Technische Universität München
Lehrstuhl für Echtzeitsysteme und Robotik

A Highly Versatile Single-Port System for Minimally Invasive Surgery

Salman Can

Vollständiger Abdruck der von der Fakultät der Informatik der Technischen Universität München zur Erlangung des akademischen Grades eines

Doktors der Naturwissenschaften (Dr. rer. nat.)

genehmigten Dissertation.

Vorsitzender:		Univ.-Prof. Dr. Nassir Navab
Prüfer der Dissertation:	1.	Univ.-Prof. Dr. Alois Knoll
	2.	apl. Prof. Dr. Hubertus A. E. J. Feußner

Die Dissertation wurde am 21.10.2011 bei der Technischen Universität München eingereicht und durch die Fakultät für Informatik am 09.02.2012 angenommen.

Abstract

Laparoscopic single-port surgery and natural orifice transluminal endoscopic surgery (NOTES) are two novel procedures with the aim to reduce trauma to the patient. Both of them are promising, but still highly dependent on the development of new, adequate support systems that are indispensable in order to perform such demanding interventions.

Primarily, the requirements of a single-port system regarding surgical as well as technical aspects were investigated. Based on this knowledge, a new robot platform was developed to extend the limited possibilities of laparoscopic single-port surgery. The design of the developed single-port platform is presented here in detail. Two manipulators with 6 DOFs and a semi-rigid telescope with 5 DOFs are combined gas-tightly into one unit to perform surgeries through a single access. The hollow structure of the manipulator allows the introduction of flexible instruments. All the joints of the platform are actuated by flexible transmission mechanisms 2m from the platform at the periphery.

This work also presents the kinematics of the flexible bending section and the manipulator that were verified and analyzed in a simulation with a simplified 3D model of the single-port platform. A velocity-based task-space control of the instruments was implemented in the simulation for kinematic analysis. The evaluation and assessment was carried out in a pick-and-place scenario. Moreover, the realized low-level control for the actuation of the manipulators in joint-space is presented.

The workspace of the manipulator and the applicable forces were evaluated. Furthermore, the results of the accomplished in-vitro as well as in-vivo laparoscopic cholecystectomy are presented. Finally, an in-vitro NOTES cholecystectomy was performed with the semi-rigid platform to assess the potentials and challenges of transluminal surgery.

Zusammenfassung

Laparoskopische Single-Port Chirurgie und die transluminale endoskopische Chirurgie über natürliche Körperöffnung (NOTES) sind zwei neuartige Verfahren mit dem Ziel das Trauma des Patienten zu reduzieren. Beide Verfahren sind vielversprechend, jedoch derzeit noch stark abhängig von der Entwicklung neuer, geeigneter Systeme, die für die Durchführung solch anspruchsvolle Eingriffe unentbehrlich sind.

In erster Linie wurden die Anforderungen an ein Single-Port System bezüglich der chirurgischen als auch technischen Aspekte untersucht. Basierend auf diesen Erkenntnissen wurde eine neue Roboterplattform entwickelt, um die begrenzten Möglichkeiten der laparoskopischen Single-Port Chirurgie zu erweitern. Das Design der entwickelten Single-Port Plattform wird hier im Detail vorgestellt. Zwei Manipulatoren mit 6 DOFs und ein halbstarres Teleskop mit 5 DOFs werden gasdicht zu einer Einheit verbunden um Eingriffe durch einen einzelnen Zugang durchzuführen. Die Hohlstruktur des Manipulators ermöglicht die Einführung von flexiblen Instrumenten. Alle Gelenke der Plattform werden durch flexible Übertragungsmechanismen in 2m Abstand in der Peripherie angesteuert.

Diese Arbeit präsentiert auch die Kinematik des flexiblen Biegesegements und des Manipulators, die in einer Simulation mit einem vereinfachten 3D-Modell der Single-Port Plattform verifiziert und analysiert wurden. Eine geschwindigkeitsbasierte Arbeitsraumsteuerung der Instrumente wurde in der Simulation für die Analyse der Kinematik implementiert. Die Evaluation und Bewertung wurde in einem pick-and-place Scenario durchgeführt. Darüber hinaus wird die realisierte low-level Steuerung für die Ansteuerung der Manipulatoren im Gelenkraum vorgestellt.

Der Arbeitsbereich und die aufgebrachten Kräfte des Manipulators wurden evaluiert. Des Weiteren werden die Ergebnisse der durchgeführten in-vitro als auch in-vivo laparoskopische Cholezystektomie vorgestellt. Schliesslich wurde ein in-vitro NOTES Cholezystektomie mit der halbstarren Plattform durchgeführt, um die Potenziale und Herausforderungen der transluminalen Operationen zu beurteilen.

Acknowledgements

First of all, I would like to thank Prof. Dr.-Ing. Alois Knoll for supervising my thesis and for the opportunity that I have received to work with the chair of robotics and embedded systems. His visionary approach in robotics and the according advice and support helped me to conduct the intended research.

I am also grateful to Prof. Dr. med. Hubertus Feussner for supervising my thesis and for the time that I have worked at the research group MITI in the Klinikum rechts der Isar. Many thanks also for the advice and support as well as the depth and variety of knowledge that I was able to acquire during my time at the clinic.

I also want to thank my colleagues at the chair of robotics and embedded systems and the research group MITI. Special thanks to Adam Fiolka and Armin Schneider for their support and the clinical evaluations. Many thanks also to Christoph Staub and Emmanuel Carlos Dean Leon for their support and reading the thesis.

I am also indebted to Viktor Wimmer from Karl-Storz GmbH and Peter Kraus from Aktormed GmbH for their support and cooperation.

Last but not least, many thanks to the Bavarian research foundation for funding my thesis!

My special thanks goes to my family, especially my parents, who have supported and encouraged me to accomplish this thesis. They were always there when I needed them and helped me to overcome any problems that I encountered.

Contents

List of Figures **vii**

List of Tables **xi**

1 Introduction **1**

1.1 Vision of the single-port surgical system . . . 4

1.2 Objectives and contributions . . . 6

1.3 Structure of the thesis . . . 7

2 Related Work **9**

2.1 Minimally invasive robotic surgery . . . 9

2.2 Enhancement of the intra-abdominal flexibility for laparoscopic surgery . . . 13

2.3 Laparoscopic single-port surgery . . . 18

2.3.1 Conventional laparoscopic single-port surgery . . . 19

2.3.2 Robot systems for laparoscopic single-port surgery . . . 21

2.4 Single-port surgery through natural orifices . . . 24

2.4.1 Current state and manual platforms for NOTES . . . 24

2.4.2 Robot systems for NOTES interventions . . . 27

3 Surgical Prerequisites and Theoretical Approach **31**

3.1 Single-port surgery from the medical point of view . . . 31

3.1.1 Shoulder girdle - arm - hand principle . . . 33

3.1.2 Description of the surgical work-flow of a single-port procedure . . . 35

3.2 Technical aspects and the impact of research and development . . . 38

3.3 Determination of the requirements . . . 41

3.3.1 Design specifications for the overall system . . . 41

3.3.2 Design considerations and corresponding restrictions . . . 43

3.4 Concept of the platform and differentiation from existing works 44

3.4.1 Description of the concept 44

3.4.2 Differentiation from existing works 47

4 The Highly Versatile Single-Port System 49

4.1 Manipulator with distal articulations 51

4.1.1 Endoscope deflecting for high dexterity 52

4.1.2 Hollow elbow joint actuated by bowden wire 53

4.2 Double-bending telescope for enhanced visualization 55

4.3 Linear and rotary articulations of the manipulator 56

4.3.1 Approach of the passive actuation mechanism 56

4.3.2 Bowden wire actuated linear and rotary articulations 59

4.4 Connection and rotation of the single-port platform at the guiding system 63

4.4.1 Requirements and concept of the rotary joint for the platform 63

4.4.2 Rotation of the single-port platform by means of a flexible shaft 64

4.5 Actuation mechanism at the periphery 66

4.5.1 Actuation unit for the deflecting and the elbow joint 66

4.5.2 Actuation unit for the linear motion of the manipulators 68

4.6 Hydraulic SoloAssist telemanipulator for guiding the single-port platform 69

5 Kinematics and Control of the Single-Port System 71

5.1 Kinematics of the flexible bending section 72

5.2 Kinematics of the single-port manipulator 75

5.2.1 Forward kinematics 76

5.2.2 Instantaneous kinematics 77

5.2.3 Numeric verification of the Jacobian 79

5.3 Simulation and kinematic analysis of the system 80

5.4 Low-level control of the single-port platform 82

5.4.1 Structure of the control hardware 82

5.4.2 Joint-space control of the manipulators with two joysticks. 82

6 Evaluations **85**
6.1 Measurement of the working range . . . 85
6.1.1 Set-up of the measurement . . . 85
6.1.2 Workspace of the bending section . . . 87
6.1.3 Workspace of the single-port manipulator . . . 88
6.1.4 Discussion . . . 90
6.2 Evaluation of the forces on the manipulator . . . 91
6.2.1 Materials and Methods . . . 91
6.2.2 Results of the force measurements . . . 93
6.2.3 Discussion . . . 96
6.3 Performing laparoscopic cholecystectomy . . . 98
6.3.1 Material and Methods . . . 98
6.3.2 Results . . . 100
6.3.3 Discussion . . . 101
6.4 Performing in-vitro NOTES cholecystectomy . . . 103
6.4.1 Material and Methods . . . 103
6.4.2 Results . . . 105
6.4.3 Discussion . . . 106

7 Conclusion **109**
7.1 Summary . . . 109
7.2 Limitations and outlook . . . 111

A Appendix **113**
A.1 Comparison of drive transmission mechanisms over long distances . . . 113
A.2 Kinematics of the SoloAssist guiding system . . . 115

References **119**

List of Figures

1.1 Vision of the single-port system. 5

2.1 Instruments with additional articulations. 16

2.2 Instruments with flexible bending segments. 17

2.3 Insertable robotic effector platform and concept of the daVinci single-port system. 23

2.4 Possible access routes for NOTES interventions. 25

2.5 Flexible platforms for transluminal surgery. 26

2.6 Design of transluminal robots. 28

3.1 Merging laproscopic surgery and gastroenterology. 32

3.2 Current approaches for single-port surgery. 33

3.3 Design of a platform that emulates the skills of the surgeons. 34

3.4 Transumblical gallbladder resection using the highly versatile single port system. 36

3.5 Surgical procedure of the single-port robotic gallbladder resection. 37

3.6 Schematic drawing of the semi-rigid single-port surgical platform. 45

3.7 Cross-section of the insert and the distal section of the hollow manipulator. . . . 46

4.1 Design of the highly versatile single-port platform. 49

4.2 The overall highly versatile single-port system. 50

4.3 Distal section of the two single-port manipulators in opposed configuration. . . . 51

4.4 Bending section of an endoscope integrated as distal deflecting of the manipulator 52

4.5 Elbow articulation of the single-port manipulator. 53

4.6 Double-bending telescope comprising two bendable sections. 55

4.7 Concepts of the linear and rotary joint of the manipulators. 57

4.8 Concept of the linear and rotary joint actuation by using bowden wire mechanism. 58

4.9 Proximal unit of the developed single-port platform. 59

4.10 Sectional view of the linear and rotary actuation mechanism of one manipulator. 60
4.11 Design of the rotation mechanism. 61
4.12 Detailed views of the wire actuation. 62
4.13 Sectional view illustrating the linear actuation mechanism of the manipulator . . 62
4.14 Concepts of the rotation for the single-port platform. 63
4.15 Rotary drive unit of the single-port platform attached to the SoloAssist link. . . 64
4.16 Sectional view of the rotary drive mechanism including the coupling of the shaft. 65
4.17 Platform of the actuation mechanism for the deflectings and the elbow joints. . . 66
4.18 Sectional view of the drive unit and bowden wire mechanism for distal articulations 67
4.19 Platform for the linear motion of the manipulators and the telescope. 68
4.20 SoloAssist hydraulic telemanipulator for guiding the single-port platform 69

5.1 Concept of the control architecture for the single-port system. 72
5.2 Bending section of the Karl-Storz gastroscope illustrating the configuration of the hinges and their orientations. 73
5.3 Schematic drawing of the manipulator and the bendable section kinematics. . . . 75
5.4 Matlab-Simulik program for the numeric verification of the Jacobian. 78
5.5 Error plot of the linear velocity of the tool tip. 79
5.6 Error plot of the angular velocity of the tool tip in quaternions. 80
5.7 Simulation environment for the evaluation of the platform and the kinematics. . 81
5.8 Velocity-based control of the single-port manipulator. 81
5.9 Control hardware of the single-port platform and evaluation of the control with two joysticks. 83
5.10 Schematic design of the realized low-level control of the single-port platform. . . 84
5.11 Matlab-Simulink program of the implemented closed-loop control. 84

6.1 Electromagnetic tracking set-up for the workspace measurements. 86
6.2 Theoretical workspace of the gastroscope bending section. 87
6.3 Measured workspace of the bending section in the horizontal and vertical planes. 88
6.4 Surfaces of the theoretical workspace of the manipulator. 88
6.5 Workspace evaluation of the distal dexterity of the manipulator. 89
6.6 Polygon mesh of the measured workspace. 90
6.7 Measurement of the forces applied by the bending section on the manipulator tip at different bending angles of the deflecting. 91

6.8 Measurement of the forces applied by the elbow joint on the manipulator tip at different bending angles of the elbow joint. 92
6.9 Linear force measurement of the prismatic joint and torque measurement of the rotational joint. 92
6.10 Results of the force measurements by horizontal deflection of the bending section 93
6.11 Results of the force measurements by vertical deflection of the bending section . 94
6.12 Results of the horizontal force measurements by bending the elbow joint 94
6.13 Results of the measured forces with the prismatic and rotational joints 95
6.14 Applicable average forces on the single-port manipulator 95
6.15 The Highly Versatile Single Port Platform 98
6.16 Set-up of the laparoscopic in-vitro and in-vivo evaluations of the single-port system 99
6.17 Laparoscopic evaluation of the platform. 100
6.18 Schematic drawing of the evaluation set-up for the transanal NOTES intervention 103
6.19 First application of the HVSPS for NOTES on the ELITE trainer performing a cholecystectomy using the transanal ISSA approach 105

7.1 Schematic drawing of a fully flexible single-port platform for transluminal surgery. 112

A.1 Design of the SoloAssist telemanipulator attached to the operating table. 115

List of Tables

2.1 List of surgical instruments with distal articulations and bending segments. . . . 14

3.1 Specification of the operating range of the individual joints 45

4.1 Assets and drawbacks of the hollow elbow articulation 53

4.2 Definition of the speech commands for the SoloAssist robot and its relation to Cartesian and invariant point control. 70

5.1 DH table of the single-port manipulator. 76

A.1 Comparison of different actuation mechanisms with flexible routing over long distances. 114

A.2 DH table of the hydraulic SoloAssist telemanipulator 116

Chapter 1

Introduction

Therapeutic interventions of any kind are inevitably accompanied by some degree of side effects or "collateral damage" which have to be accepted to reach the therapeutic goal. Within the ongoing third era of scientific surgery it has been the aim to reduce the side effects or trauma of the operative treatment as much as possible without compromising the curative effect [1]. One central issue thereby is minimizing the trauma of surgical access by replacing long surgical incisions with tiny insertion ports for laparoscopic trocars. The next level is to perform "scarless surgery" via the gastrointestinal tract. The more ambitious the new approaches, however, the more they depend on new technological support.

The initial euphoria that reigned at the end of 20th century encouraged the belief that laparoscopic surgery would penetrate the operating rooms and 80-90% of all surgical operations would be performed laparoscopically. The results have been less than was expected. Nevertheless, minimally invasive surgery has become the gold standard for such procedures as cholecystectomy and fundoplication [2]. In numerous indications, however, minimally invasive surgery could not be introduced as intended despite the fact that the advantages of laparoscopic surgery (less pain, shorter hospitalization, better cosmetic results, etc.) were proven convincingly. More complex operations, in particular oncological ones, are still performed via the conventional open access.

One of the main drawbacks of laparoscopic surgery is the restricted flexibility of the instruments which are limited due to the trocar port to 4 DOF. The access through the trocar acts as a fulcrum. As a result, the surgeon must cope with counter intuitive, unfamiliar manipulations of the rigid instruments, the experience of which is similar to the chopstick effect. Another drawback is the limited, cone-shaped working range of the instruments that depends on the port placement. A change or extension of the workspace always demands the placement of new trocar ports, which in turn increases the trauma to the patient. Therefore, operations such as a partial bowel resection, which require a large workspace (in part over several quadrants of the abdomen), are often performed through an open access. Moreover, sophisticated surgeries such as those of the lower abdomen are difficult to perform laparoscopically due to restricted accessibility. Considerable progress that has been achieved by developing new instruments could partially improve the limited dexterity. However, the impact has been low and surgeons are still hampered during laparoscopic surgery.

In addition to the limited flexibility and workspace, the limited visual access to the situs is a further disadvantage. The surgical target is observed and operated in a prograde direction. A lateral or retroflexed view, which would have a huge influence on the outcome of the operation, is limited at best. In laparoscopic surgery, the telescope is usually held by an assistant physician and guided according to the commands of the surgeon. Besides the additional cost factors, the surgeon must cope with the tremors of the assistant during long interventions or a misunderstanding of the instructions. Another serious drawback is the counter-intuitive way of working by observing the endoscopic view on the monitor, whereby the overview on the performed hand movements is lost. The surgeons must perform challenging interventions in an unergonomic posture that hinders their abilities. In addition to the aforementioned drawbacks, inaccurate manipulations resulting from tremors and lack of depth perception, the lack of adequate instruments with integrated sensors and force feedback, and the need for extensive training are further limitations of laparoscopic surgery, which require new developments. These drawbacks of laparoscopy can be partially overcome by the introduction of computer aided systems and telemanipulators (robots) integrated into the operating room [3, 4].

Although extensive research on new support systems, telemanipulators and robots have been carried out during the last two decades, only a few of these systems have been able to achieve acceptance and application in the clinical routine (For further details see Chapter 2: State of the Art). The daVinci is one of the well known master-slave manipulators that has been applied in many surgical areas including cardiology, urology and visceral surgery. Due to its limited benefits, which do not meet the requirements of the other surgical areas, the daVinci is currently being used mainly in urology. There are still many problems such as bulky construction, limited flexibility, lack of navigation and very high investment and running costs. The superiority of robots in the clinical routine has not yet been proven. Extensive research is required to achieve a breakthrough. In addition to the hardware developments in regard to optimization and miniaturization, many other aspects such as new sensor modalities, intuitive user interfaces, medical imaging and computer vision, integration of workflow management systems and partial autonomy are being investigated by various research institutes. The focus of most ongoing research is the development of new systems that meet the specific requirements of a given field of application.

Extremely high mechanical precision is a traditional requirement of medical robots which makes them rather rigid and inflexible. A very high level of precision is undoubtedly necessary in neurosurgery or orthopedic surgery. In surgical disciplines dealing with soft tissue, such as visceral surgery, different criterions are more important. A very high maneuverability is essential since anatomical structures such as the bowel, the stomach or the liver frequently shift their shape and position as soon as surgical manipulations are exerted. The operating field is larger, and changing the working position from one quadrant of the abdomen to another is frequently necessary. Surgical instruments for dissection, coagulation, suturing or stapling often have to be changed. This is less than ideally solved in current concepts of master-slave systems. Last but not least, serious emergencies, such as bleeding, requiring immediate conversion to open surgery are more likely to occur in abdominal surgery than in other disciplines. Accordingly, the bulky construction of current master-slave systems, consuming considerable time, is unfavorable and a source of worry for the surgeon. General -or visceral surgeons would prefer a system which does not require more space at the surgical table than a human assistant. The intraabdominal versatility should be more or less comparable to the human arm, hand, and fingers to extend the limited possibilities of laparoscopic surgery.

Besides the achieved developments and progress of minimally invasive robotic surgery, physicians are trying to develop new surgical procedures and techniques that could reduce patients' trauma without compromising surgical ability. There are two popular surgical approaches, which are promising due to the enhanced technical possibilities:

- The laparoscopic **Single-Port Surgery** is performed through one port in the abdominal wall where all required manipulators, usually up to three or four instruments, are inserted.
- For **NOTES** (Natural Orifice Transluminal Endoscopic Surgery), the access through the abdominal wall is completely avoided and the surgeries are performed through a natural orifice (transoral, transvaginal, transurethral, transanal or a combination of these).

Both methods place similar demands on the operational platform. It would be ideal to be able to have several independently controllable instruments and manipulators bundled and introduced through a single shaft (carrier). Similar to flexible endoscopy, the introduction of the instruments is performed using the same access path through the carrier. However, at the target it can change from a single carrier to several manipulators to enhance the flexibility required for the operation. In addition, a triangulation i.e. the opposition of both main manipulators is indispensable to achieve controlled and precise preparation and dissection as well as the reconstruction of anatomical structures. Compared to conventional laparoscopy and single-port surgery, the access path is a further challenge for NOTES which can only be overcome by fully flexible systems.

These new surgical approaches have also stimulated the industry and the research institutes that are developing new systems in this regard to identify the technological possibilities. While the industry is developing simple and robust systems for clinical applications, engineering scientists are conducting basic research to provide new technologies for this purpose.

1.1 Vision of the single-port surgical system

We are firmly convinced that a new concept of a single-port robotic system would be superior to conventional solutions. The idea is, literally spoken, to bring the surgeon's head, shoulders and arms into the abdominal cavity to regain the same flexibility as in open surgery. This can be achieved through the development of new manipulators with a kinematic structure that reflects the degrees of freedom of the surgeon's body. Two such manipulators that correspond to the arms of the surgeon, and a telescope for the visualization are combined in one platform and introduced together through a single incision into the abdominal cavity.

The high flexibility of the manipulators enables an opposed configuration of the instruments to exert traction and counter-traction on the target tissue. Anatomical structures can be dissected thereby in a controlled and precise manner. As a further important property, the single-port platform enables the accomplishment of complex and demanding surgical procedures in a large workspace over several quadrants of the abdomen. The dimensions of the manipulators as well as the working range are defined according to the surgical task and can be variably adapted. Despite the large number of articulations and the flexible structure, the manipulators provide a rigidity sufficient to exert high forces for precise manipulations. Moreover, a modular conception of the entire platform enables the sterilization and maintenance of the individual components.

As shown in Figure 1.1, the single-port platform is held and guided by a telemanipulator attached to the operating table. Therefore, when carrying out single-port interventions, the necessary space for the slave system (the guiding manipulator and the single-port platform) at the operating table can be reduced drastically. The surgeon controls the overall system in an intuitive manner on the master console. His motions are tracked and transmitted after scaling and tremor filtering to the slave manipulator. Additional user interfaces such as speech and gesture recognition or eye tracking enable the simultaneous control of additional functionalities such as the navigation of the telescope or the exchange of the instruments. In the opposite direction, the endoscopic image is transmitted after processing and integrating the required information to the master console and observed by the surgeon. Stereo endoscopy or additional depth information enable thereby the reconstruction of the scene that is used, for example, for the navigation, the definition of virtual fixtures or the observation in different perspectives.

Figure 1.1: Vision of the single-port system: The intuitive master console on the surgeon's side and the guiding manipulator with the single-port platform on the patient's side (MITI, Klinikum rechts der Isar, Germany).

A multitude of sensor modalities such as position, force and optical sensors are integrated in the manipulators in order to provide further information about the interaction between the system and the patient. For the force feedback, the effective forces on the instruments are measured with kinesthetic force-torque sensors on the one hand, and on the other hand localized surface structures are identified by tactile sensor matrices. These forces are transmitted to the input devices of the master console and perceived by the surgeon. Furthermore, adequate position sensors in small sizes are used to determine the mechanically inaccurate determinable position of the manipulators. In addition to the position of the instrument tip, the spatial structure of flexible manipulators is measured in order to predict precisely the lateral collision of the manipulators. The integration of miniaturized optical sensors in the tool tip enables a detailed visualization of the instrument or surgical field in different perspectives in addition to the overview presentation of the telescope.

Last but not least, the design of the overall system with standardized interfaces provides a simple integration into the operating room. This enables the transmission of the acquired information into a superior entity, in which the entire surgical workflow is recorded. By using the previously gathered interventions in a database, the current sequence of the surgical procedure is determined and the subsequent steps can be predicted accordingly. In this way, recurring tasks are performed semi-autonomously, on demand. This includes, for example, the automatic preparation and introduction of the instruments by a tool changer or the supportive, self-running sequences such as camera guidance or knot tying, which can be retrieved by the surgeon.

1.2 Objectives and contributions

The main purpose and objective of this work is the development of a semi-rigid platform for single-port surgery in order to enable the accomplishment of new surgical procedures. This intention raises questions such as how the kinematic structure of the system should look and how it can be implemented technically. Furthermore, the question of how such a system can be controlled intuitively by a single surgeon arises. Based on these questions, this thesis presents the following contributions:

- **Single-port surgery:** There has not yet been much investigation on the topic of single-port robotic surgery. Therefore, the requirements for a single-port surgical robot were first determined in close cooperation with the physicians. The technological possibilities and challenges of the intended developments or research were identified accordingly. A new approach of a shoulder girdle-arm-hand principle is presented whereon the design concept of the developed platform was based. Furthermore, the surgical procedure of a single-port intervention was determined by means of functional models and evaluations that serve as a basis for further developments.

- **Hardware development:** A new, highly versatile, single-port platform with two manipulators and a telescope was designed and manufactured to perform surgical interventions through a single incision. The developed hollow manipulator with 6DOFs and an enhanced dexterity enables the insertion of flexible instruments that can be easily exchanged during surgery. All the bowden wire actuated joints of the platform are controlled from a distance of 2m at the periphery. Thereby, bulky and heavy construction as well as the electromagnetic interference caused by having the motors near the patient, is avoided. The rotation and guidance of the overall platform is achieved with the additional rotary joint that is attached to the SoloAsssist guiding system.
- **Kinematics and control:** One of the major problems for the control arises from the large number of degrees of freedom of the single-port system that must be intuitively operated by a single surgeon. Therefore, the kinematics of the flexible bending section and the manipulator was determined for the implementation of the control. Accordingly, a velocity-based task-space control was implemented in a simulation, in which the manipulators, the telescope as well as the overall platform attached to the guiding system are operated by a space mouse. The simulation provides a simplified 3D model of the platform and enables the evaluation and kinematic analysis of the system. Moreover, a low-level joint-space control of the platform was implemented and evaluated with two joysticks as the input device.
- **Evaluation of the system:** The working range of the developed system and the applicable forces on the manipulators were measured and evaluated according to the defined specifications. In addition, by performing in-vitro or in-vivo experiments, the feasibility of single-port surgeries was determined in simple interventions such as the resection of the gallbladder. Moreover, an in-vitro transluminal surgery was accomplished and the challenges of NOTES interventions as well as the requirements for a fully flexible system were identified.

1.3 Structure of the thesis

Chapter 2 presents the related work comprising the minimally invasive robotic surgery, a detailed survey of articulated instruments and the laparoscopic and transluminal single-port surgery including the robot systems, which have been developed so far for these new approaches.

Chapter 3 gives a brief description of the single-port surgery from a medical point of view followed by the explanation of the shoulder girdle-arm-hand principle. The technical aspects of single-port surgery and the manual and robotic single-port procedures are described as well.

The requirements for a single-port platform are identified and the concept of the developed system is described including the differentiation from existing works.

Chapter 4 presents the developed single-port system. After a brief overview of the entire system, the individual subunits including the single-port platform, the manipulator, the telescope, and the actuation unit are described in detail. Moreover, an additional joint for the rotation of the overall platform that is attached to the SoloAssist guiding system is presented.

Chapter 5 introduces the kinematics of the flexible bending section and the manipulator. It also presents a simulation with a velocity-based task-space control for the evaluations and kinematic analysis. Furthermore, the implemented low-level control for the actuation of the manipulator in joint-space is described.

Chapter 6 presents the accomplished evaluations. An experiment was carried out for the measurement of the working range as well as the achievable forces, which are described and discussed in this chapter. Furthermore, the accomplished in-vitro evaluations with a human mock-up and in-vivo animal experiments are described with respective results.

Chapter 7 concludes the thesis with a summary including the contributions. Finally, suggestions and future works are described in an outlook.

Chapter 2

Related Work

The intended research focuses on robotic systems for laparoscopic surgery. Therefore, a brief literature survey on minimally invasive robotic surgery was conducted. Some of the well-known master-slave robotic systems for laparoscopic abdominal surgery are briefly described to illustrate its potentials. Since the limitations of the single access into the abdominal cavity demands additional flexibility, a detailed literature survey on articulated instruments was accomplished and is presented in this chapter. Subsequently, the related work in the field of laparoscopic single-port surgery as well as the single-port surgery through natural orifices was investigated. For both of these approaches, a literature survey, consisting of the evaluation of the conventional instruments or platforms and the recent developments of robotic systems for these procedures, was accomplished. Because of the different challenges and requirements from a clinical and technical point of view, the laparoscopic and transluminal surgery are presented separately.

2.1 Minimally invasive robotic surgery

The application of robots for surgery was pioneered in the late 1980s in the fields of neurosurgery and orthopedic surgery [5]. The rapid advance of laparoscopic surgery and its potentials stimulated the broad spectrum of robot development in the early 1990s [6]. Preliminary, industrial robots were adapted for medical application without being optimized for the characteristics of specific surgical tasks [7]. Surgical robots should be viewed as "extending or enhancing human capabilities" rather than replacing humans, in contrast to the example of industrial automation [8]. NeuroMate, Robodoc and CASPAR are some examples of adapted programmable industrial robots applied in the operating room (OR) with limited output and success. For example, many patients in Germany who had hip replacements which were accomplished with the Robodoc had to be reoperated on due to technical complications. This led to a flood of lawsuits, the company was closed and the robot disappeared from the market [9]. Nevertheless, robotic surgery could penetrate the OR after being redeveloped. To date, however, only a few have overcome the barriers to acceptance and have been applied in surgical interventions. FDA approved robots such as AESOP, ZEUS (Computer Motion, USA) and daVinci (Intuitive Surgical, USA) have found their way into the OR [10, 11, 12, 13]. These systems have established their ability to augment a surgeon's dexterity in minimally invasive procedures and have the potential to enhance treatment outcome.

Generally, surgical robots can be classified into the groups of programmable robots or master-slave systems. Camera guiding systems are a splitting of the latter. The AESOP camera guiding system, an inherent part of the ZEUS master-slave system, was also employed as stand-alone solution in many clinics for various surgical procedures (e.g. [14, 15]). Many comparative studies have been carried out with the AESOP system that demonstrate its feasibility. However, there are still drawbacks like loss of comfort and time as well as safety aspects. Because it was not widely accepted, the system disappeared from the market [16]. This was followed by other camera guiding systems such as LapMan [17] and EndoAssist [18] which were not able to prevail due to similar outcomes and drawbacks. Newer systems such as the ViKY [19] or the FreeHand [20] have to prove their advantages in extensive studies to attain the required acceptance of the community.

One of the first master-slave systems was the ARTEMIS, which was developed at the Karlsruhe Research Center [21, 22]. The system consists of three adapted 4 DOF spherical slave manipulators guiding articulated multi-link instruments with additional 2 DOF. A custom-made HT2 master system was used to control and evaluate the instruments in animal studies. This research was discontinued because of limited funding resources. Black Falcon, developed by Madhani et al. at MIT, is another manipulator system with articulated instruments [23]. The 8 DOF manipulator system consists of a base unit and a wrist unit with 4DOF that is controlled by wires. This research system was also discontinued. There are only a few master-slave systems that have been used clinically and have achieved wide acceptance. For example, Guthart et al. performed abdominal surgical procedures using the daVinci system [24]. Marescaux et al. performed the first transatlantic robot-assisted telesurgery with the ZEUS system [25]. Intuitive Surgical merged, in 2003, with its competitor, Computer Motion, and the ZEUS system was phased out in favor of the daVinci system. By increasing intra-abdominal articulations while operating through small incisions, the daVinci was already used for a large number of visceral and solid organ operations, including those for the gallbladder, liver, pancreas, spleen, kidney and colon [26, 27, 28, 29]. The daVinci can actually be considered to be the state of the art for the many medical robot systems that have been developed. The system was primarily applied in general laparoscopic procedures in 2000 [24] and found its way to urology and gynecology where it is mostly used nowadays. Prostatectomy and hysterectomy are two of the surgeries most performed with the daVinci system [30, 31]. After the standard daVinci and the daVinci S surgical system, the newest daVinci Si was launched in April 2009.

The daVinci master-slave system comprises the surgeon console, patient-side cart and the 3D vision system. The robotic camera arm is manipulated by pressing the camera foot-switch pedal. This locks the instrument arms and gives the operator control of the camera through the master manipulators. The daVinci system has the main technological advantages of realistic 3D imaging, motion scaling and tremor filtering with the 7 degrees of freedom "EndoWrist" instruments [24]. With the introduction of the new daVinci patient-side cart in 2002, the surgeon has the ability to change to a third instrument by foot pedal to use additional instruments at the same time [12]. Additional functionalities introduced with the actual daVinci Si system are: 3D-HD visualization, enhanced user interface and ergonomics with an integrated touchpad, an extensive array of wristed instruments, motorized and adjustable patient cart, dual console capability and the TilePro multi-input display to also view ultrasound and EKG video sources.

For the moment, the costs of the daVinci system (1.25 million excl. service cost of 0.11 million EUR per year [32]) are prohibitively high for widespread application. The daVinci robot proved its usability in comparison to conventional laparoscopic interventions; a routine use is still not justified because of lack of benefits [33, 34, 35]. This is caused by significantly higher procedural costs and prolonged overall operating time. To date, the superiority of robots on the market could not be proven. As a result, improvements and new developments are required. There are several problems to be solved such as difficult handling, bulky construction, limited flexibility, training systems for surgeons, lack of navigation systems and very high investment and running costs.

There are many studies and system developments that have been conducted in the field of minimally invasive robotic surgery to overcome the aforementioned drawbacks. One of these studies is the extensive MiroSurge master-slave robot system developed by the German Aerospace Center (DLR). It could compete with the daVinci system [36, 37]. Compared with the daVinci, the MiroSurge is designed modular and allows greater flexibility in the constellation of individual robot arms. Each light-weight robot arm with 7 DOF allows the positioning of one

MICA Instrument. These instruments, with a distal cardan joint and a hexapod equipped with force sensors, permit additional dexterity. The robot arms can be controlled either by position control or torque and impedance control. Providing the torque needed to sustain the weight of the robot and the tool, the surgeon is able to position the robot by hand in an intuitive manner. The current master console includes a stereo display and two Sigma7 haptic devices (Force Dimension) [38].

In many other ongoing studies, specific issues such as flexibility, force feedback or the interface are being examined more closely. Mitsuishi et al. at Tokyo University in Japan have developed a three arm master-slave system with integrated force feedback and instruments with an additional articulation [39, 40, 41]. The mechanism of the SCARA-like slave manipulator permits the maintenance of the fixed insert position so that patient safety is ensured. The link driven 4 DOF bending forceps were developed to perform difficult suturing tasks. Force sensors are integrated on the push/pull rod of the instruments providing the surgeon with haptic sensing on the self-made master console. Using this master-slave system they were able to perform a remote telesurgical experiment between Japan and Korea [42]. Another master-slave system was developed by Cavusoglu et al. at UCB/UCSF in California. That robotic telesurgical workstation comprises two 4 DOF gross positioning slave robots and instruments with 2 DOF wrists that are actuated by wires [43]. The parallel arrangement of these robots increases rigidity on a small footprint and the complete system is controlled over the master workstation using two 6 DOF Phantom haptic devices. The authors point out that the 2 DOF wrists greatly improve the ability to suture and tie knots, however, the available range of motion is quite restrictive.

Hermann et al. at the TU Munich in Germany developed the EndoPAR system for minimally invasive cardiac surgery [44]. They integrated force feedback on the daVinci instruments and controlled them by three Mitsubishi robots mounted on the ceiling. By performing skill transfer, this system permits automated trajectory planning and knot tying using fluid dynamics [45]. KaLAR [46] or CURES [47] are two manipulators developed by Kim et al. at KAIST in Korea for laparoscopic surgery. The CURES is a 5 DOF, light-weight surgical robot with a spherical mechanism permitting sufficient workspace and adequate force. In contrast, the KaLAR is a 3 DOF laparoscope with a distal bending segment which is attached to a laparoscopic holder. More recently, the completely wire actuated 7 DOF telesurgery system RAVEN was developed by Lum et al. at the Univ. of Washington in the USA [48, 49]. The 4 DOF spherical positioning and additional 3 DOF for wrist articulation and grasping were identified using the kinematics and dynamics determination system BlueDragon [50]. All the actuators of the system are located on a static base.

In nearly all of the systems mentioned above it is being attempted to increase the intra-abdominal flexibility by distal articulation. Therefore, we identified and compared current studies regarding the enhancement of intra-abdominal flexibility in minimally invasive surgery.

2.2 Enhancement of the intra-abdominal flexibility for laparoscopic surgery

The enhancement of the intra-abdominal dexterity is indispensable for the accomplishment of complex surgical procedures in minimally invasive surgery with sophisticated tasks such as suturing or knot tying [51]. This was recognized early by many research groups which have developed new instruments with articulations at the distal end [52, 23, 53]. Simaan et al. have published a literature survey of dexterity enhancement in minimally invasive surgery [54] and Webster et al. a literature survey of snake-like robots [55]. An extensive literature search was conducted by us to collocate and compare instruments with flexible, articulated joints (Table 2.1). The following literature survey includes and extends the aforementioned literature surveys of articulated instruments for minimally invasive surgery. The classifications were inspired by these reviews and enhanced as well.

Most of the identified publications deal with instruments for robotic surgery [24, 40]. However, there are also some instruments that were designed for manual operation [56, 57]. These instruments with distal articulations have either a parallel [58, 59] or a serial kinematics [60, 61, 62]. The latter can be classified into instruments with discrete [23, 43, 63] or continuous bending articulation [64, 65, 66]. Discrete instruments have one or several joints at certain intervals. In contrast, continuous instruments offer snake-like structures with one or several bending segments. In the collocated literature, the instruments with bending segments can be regarded as quasi-continuous and are getting close to a pure, theoretical continuity.

The number of joints and degrees of freedom of the distal part of these instruments are widely diversified. There are instruments with one distal articulation and one DOF [64, 67] and up to several articulations with, in total, 6 DOF [52, 60]. We have distinguished here between degrees of freedom for the entire instrument and degrees of freedom for bending. Thus, neither the gripper-joint nor the instrument rotation were considered for the determination of the entire deflection. The maximum achievable bending angle varies between 40° [37] and 360° [68].

Table 2.1: Chronological list of surgical instruments with distal articulations and bending segments.*

Literature	Institution	Manual/ Robotics	Discrete/ Continuous[1]	Serial/ Parallel	DOF[2]	Diameter [mm]	Force [N]	Bending Angle	Actuation	Application
RAMS (Schenker1995) [52]	CIT, California, USA	R	D	S	6	25	—	180°	Wire	Microsurgery
Black Falcon (Madhani1998) [23]	MIT, Massachusetts, USA	R	D	S	4	13	4.4	180°	Wire	Laparoscopy
Instrument Tip (Peirs1998) [69]	KUL, Leuven, Belgium	R/M	C	S	3	6	6	90°	SMA[3] Wire	Minimally Invasive Surgery
DALSA (Minor1999) [70]	MSU, Michigan, USA	R	D	S	3	10	5	180°	Gear/ Wire	Laparoscopy
Parallel Wrist (Reboulet1999) [58]	ONERA, Toulouse, France	R	D	P	3	5	—	60°	Rod	Minimally Invasive Surgery
Laparoscope (Fischer1999) [71]	KRC, Karlsruhe, Germany	M	C	S	2	10.5	—	90°	NiTi Wire	Laparoscopic Endoscope
ARTEMIS (Schurr2000) [53]	KRC, Karlsruhe, Germany	R	D	S	2	10	—	90°	Wire	Laparoscopy
EndoWrist (Guthart2000) [24]	IS, California, USA	R	D	S	2	8	—	90°	Wire	Laparoscopy
Arthroscope (Dario2000) [64]	SSSA, Pisa, Italy	M	C	S	1	4	1	110°	Wire	Arthroscopy
Forceps (Nakamura2000) [56]	UT, Tokyo, Japan	M	D	S	2	6	4.4	90°	Wire	Laparoscopy
Hyper Finger (Ikuta2002) [60]	NU, Nogoya, Japan	R	D	S	6	10	—	120°	Wire	Laparoscopy
Micromanipulator (Ikuta2002) [72]	NU, Nogoya, Japan	R	D	S	2	3	—	150°	Wire	ENT Surgery
RTW Instrument (Cavusoglu2003) [43]	UCB/UCSF, California, USA	R	D	S	2	15	1.5	135°	Wire	Laparoscopy
KaLAR (Lee2003) [73]	KAIST, Daejeon, Korea	R	C	S	2	4.2	—	90°	Wire	Laparoscopic Endoscope
Instrument Tip (Peirs2002) [65]	KUL, Leuven, Belgium	R	C	S	2	5	—	90°	Wire	Laparoscopy
Linkage Forceps (Yamashita2003) [57, 63]	UT, Tokyo, Japan	R/M	D	S	2	9	5.4	90°	Linkage/ Rod	Laparoscopy
MARGE (Dombre2004) [74]	LIRMM, Montpellier, France	R	D	S	4	10	—	270°	Gear/ Motor	Cardiac Surgery
Microforceps (Asai2004) [67]	UT, Tokyo, Japan	R	C	S	1	5	—	90°	Wire	Neurosurgery
Linkage Forceps (Arata2005) [40]	UT, Tokyo, Japan	R	D	S	2	10	1	70°	Linkage/ Rod	Laparoscopy
Endo-Periscope (Breedveld2005) [75]	DUT, Delft, Netherlands	M	C	S	2	5	—	110°	Wire	Laparoscopy
Micromanipulator (Harada2005) [61]	WU, Tokyo, Japan	R	D	S	2	2.4	—	90°	Wire	Fetal Surgery
MICA Instrument (Seibold2005) [76, 37]	DLR, Munich, Germany	R	D	S	2	10	10	40°	Wire	Laparoscopy
DDU (Simaan2004) [66, 77]	ARMA, New York, USA	R	C	S	4	4.2	1	180°	NiTi Rod	Laryngeal Surgery
Laprotek (Dachs2006) [78]	PU, West Lafayette, USA	R	D	S	5	10	13	180°	Wire	Laparoscopy
Dext. Manipulator (Song2006) [62]	KAIST, Daejeon, Korea	R	D	S	4	10	2	180°	Wire	Laparoscopy
HARP (Degani2006) [79]	CMU, Pittsburgh, USA	R	C	S	3	12	1-5	240°	PE[4] Cable	Cardiac Surgery
COLOBOT (Chen2006) [80]	INSA, Lyon, France	R	C	S	3	17	—	120°	Pneumatic	Colonoscopy
Robotic Forceps (Hashizume2008) [81]	KU, Fukuoka, Japan	R	D	S	2	10	—	90°	Wire	Laparoscopy
INKOMAN (Roese2009) [59]	TUD, Darmstadt, Germany	M	D	P	3	10	—	80°	Rod	Laparoscopy
IREP (Xu2009) [68]	ARMA, New York, USA	R	D	S	5	6.4	2	>360°	NiTi Rod	Laparoscopy
Catheter (Camarillo2009) [82]	SU, Standford, USA	R	C	S	3	4	—	270°	Wire	Interventional Cardiology
Outer Sheath (Yamashita2009) [83]	UT, Tokyo, Japan	R	C	S	2	16	3.6	180°	Wire/ Pneum.	Laparoscopy

[1] Quasi continuous (Snake-Like) [2] Degrees of freedom for distal bending section [3] Shape Memory Alloy [4] Polyethylene * This are only examples and the list does not claim completeness!

The diversity of the application area is also reflected in the definition of the outer diameter. Except one or two special cases it can be noted that the instruments are smaller than 10mm in diameter. Because of low rigidity, less force can be applied on the gripper of these articulated instruments. The achievable force therefore lies between 1 N [40] and 10 N [37]. Of course, here the tendency is to develop instruments with a small diameter and high load capacity, which are standing in compromise to each other.

The greater part of the instruments found, more than two-thirds, are actuated by wires (e.g. [67, 81]). According to the application, the actuation wire of these bending joints are made of stainless steel [56], polyethylene [79] or shape memory alloy (SMA) using superelastic materials such as CuAlNi [69] or Nitinol (NiTi) [71]. As a special case, Minor et al. developed a bending segment with gears, which is actuated by wires as well [70]. In contrast, the joints with parallel kinematics [58, 59] or linkage mechanism [63, 40] are actuated by rods. Furthermore, Simaan et al. developed a push-pull actuated bending segment using tubes made of superelastic NiTi material [66]. In a concept Dombre et al. have developed a direct drive, where they have integrated micro motors in the joints, so that the movements are transferred by gears [74]. In addition to the mechanical drives, there exist also pneumatic actuators for the control of the flexible segments. For example, Chen et al. developed a silicone-rubber bending tip with three specific chambers that are controlled pneumatically [80]. In an application, where the bending segment is operated by wires, Yamashita et al. developed a nonmagnetic outer sheath with a pneumatic interlocking mechanism [83].

As one of the greatest application areas, more than half of the instruments found were developed for laparoscopy (e.g. [24, 76, 78]). Some of these instruments with flexible bending segments were implemented as laparoscopic endoscopes (laparoscope) [71, 73]. Further application areas for instruments with additional flexibility are microsurgery [52] or neurosurgery [67, 81], arthroscopy [64], ENT surgery [72] or laryngeal surgery [66, 77], cardiac surgery [74, 79], fetal surgery [61], colonoscopy [80] and interventional cardiology [82].

Related to the proposed system development, we should also differentiate between instruments with an integrated gripper at the top, which affects the majority of the listed instruments, and those with a hollow structure that allows, as a guiding-manipulator, the introduction of flexible instruments, similar to endoscopy (e.g. [65, 75]). The latter would offer the possibility to introduce instruments that are provided by a tool changer at the periphery. However, a hollow structure limits the implementation of the articulation mechanism and furthermore, such an instrument has a comparatively lower stiffness.

Except the wire actuated daVinci Endowrist, all the listed instruments are research systems that have not clinically been used to prove their functionality. Due to poor sterilization conditions and increased risk of wire-tearing, the use of the Endowrist instruments is limited to 10 applications. Consequently, all wire-actuated instruments under development have to deal with similar challenges. Some of the instruments are described subsequently in detail to show the possibilities for the intended research. Because of the diversity of instruments, we will classify them as the ones with flexible bending segments (snake-like structures) and those with serial joints that are actuated over cable or shafts.

Starting with the latter, the Endowrist instruments of the daVinci have up to four DOF including opening and closing of the forceps that are actuated by cables (Figure 2.1a). The outer diameter of the instruments varies between 5 and 12 mm. As modular units, they can be sterilized and attached to the individual robot arms that are covered with plastic envelopes. The electrical drives of the instruments are integrated into the tip of each robot arm and they actuate the four rotatory joints in the proximal instrument housing. The MICA instruments developed by German Aerospace Center (DLR) have a cardan joint with two additional DOF and a forceps actuated by cables as well (Figure 2.1b). These instruments with 10 mm outer diameter have, furthermore, a 6 DOF force measuring sensor that is integrated into the tip between the forceps and the cardan joint. Thielmann et al. recently published the actual state of ongoing developments [84]. The drive unit for the instruments, with three motors integrated upon each other, actuates the proximal cable joints by three rods.

In a different approach, Yamashita et al. from the University of Tokyo developed a hand-held multi-slider linkage forceps (Figure 2.1c). They control, in a serial chain, four joints, two for each direction, that provides an individual bending of ±45° per joint and ±90° in each direction.

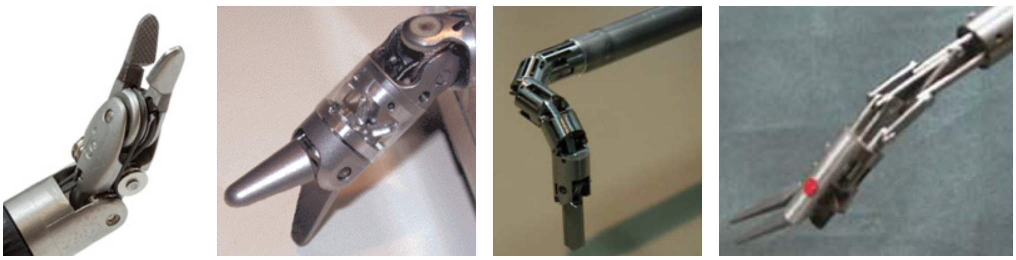

(a) Endowrist (b) MICA Instrument (c) Linkage Forceps (d) Multi DOF Forceps

Figure 2.1: Instruments with additional articulations: a) Endowrist Instrument [24] b) MICA Instrument [76] c) Hand-held multi-slider linkage forceps [63] d) Link driven multiple DOF forceps [40]

Each joint is actuated by two sliding linkages that are controlled by pulling and pushing of the specific links trough the instrument shaft. The instrument shaft can be decoupled for the sterilization of the unsterile linear drive unit. The published instrument with a 9 mm outer diameter and less than ±1 mm repeatability, provides a load capacity up to 5 N. As a further example for link driven instrument mechanisms, Arata et al. developed a four DOF instrument that comprises two DOF bending, one DOF grasping and the rotation of the instrument (Figure 2.1d). The instrument with a 10 mm diameter and $\pm 50°/70°$ bending range is attached to the drive unit housing (∅30x58mm). The maximum applied force on the instrument was 1 N. It can be assumed, that the link driven joints have a higher stiffness and load capacity in comparison to the cable driven joints. In contrast, cable driven mechanisms have a higher flexibility and working range. Furthermore, they are easy and cheap to manufacture.

The second classification of the instruments includes the snake-like bending segments. The Distal Dexterity Unit (DDU), developed by Simaan et al., is a multi-backbone, snake-like unit and has two DOFs composed of several discs and four super-elastic NiTi tubes (Figure 2.2a). All the discs are attached to the central tube, or the so called “primary backbone”. Three further tubes are used for bending which are only attached as secondary backbones to the end disc. A first prototype with a diameter of 4.2 mm can be bent more than 70° in any direction and provides more than 1 N force at the instrument tip. Breedveld et al. developed the Endo-Periscope, a bending segment for the steerable endoscope (Figure 2.2b). The first prototype of 15 mm diameter, composed of ring-springs, can be bent up to 180°. Several redesigns lead to the actual design of the Endo-Periscope III, a tentacle-inspired mechanism with a diameter of 5 mm, a bending range up to 110° and a small bending radius. The diameter of the instrument can be reduced to less than 2 mm and the hollow structure allows the introduction of a camera and the light source.

(a) DDU (b) Endo-Periscope (c) Flexible Instrument (d) Micro Manipulator

Figure 2.2: Instruments with flexible bending segments: a) Snake-Like Distal Dexterity Unit (DDU) [66] b) Endo-Periscope [75] c) Flexible Instrument Tip [65] d) Bending Micro Manipulators [61]

Instead of several assembled parts for the bending segment, Peirs et al. published a one piece NiTi bending tube with a 5 mm diameter whose joints are manufactured with wire-EDM (electro-discharge machining) (Figure 2.2c). A prototype with a length of 22.5 mm has 2 times 12 pairs of joints and provides a bending of ±90°. With the trend towards developing smaller instruments for micro surgery, Harada et al. proposed a bending micro manipulator with a 2.4 mm diameter (Figure 2.2d). The proposed bending mechanism is composed of cylindrical parts with four holes for the wires and spheres with a central hole. A laser fiber is inserted centrally through the manipulator to perform laser ablation during intrauterine surgery.

Snake-like bending segments possess higher manipulability compared to multi joint instruments [85]. A further increase of dexterity is conceivable by serial concatenation of several of these joint mechanisms into a highly flexible manipulator. To give an example, an instrument could have a bending section which is followed by one or two additional distal or proximal joints. The research group of Simaan et al. are also working on a single-port platform called IREP related to the proposed system (A detailed description follows in next chapter) [68]. They are connecting two DDU bending segments of 4.2 mm in diameter consecutively to augment the intracorporeal flexibility. Such instruments would also provide further functionalities due to the resulting redundant configuration. It should be considered, however, that the smaller the outer diameter of the instruments and the longer the bending section, the lower the achievable load capacity and stiffness will be.

2.3 Laparoscopic single-port surgery

Compared to laparoscopy, where 3-5 trocars (ports) are usually inserted at different positions in the abdomen, the single-port surgery is performed only through a single trocar. This trocar is usually introduced through the umbilicus and barely leaves cosmetically visible scars. One of the main advantages of the single-port operation technique is reducing trauma by diminishing the amount of ports. However, the additional restriction of one port calls for the introduction of all the required instruments through the same access in the abdominal cavity. There are already several terms being used for single-port surgical procedures. One of the popular names is "single-incision laparoscopic surgery". Other well known terms are "single-port access", "laparo-endoscopic single-site", "transumbilical endoscopic surgery" or "natural orifice transumbilical surgery" [86]. To date there has been no consensus reached on what the terminology for these surgical interventions should be.

2.3.1 Conventional laparoscopic single-port surgery

The single-port technique has been used to perform a variety of general surgical, gynecological and urological procedures. Although many years ago, single-port operations were carried out (e.g. appendectomy or tubal ligation), the research interest for single-port operations has increased with the development of new technological instrumentation. Most of the publications that have come out in recent years have been in the field of urology. In 2007, Raman et al. first performed a single keyhole umbilical nephrectomy using RealHand instruments (Novare Surgical) and a 5mm deflectable endoscope (Olympus). The single-port access was realized by inserting three trocars together through the umbilicus [87]. Rane et al. then accomplished a single-port access nephrectomy and other urologic procedures with the R-Port (Advanced Surgical Concepts). This single-port trocar (device) consists of three channels for the introduction of two 5mm instruments and a 10mm endoscope. These experiments were performed with conventional laparoscopic instruments so that they confirm the loss of triangulation and the handling difficulties which may be, in part, overcome by using multi-angled instruments [88].

This was followed by further clinical applications where similar trocar-like devices were used. For example, a single-port laparoscopic cholecystectomy was accomplished in a human case using the TriPort device and Roticulator instruments [89]. They report the feasibility of single-port cholecystectomy; however, they also mention that the absence of articulating instruments causes in-line viewing, which leads to the external collision of hands as the working space is small. Leblanc et al. published a review article where they consolidated single incision laparoscopic colectomy using the SILS Port (Covidien), Triport (Advanced Surgical), Uni-X (Pnavel Systems) or GelPoint (Applied Medical) and analyzed the technical aspects, feasibility and expected benefits [90]. They came to the conclusion that for experienced laparoscopic colorectal surgeons, single incision laparoscopic colectomy is safe and feasible, although technically more difficult than straight multiport laparoscopic colectomy. In gynecology there are also single-port feasibility studies that have been carried out in the last few years and they report similar outcomes due to limited technological possibilities [91].

The possibilities of the single-port surgery are limited due to the lack of appropriate instruments. Overcrowding and clashing of the instruments is an inevitable impediment to the single-port technique when standard laparoscopic instruments are used. To overcome this, bent and flexible instruments are being used to facilitate manipulation and dissection through a single incision. Actually available RealHand (Novare Surgical) and Autonomy Laparoangle (Cambridge Endo) instruments have a flexible distal segment and a shaft that can be rotated.

In contrast, there are also pre-bent instruments which are adapted to the intended operation and also allow a partial triangulation. For the visualization of the surgical field, either endoscopes with a flexible distal segment (Endoeye, Olympus or Ideal eyes, Stryker) or endoscopes with the possibility of selecting the viewing direction (Endochameleon, Storz or Eyemax, Wolf) are used [92].

All previous experimental and clinical results for manual single-port surgery point out that this technique falls far short of expectations because of the substantial conflicts between the instruments and the laparoscope that are passed through a small incision. Currently, the following limitations of single-port surgery have to be overcome: Crowding of instruments, triangulation, visualization, retraction and port related problems [93]. For example, the viewing angle during laparoscopic single-port procedures is considered as suboptimal. An off-axis visualisation, which is a primary requisite in laparoscopic surgery, is not possible. The triangulation of instruments is required for proper tissue retraction or dissection and the a loss of triangulation results in loss of depth perception. Instruments with distal bending segments allow some degree of triangulation; however, the surgeon has to cross instruments and his or her hands, therefore, which requires counterintuitive movements on the outside and substantially reduces the surgical performance.

As a new platform for single-port surgery, the company TransEterix developed the passive, sterile and one-way SPIDER system that achieves a better triangulation than laparoscopic instruments with a distal bending [94]. The system has four working channels and the outer diameter is 18 mm. Two controllable, flexible working channels are provided for the introduction of flexible instruments to the surgical site. They are actuated by a gimbal system at the proximal end which provides a motion range of 360 degrees in two directions at the distal end. Two rigid channels, superiorly and inferiorly, can accommodate an endoscope or any rigid surgical instruments with a dimension of less than 6 mm. The system has three distinct ports for insufflation or smoke evacuation. The SPIDER is gas-tight and allows the maintenance of the pneumoperitoneum through valves. Four single-port cholecystectomies were successfully completed with the TransEnterix single-port system in an average operative time of 39 min. The published article does not describe how the whole system is operated and how many people were needed for the operation of all the manual functionalities. Although the system offers better conditions than laparoscopic instruments, the working range is limited and the triangulation is not sufficient. The representation of the entire situs and exposure of the instruments as an additional limitation is not attainable by using a rigid endoscope.

The LESSCAR consortium was formed in the United States to advance the field of single-port surgery. In 2010 a consensus paper for laparoendoscopic single-site (LESS) surgery was published [95] where they conclude that LESS is the most accurate term for single-port surgery and has the potential to reduce the operative trauma of access to levels hitherto not realized. They also mention that the ability to triangulate and grasp tissues firmly enough to allow traction and countertraction for exposure and dissection is a basic requirement of surgery. Industry is pursuing solutions to many of these problems through the development of next-generation flexible, articulating, or motorized instruments. Computer-assisted robotic technologies represent possibilities that could potentially resolve the problems imposed by restricted range-of-motion and in-line work and vision. A stable, multitasking robotic platform dedicated to single-port procedures could address these issues and enhance instrument manipulation and freedom.

2.3.2 Robot systems for laparoscopic single-port surgery

The daVinci robot that is already in use in urology, was initially also utilized for single-port urologic procedures. Started in 2008, the system was used to carry out nephrectomy or reconstructive urology as hybrid NOTES interventions in animal experiments [96, 97]. One port was introduced trough the umbilicus and the others via the vagina or/and colon into the abdomen. These studies pointed out that even if the robotic system currently offers many potential advantages, technical difficulties such as robotic arm collision, limited triangulation and counterintuitive camera angles still need to be overcome.

Based on these experiences with a percutaneous transvesical approach for simple prostatectomy, Desai et al. assessed the technical feasibility of performing transvesical robotic radical prostatectomy in a cadaver model with the daVinci-S robot system [98]. They inserted a four-lumen Quadport (Olympus) single-port device percutaneously through a 3cm skin incision into the bladder. One of the main technical difficulties of this single-port procedure was the overcrowding and clashing of the instruments or arms. Due to the limited flexibility and working range, the daVinci system is not suitable to perform difficult procedures such as lymph node dissection. The authors pointed out that a robotic platform, specifically designed for single-port surgery, might overcome existing difficulties. In 2008, Kaouk et al. reported the first successful series of single-port robotic procedures in humans, including radical prostatectomy, dismembered pyeloplasty and radical nephrectomy [99]. A 12mm telescope and 5mm grasper were introduced through the multichannel R-Port, while an additional 5mm port was introduced through the same 2cm umbilical incision alongside the multichannel port to introduce the second daVinci instrument. In these experiments an improved facility for intracorporeal dissecting and suturing due to robotic instrument articulation and stability was noted. The same group reported further clinical applications such as partial or radical nephrectomies using the daVinci system and concluded that similar technological problems have to be overcome for an acceptable robotic single-port surgery [100, 101].

The technical limitations such as clashing instruments and limited working range due to the bulky construction of the daVinci robot, initiated two animal, single-port experiments that were carried out with the ViKY camera guidance system (EndoControl, France). The compact ViKY is controlled by voice or foot pedal and provides enough space for the manipulation of the manually controlled instruments with articulations and rotating tips [102, 103]. The authors conclude that the combination of a robotic telescope holder and articulated instruments operated by one surgeon for single-port surgery is feasible. Although ViKY affords an improved range of motion, it will not overcome all the limitations of single-port surgery.

Currently, an attempt is being made to improve the previous single-port methods with the daVinci robot through technical optimization, since no alternative, specifically for single-port, exists. To ensure a certain triangulation for the single-port technique, the instruments of existing systems or methods should be crossed at the invariant point [104]. However, working with manual instruments and crossed hands is a burden for the surgeon that could be overcome with the use of appropriate robots. To solve the challenges related to the arrangement of the instruments, Joseph et al. have proposed the so-called “chopstick” surgery technique using the daVinci robot arms [105]. The chopstick arrangement crosses the instruments at the abdominal wall so that the right instrument is on the left side of the target and the left instrument on the right. This could prevent a collision of the arms outside the body. At the console, the surgeon controls, in an intuitive manner, the “left” instrument using the right hand and vice versa. The authors report an increased dexterity for the surgeons and global performance through significantly improved performance times and the elimination of instrument collision by using the “chopstick” method. It should also be mentioned that Intuitive Surgical is currently working on developing a new single-port system as shown on figure 2.3b, which they have claimed in a patent [106]. However, there are not yet any further details or publication related to this.

The research group of Simaan et al. at the University of Columbia, USA are currently developing a single-port surgical system called IREP (Figure 2.3a), that comes close to the proposed developments [68]. Initially, the system was designed for laryngeal surgery [66] and the research regarding this application is still in progress [77]. Two bending segments of 4.2

mm in diameter, a distal DDU of 12 mm in length and a proximal DDU of 23 mm in length, are unified to one manipulator which is guided by a parallel robot and the complete dual-arm robotic slave system has 20 actuated joints. The daVinci master interface is used to control the slave manipulators. Similarly, the IREP system is designed for laparoscopic surgery. Two aforementioned manipulators of 6.4 mm in diameter and a stereo optic of 6.5 mm are combined together to a unit which has a 15 mm outer diameter in a folded state. Each snake-like manipulator has two further DOF that are implemented by a parallelogram mechanism and the rotation of the forceps is realized at the tool tip. Design alternatives of the overall system with 17 DOF [68] and recently the kinematic alternatives for the manipulators have already been presented [107]. The required workspace is defined to be more than 50 × 50 × 50 mm and the working load is 2 N. The detailed specification of the IREP system as well as the suturing and performance evaluations are presented in the paper [107].

(a) IREP system

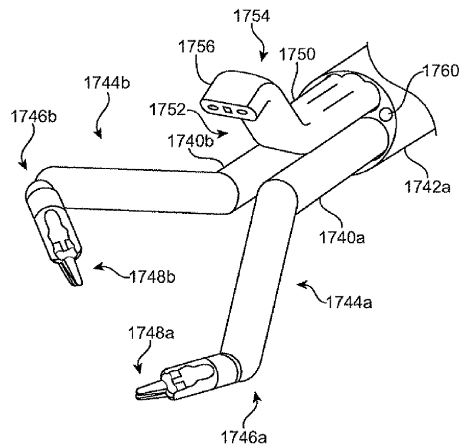

(b) daVinci single-port system

Figure 2.3: a) Insertable Robotic Effector Platform (IREP) for Single-Port Access (SPA) Surgery [68] b) Concept of the daVinci single-port system as claimed in the patent [106] (Intuitive Surgical, USA)

A further single-port system called SPRINT robotic system is being developed by the research group of Dario et al. within the ARAKNES project [108]. The design of the 6 DOF manipulator and preliminary tests were published for this system. The single-port laparoscopy bimanual robot consists of two manipulators, that are inserted one after the other through a 30 mm umbilical access port. The four distal joints of the manipulator are actuated by on-board motors, while the two proximal DOFs of the shoulder are actuated by external motors. Three motors integrated in the forearm provide the actuation of the wrist joints with a peculiar differential mechanism. Performance tests of the first prototype of the manipulator with a 23 mm diameter and a length of 142 mm resulted in a force of 5 N and linear speed of 1 m/s. A position error of 8 mm was measured at the end-effector by using magnetic tracing sensors.

2.4 Single-port surgery through natural orifices

The interest in Natural Orifice Transluminal Endoscopic Surgery (NOTES) started its upswing in the USA where it was supported by much funding. In 2005, the ASGE/SAGES working group on natural orifice transluminal endoscopic surgery was established and published the NOTES white paper [109]. This document includes inter alia the challenges like surgical access to the peritoneal cavity, the closure of the access, the mechatronic multitasking platform and spatial orientation and navigation.

The intention of NOTES is the consolidation of laparoscopic surgery and gastroenterologic endoscopic interventions, to create an access to the peritoneum through a natural orifice and perform surgical procedures as in laparoscopy. So far, four different access routes have been used to perform NOTES surgery: the stomach, colon, bladder, the vagina for female patients and the combination of several of these approaches (Figure 2.4). Every single access route has its advantages and disadvantages. As a result, none of them could be proven as ideal [110]. With the tansgastric approach, accessibility to the upper abdomen is limited, whereas the transvaginal access is only available for about half of the patients. The transcolonic access provides an easy and short access route to the abdominal cavity, however, it has the greatest disadvantage of a high risk of contamination. We developed an instrumentation set for the so-called “innovative, safe and sterile sigmoid access” (ISSA) approach [111, 112], that was also used for the evaluation of the proposed single-port system [113].

2.4.1 Current state and manual platforms for NOTES

A variety of NOTES interventions with different approaches have been carried out and published so far [114, 115]. Most of them are usually performed by modified or standard endoscopes that are controlled manually [116, 117]. Due to the lack of a necessary platform, these interventions are accomplished by the assistance of additional instruments introduced either through an access in the abdomen or through a further transluminal access. Hence, such operations have been performed to date by several surgeons and assistants revealing additional difficulties like communication and coordination between the surgeons or the allocation of the tasks [118].

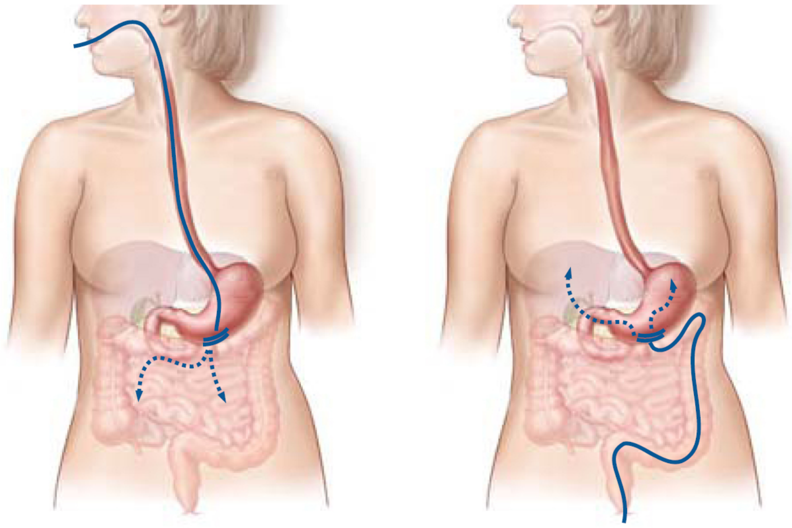

Figure 2.4: Possible access routes for NOTES interventions: Transgastric access is illustrated at left and the transrectal at right (MITI, Klinikum rechts der Isar, Germany).

With the exception of the vaginal access, no transluminal access is clinically mature yet [119, 120]. There are still too many unsolved problems which impair the further progress of NOTES interventions. Among others, one serious problem is the limited intraoperative performance (limited flexibility and working range, no triangulation, difficult handling etc.). There is a wide consensus that these problems will be overcome as soon as innovative mechatronic platforms are available. Some solutions have already been suggested, that have been already published in summary by us in [121]. These systems are evidently not yet ready for routine clinical use and their current impact is low. There are other publications which also present an overview of some of the existing systems [122, 123]. Subsequently, we will give a brief description of some of these important platforms which definitely show the trend of development.

"Cobra" and "Transport" (USGI Medical, USA)

Both of these multifunctional platforms were developed by USGI Medical in cooperation with the research group of L.L. Swanstrom from Legacy Health, USA. The Cobra device relies on the structure of flexible endoscopes and includes two independent manipulators and a flexible optic which are introduced transluminally through the same platform tube in the abdominal cavity [124]. The shaft can be rigidly positioned at the desired place using shapelock technology. This provides the transmission of the required forces over the two manipulators to perform the required manipulations.

The Incisionless Operating Platform (IOP) Transport (Figure 2.5a) is a multi-lumen operation platform similar to a multi-channel endoscope [125, 126]. Like the Cobra system, the shaft of the Transport can be interlocked in any position using shapelock technology. Important features of the system are the four working channels (7 / 6 and 2 × 4 mm), an insufflation channel and the flexion of the tip in four directions. A flexible endoscope is inserted through the 6mm channel for visualization. Conventional instruments such as needle-knife or clip pliers and sturdy tools in the form of special grippers or suture instruments can be introduced through the three working channels. After the stiffening of the shaft in the desired position, the surgical operation can be carried out by steering the individual instruments.

Both platforms offer advantages compared to conventional endoscopes. The required flexibility is, however, not enough to perform sophisticated manipulations. Furthermore, the triangulation of the transport platform is limited due to the parallel alignment of the instrument and optical axis. These platforms are being continuously enhanced, optimized and evaluated.

(a) IOP Transport (b) Endo Samurai (c) DDES (d) Anubis Scope

Figure 2.5: Flexible platforms for transluminal surgery: a) Incisionless Operating Platform Transport (USGI Medical, USA) [126] b) Endo-Samurai (Olympus, Japan) [127] c) Direct Drive Endoscopic System (Boston Scientific, USA) [123] d) Anubis Scope (Karl-Storz, Germany) [128]

"R-Scope" and "Endo-Samurai" (Olympus, Japan)

Olympus, in Japan, are also developing new systems such as the R-Scope endoscope and the Endo-Samurai platform in cooperation with the research group of L.L. Swanstrom to perform transluminal surgery. The R-Scope with a 14.3 mm diameter is a modified form of a double channel endoscope for extended transluminal resections and NOTES [129]. This endoscope has two distal bending segments and can adopt an S-shape that provides a higher manipulability. After blocking both bendings in the desired position, fine retraction, dissection and manipulation can be performed with the two 2.8 mm instruments. Each instrument can be pivoted in a plane perpendicular to the other. The additional degrees of freedom, which are controlled manually, make it difficult to use and it can hardly be controlled by a single surgeon.

The Endo-Samurai platform (Figure 2.5b) is structurally similar to the Cobra system [127]. Both flexible manipulator arms are rigidly fixed to the distal end of the carrier tube and allow a small triangulation of the instruments. Apart from the two instrument channels through both manipulators, the system has a further instrument channel for the introduction of a third instrument. The optic of the Endo-Samurai is rigidly integrated in the flexible carrier tube, so that the view on the instruments is limited, similar to conventional endoscopy. An independent examination of the surgical field from different perspectives is, therefore, not possible.

"Direct Drive Endoscopic System" (Boston Scientific, USA)

Another type of support system for transluminal surgery is the Direct Drive Endoscopic System (DDES) (Figure 2.5c) developed by Boston Scientific in cooperation with the research group of C.C. Thompson [123]. The DDES consists of three main elements: 1) a flexible guiding tube with three channels (6 mm visualization channel and two 4 mm instrument channels), 2) a set of 4 mm instruments and 3) a platform rail. At the surgical site, the distal part of the DDES guiding tube allows movements in the horizontal and vertical plane similar to an endoscope. The proximal part is mounted on the stable guiding rail. The instruments, that slide on individual rails, have control handles so that the hand movements are transmitted to the instrument tips with 5 DOF without changing the visual perspective.

"Anubis Scope" (Karl-Storz, Germany)

In Germany, Karl-Storz is developing the innovative Anubis Scope (Figure 2.5d) that is characterized by the distal tip, in cooperation with the research group of J. Marescaux [128]. Two half-shells in the folded state facilitate the penetration of the abdominal cavity. Within the abdominal cavity, the two flaps are unfolded and press the adjacent organs aside. Simultaneously, they carry the instruments from the inside out, so that a certain triangulation is afforded. Flexible articulating instruments are available that provide almost all the functionalities of conventional laparoscopic instruments. The optic is rigidly integrated in the flexible carrier tube similar to the Endo-Samurai platform, that possesses the same drawbacks of visualization. An interlocking mechanism, similar to the Trasport platform, is not provided.

2.4.2 Robot systems for NOTES interventions

The aforementioned single-port platforms pushed by the industry are application oriented and manually operated systems. There are also research activities accomplished parallel to these developments, where fully flexible robots are being developed for NOTES interventions. Subsequently, some of these systems and their functionalities will be briefly described to give an overview of the possible techniques.

Initial approaches of multifunctional transluminal robots have been realized by unifying a conventional endoscope and two flexible instruments with distal articulation in a carrier tube. One of these first solutions was published by Hattori et al., who developed a robot system with two forceps attached distally on both sides of an endoscope [130]. Each forceps is controlled by three wires guided through a 3.5 mm elastic metal tube. Additionally, a magnetic tracking sensor is attached to the tip for the navigation of the robot. The endoscope is operated manually by a surgeon and the forceps are controlled by a further surgeon on a master console.

Similar to the slave manipulator above, a robotic system for transluminal surgery (Figure 2.6a) with a specific master controller has been developed by Phee et al. [131]. The first prototype of this system includes two 5 DOF manipulators, that are attached distally to an ordinary endoscope and controlled by tendon-sheath mechanism. The articulation of the slave manipulator is modeled similar to the human arm and controlled by a 6 DOF master console, where the motion of the shoulder, elbow and wrist of the arms are tracked by different sensors. In a second prototype, with 9 DOF in total and a 22 mm external diameter, the articulated length of the manipulators is reduced to 42 mm, which affords forces up to 3 N. The authors conclude that the biggest problem is the non-linear characteristic of the tendon-sheath mechanism due to the friction between the tendon and the sheath.

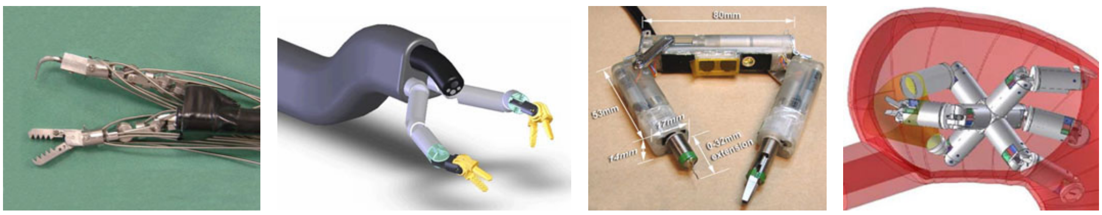

(a) Transluminal robot (b) ViaCath robot (c) NOTES robot (d) Modular robot

Figure 2.6: Design of transluminal robots: a) Transluminal endoscopic robot [131] b) ViaCath endoluminal robot [132] c) Miniature NOTES robot [133] d) Reconfigurable modular endoluminal robot [134]

The ViaCath robot system (Figure 2.6b), which is in concept similar to the DDES, offers more functionalities than the aforementioned systems [132]. In a first generation, two 7 DOF instruments of 5 mm in diameter were developed and introduced alongside of a standard gastroscope. The instruments are controlled using the Laprotek surgeon console. Two bending sections of the instruments (10/25 mm length) enables a S-curve for higher flexibility. However, these instruments produce only 0.5 N lateral force so that a new system is being developed. The outlined platform has a steerable overtube of 19 mm diameter and the instruments of 7.2 mm diameter provides 9 DOF.

In a different approach Lehman et al. developed a miniature robot (Figure 2.6c), that is inserted as a whole through an overtube into the abdominal cavity [133]. The robot consist of two prismatic arms, each connected to the central body by a rotational shoulder joint. After introduction, the robot with the embedded magnets is attached to the interior abdominal wall with magnets housed in the external magnetic handle. Gross repositioning of the robot is realized by the external handle. A stereo camera and motor drives are integrated into the body, and the electrical cable is fed through the overtube outward. This robot has limited flexibility and the positioning in the body is restricted to the surface of the abdominal wall.

A further miniature robot that is introduced as a whole into the body, is the wireless reconfigurable modular robot (Figure 2.6d) proposed by Harada et al. [134]. The robot modules are ingested and assembled in the stomach. Each module with 2 DOF ($\pm 90°$ bending and $360°$ rotation) measures 15.4 mm in diameter and 36.5 mm in length. The integrated wireless control board provides control from the outside. Although this approach is very innovative, extended evaluations are required to demonstrate its feasability in real environments.

Chapter 3

Surgical Prerequisites and Theoretical Approach

The goal in this chapter is the examination of the single-port surgery from the medical and technical point of view, the identification of the requirements and the derivation of a concept. The possibilities and potentials from the medical point of view are based on the accumulated knowledge from the numerous experimental NOTES interventions that were performed by the physicians at the Klinikum rechts der Isar. The idea of the shoulder girdle - arm - hand principle was inspired by these experiences. Also, the work-flow of a manual and robotic single-port cholecystectomy, as well as the technical aspects of the single-port surgery, resulted from the accomplished interventions. Moreover, the requirements for a robotic platform were determined in close cooperation with the physicians. Finally, our concept of the single-port platform was developed according to these requirements and differentiated from the existing works.

3.1 Single-port surgery from the medical point of view

Minimization of trauma and the investigation of new fields of indication are two topics that are currently being focused on for the enhancement of minimally invasive surgery. In general, the accomplishment of laparoscopic surgery is bound to so-called "ports" (at least three and for some indications even more) through the abdominal wall that significantly restrict the flexibility of the instruments. Limited flexibility of rigid instruments, restricted working space and lack of force-feedback or navigation are some of the obstacles that prevent the application of minimally invasive surgery in further fields of indication in particularily complex tumor surgery. Computer assisted surgery and master-slave systems are some of the approaches used in order to overcome the existing limitations of laparoscopic surgery.

On the other hand, the predominantly conservative or diagnostically oriented gastroenterology is gaining increasing significance in the accomplishment of interventional therapy. The removal of small specimens with the biopsy forceps, the removal of polyps/tumors with loops or the endoscopic mucosa resection are some possible interventions that can be performed by using flexible endoscopes. Due to the technical limitations of the conventional endoscopes, these interventions are limited to only small areas of less than 2 cm. Moreover, wide experience and skills are necessary to perform these operations with the existing opportunities.

An established method to expand the possibilities of minimally invasive surgery and to reduce trauma to the patient, is the accomplishment of combined laparoscopic-endoscopic interventions in which interdisciplinary skills are required [135, 136]. This includes, for example, the resection of colorectal polyps and gastric wedge resections. Such interdisciplinary interventions stimulated the research of new surgical approaches such as the natural orifice transluminal endoscopic surgery (NOTES). Up to now, a broad range of NOTES interventions have been carried out in order to identify the possibilities and limitations. Disenchantment came very early. Using the existing technical possibilities, these interventions can only be realized in a very limited scope. New, flexible platforms must be developed to accomplish such innovative approaches. As illustrated in Figure 3.1, both the skills of a laparoscopic surgeon as well as that

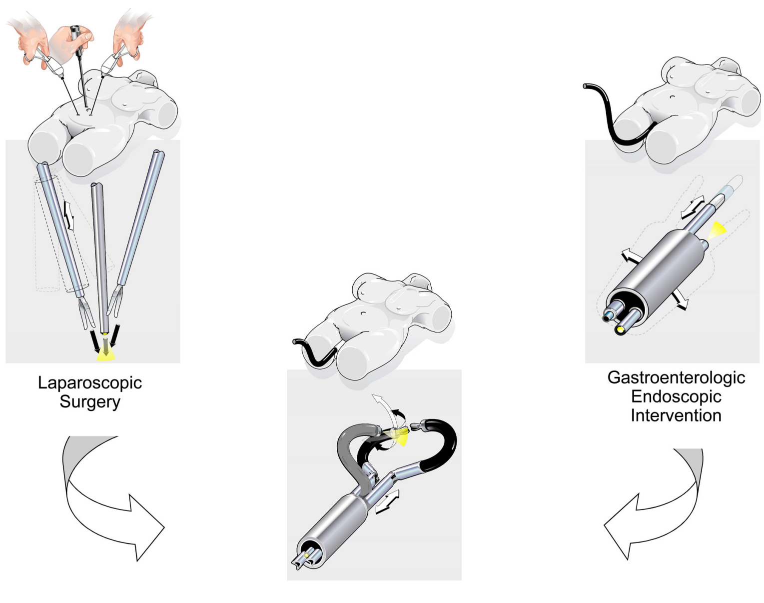

Figure 3.1: Merging laproscopic surgery and gastroenterology to develop an ubiquitous surgical platform.

of an endoscopist should be combined in one system that offers enough dexterity to perform the intended transluminal interventions.

The exciting possibility of transluminal surgery with a high potential of trauma minimization and the ongoing technological developments have also incited the approach of laparoscopic single-port surgery. At first, such interventions were performed by the introduction of all required laparoscopic instruments through a single incision. The limited flexibility of the conventional rigid instruments, however, calls for new designs that include additional distal articulations. New single-port access devices as well as articulated or bended laparoscopic instruments are currently used products for single-port interventions, which are provided by the industry. Similar to transluminal surgery, it is obvious that the full potential of laparoscopic single-port surgery can only be exploited if new appropriate platforms are developed.

3.1.1 Shoulder girdle - arm - hand principle

When performing a "manual" single-port intervention in which all conventional instruments are introduced through the same port, the ability of the surgeon is drastically restricted. The parallel adjacent instruments limit the workspace of the surgeon so that they cross the instruments in order to have some more space for motion. However, this is only feasible if the trocar channels are deflectable and the instruments provide a certain amount of flexibility (distal articulations). By doing so, the surgeon takes on a further burden when operating with crossed instruments/hands, which is counterintuitive and not simple to handle. As schematically shown on Figure 3.2a, a robot could manage the crossing of the instruments in a manner

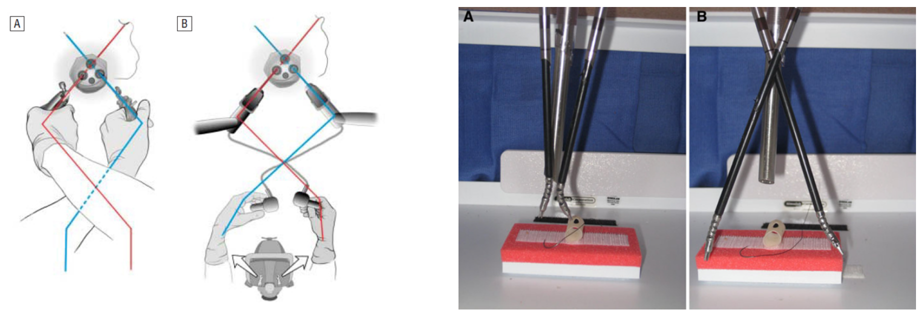

(a) Operation with crossed instruments (b) Configurations of the daVinci instruments

Figure 3.2: Current approaches for single-port surgery: a) Comparison of the conventional (A) and robotic (B) single-port surgery b) Standard (A) and chopstick setup (B) of the daVinci instruments [104, 105]

so that the surgeon controls with the left hand the right manipulator, which corresponds to the left instrument in the patient's body.

Joseph et al. performed dexterity evaluations with daVinci instruments in crossed configuration ("chopstick" surgery) as shown on Figure 3.2b [105]. They report that the operation performed with the aid of a robot with crossed instruments improves the surgeon's dexterity, and the external collisions of the arms are reduced. Furthermore, they point out that the instruments should only be crossed below the abdominal wall in order to prevent port or camera collision. Although this study presents enhancements relative to manual single-port surgeries, there are still problems that must be solved to satisfy all requirements of the surgeons. The workspace is still too small and restricted in such surgeries as in the conventional laparoscopy. Vigorous movement of the instruments at the incision site causes lateral stress, and the collision of the instruments and/or arms can not always be prevented. A reorientation, the rotation of all instruments including the telescope around the incision axis, is not easy to achieve. Furthermore, the representable range with the telescope is still limited and a volatile positioning or an ill-defined crossing point of the instruments demands an appropriate referencing.

As long as these drawbacks are not addressed by new, adequate telemanipulators (robots), the option of performing open surgery, where all these restrictions do not exist, is contemplated more often than expected. The main challenge still lies in the development of new, sophisticated systems to overcome the existing barriers. As already described in the vision, our intention is, literally spoken, to bring the surgeon's head, shoulders and arms into the abdominal cavity in order to regain the same flexibility as in open surgery. Figure 3.3 illustrates schematically the

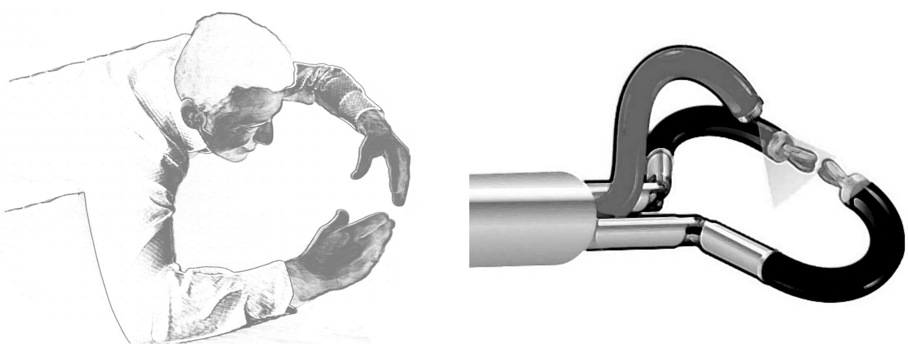

(a) Dexterity of surgeons upper body

(b) Corresponding platform design

Figure 3.3: Design of a platform that emulates the skills of the surgeons, as if his upper body could be introduced through a small incision into the abdominal cavity.

intended dexterity of the surgeon in the abdominal cavity and the corresponding implementation of a platform which meets the requirements.

Two manipulators and a telescope are integrated parallel to each other in an insert (emulating the torso) as illustrated in Figure 3.3b. Similar to the shoulder girdle, the system provides appropriate degrees of freedom to ensure the motion of the manipulators in the insert. Each manipulator, which corresponds to one arm of the body, has enough flexibility to manipulate the instruments at the tip. This is realized by a shoulder, elbow and wrist articulation in a serial configuration. The wrist articulation comprises three degrees of freedom for the orientation of the instrument, which represents the hand of the surgeon. Both manipulators are visualized by an articulated telescope with at least three distal degrees of freedom in the entire workspace. As one of the greatest advantages, the platform, including both manipulators and the telescope, can be manipulated by an external guiding system in all four quadrants of the abdomen. Thereby, the potential of surgical interventions can be significantly expanded.

3.1.2 Description of the surgical work-flow of a single-port procedure

Conventional, manual single-port cholecystectomy

There are several devices and approaches proposed so far to perform diverse single-port procedures. However, these are by far not standardized like the conventional laparoscopic cholecystectomy. Currently, most efforts are set on the development of new trocars with multiple channels and manual instruments with one or two distal articulations that provide, in the short-term, the accomplishment of clinical single-port interventions. A review paper that includes the single-port cholecystectomy, carried out through the abdominal wall, was published by Chamberlain et al. [137]. They summarize all technical variants which are available for the gallbladder resection. A variety of different trocars and new curved or articulated instruments are proposed by the industry which are facilitating the performance of the operations [128].

Certain prerequisites and sequences in all these performed single-port cholecystectomies are equal or similar, so that a rough process can be described. In the first step, the access through the abdomen is created (usually through the navel) and the single-port trocar is introduced into the body. The pneumoperitoneum is established and maintained through a trocar channel. Thereafter, a (semi-rigid) telescope is inserted through one channel and the trocar is positioned towards the gallbladder after observing the intra-abdominal situs. The required (curved, articulated) instruments are inserted through two further channels. The dissection of the gallbladder is then accomplished similar to the conventional laparoscopy, except that the instruments are introduced through the same trocar. After a thorough hemostasis, the resected gallbladder is held with an instrument and recovered together with the trocar. Finally, the intervention is completed by suturing the access.

Some of the important aspects that must be considered in all procedures are: Maintaining the gas-tightness by using new sealing mechanisms, channels with interchangeable diameters providing the introduction of various instruments, ability to triangulate and grasp tissues firmly enough to allow traction and counter-traction, reduction of repetitive instrument exchange by providing new tools such as staples, clips and sutures for hemostasis and the conversion to open surgery in case of unforeseen emergencies. The manually operated and disposable SPIDER platform, developed by TransEnterix, offers advantages such as the device insertion, ease of flexible instrument exchange, and triangulation [138]. However, there are still unsatisfactory properties such as instrument retraction and lack of depth control during dissection.

Robotic single-port cholecystectomy

The surgical procedure of the robotic single-port gallbladder resection proceeds, in general, similar to the manual single-port cholecystectomy. The robotic intervention includes in additional the assembly and disassembly of the system and the integration of the required resources (see Figure 3.5). The robot system (guiding system and single-port platform) has to be assembled before the surgical procedure begins. First, as in the conventional procedure, the access to the abdominal cavity should be created to introduce, afterwards, the specifically designed trocar for the platform into the body. After establishing the pneumoperitoneum, the single-port plat-

Figure 3.4: Transumblical gallbladder resection using the highly versatile single port system.

form is introduced, together with the manipulators and the telescope, through the trocar into the body. The manipulators and the telescope have a folded-straight configuration during the introduction and are unfolded in the abdominal cavity as shown on Figure 3.4. One of the important points to be considered, thereby, is the prevention of injury to the organs during the insertion phase! Therefore, the telescope should provide the view during introduction.

In the next step, the platform is steered to the gallbladder by the guiding system. After positioning the platform at the desired place, the manipulators with the introduced instruments can be operated to resect the gallbladder. Necessary instruments are exchanged by a tool changer according to the requirements. After resection of the gallbladder and hemostasis, the platform with the manipulators and the telescope are guided to the initial position. By holding the gallbladder with an instrument and keeping the folded-straight configuration, the platform is pulled out of the body. In the final step, the system is disassembled after suturing the access.

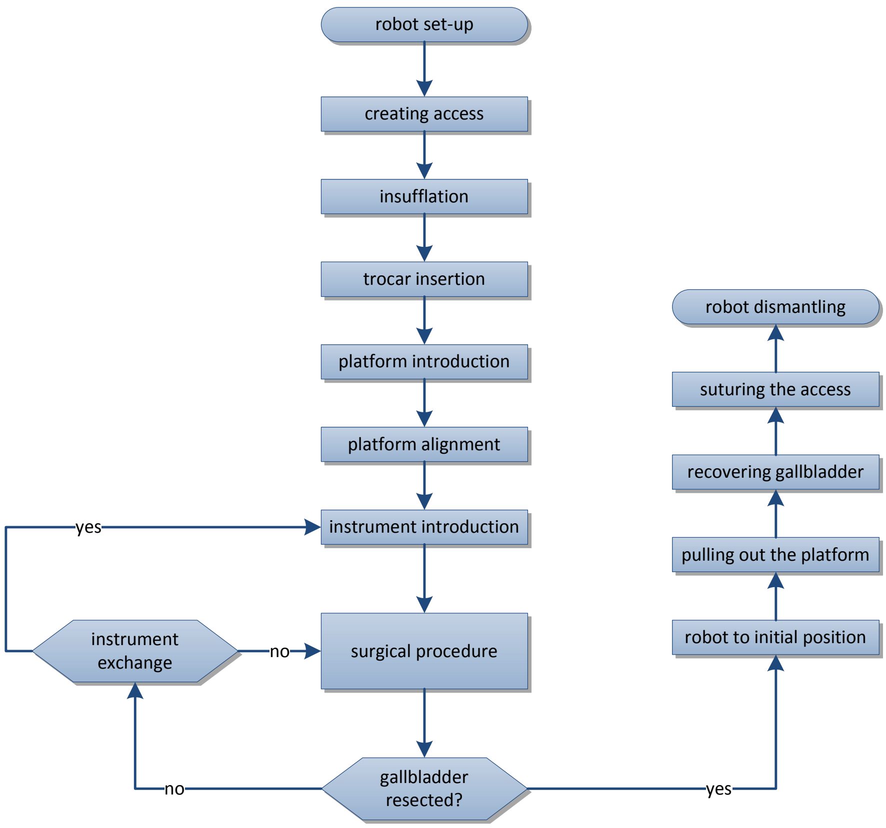

Figure 3.5: Surgical procedure of the single-port robotic gallbladder resection.

3.2 Technical aspects and the impact of research and development

Limited technical possibilities hinder the accomplishment of the new, demanding surgical procedures such as single-port or transluminal surgery. This was already pointed out by the ASGE/SAGES working group on NOTES, who published the white paper [109]. Being aware that single-port or NOTES operations depend even more on technological support systems (robots), a consensus document on robotic surgery was published by the SAGES-MIRA group [139]. A further consensus statement for laparoendoscopic single-port surgery was recently published by Gill et al. [95]. Based on these publications and our own experience, the following technical aspects for single-port surgery, pointing out the impact of research and development, have been worked out. This has already been partially published in [140].

Access to the peritoneal cavity

The access for NOTES intervention is more challenging in comparison to laparoscopic single-port surgery, which is usually performed through the umbilicus. Due to the bigger size of the entrance, new access devices should be developed for single-port surgery that provide the introduction of the required instruments and prevent air leakage by using novel sealing mechanisms. The instruments for the creation of a NOTES access are far more demanding. This applies particularly to the transgastric approach with the long access route up to the stomach. The transcolonic, transvaginal and transvesical approaches offer the advantage of a short and easy access path, however, they have the main disadvantages of the contamination for transcolonic access, the small diameter for transvesical access and the restricted applicability to female patients for transvaginal access. It is very likely that the access must be chosen according to the specific procedure. Although some devices have already been proposed, development of adequate access instrumentation for the individual approaches remains one of the main challenges.

Mechatronic support platform

Conventional instruments and/or flexible endoscopes are not suitable for single-port procedures. The existing master-slave systems also do not offer potential support for the accomplishment of such demanding surgeries. A single-port system should provide access through only one port, where all the instruments are introduced (natural orifice for NOTES and e.g. transumblical access for laparoscopy). Necessarily, the outside diameter of a system that meets the appropriate requirements must not be much larger than that of a flexible endoscope. The realization of the triangulation is essential, so that traction and counter-traction can be exerted with opposed end-effectors. Therefore, at least two instruments and the optics must provide independent manipulations. Furthermore, the integrated “intelligent” instruments should comprise “smart sensing” capabilities to provide the surgeon with information such as forces, position and tissue properties. The following points can be considered as design criteria for such systems: Miniaturization, high flexibility, intuitive manipulation, free navigability, embedded into an overall control system and partial autonomy.

The establishment of an intuitive man-machine interface plays a critical role. Two interfaces should be considered here: The interface between the anatomy and the machine and the interface between the machine and the operator. Since the surgeon can only handle two instruments or a telescope at the same time, we also need an intelligent approach to change the connection between the interface and the end-effectors dynamically at runtime of the system. Instruments which are not controlled by the surgeon could, for example, take over partial autonomous tasks such as force-controlled pulling or holding a position. If the intuitive, intelligent platform has brought the optics and the instruments into the ideal position, the synergistic interaction of at least two surgical tools (effectors) in the visual range of the camera is required. The system should provide more complex manipulations in order to realize the single-port concept in a clinical environment. Probably this is only achievable if the end-effectors have some degree of autonomous capabilities.

Spatial orientation and navigation

Endoscopists are accustomed to working in-line with their cameras and light sources and laparoscopic surgeons are aware of the problems that arise when working beyond the camera axis. During single-port or NOTES interventions, physicians are confronted with both of these challenges. New single-port devices with a distally articulated telescope, such as proposed here, provide manipulations beyond the camera axis. However, by bending and/or rotating the camera, the surgeon loses the spatial orientation. For example, in retroflexed orientation, the image is upside-down and it is impossible for the surgeon to perform the procedure without technical help. As a result, auxiliary systems are required which offer, for example, a real-time anatomical horizon adjustment. A continuous description of the system configuration using different sensor modalities and navigation is just as important in order to detect, for example, a retroflexed/inversed configuration or loop formation.

Integrated operating room

The more complex the specific working environment becomes, the more important an integrated system control is, i.e. a central intelligent control entity. A reasonable, common use of different technological modules presupposes coercively an integrated network. A target/actual-adjustment can be achieved on the basis of continuous, real-time status information from the individual sensors integrated in the operating room. The constant workflow analysis allows not only the specific prediction of other necessary steps (important for the logistics), but also things like warnings to the surgical team and, in an emergency, the independent alerting of control entities. Naturally, the "intelligent operating room" with the property of the "situation awareness" should afford a situation-suitable provision of preoperative information and facilitate necessary communication to the outside (such as the entering of information into a hospital information system). The automated process protocol (i.e. operation protocol) is a welcome side aspect inter alia for quality management.

Training and simulation

As pointed out by the SAGES-MIRA consensus group, for maintaining the highest level of patient care, it should be ensured that surgeons are adequately trained in the use of surgical robots before applying them in a clinical setting [139]. The following two aspects are mentioned therefore: At first, the surgeon must have a knowledge base and a practical working familiarity with these complex devices before clinical use (technical training and capability), and, thereafter, as a second training aspect, the robot must be used for specific operations. Simulation and training systems, therefore, play a central role in robotics surgery.

However, even relatively high-tech procedures such as laparoscopic surgery are still not satisfactorily simulated in virtual reality. This applies even more to single-port procedures, in which the conditions for intervention are much more dynamic than in the minimally invasive abdominal surgery. The requirements for an ideal training unit are versatile and some important aspects of them are: 1) realistic anatomy and tissue coloring, 2) authentic haptics, 3) suitability for laparoscopy, NOTES and hybrid procedures, 4) the provision of different access routes to the operating field and 5) suitability for intra-operative navigation. As a special feature of transluminal or single-port surgery, the cognitive ability and manual skills of an endoscopist and, simultaneously, those of an experienced laparoscopic surgeon, are required. Until now, this training necessity and opportunities have only been met by animal experiments.

3.3 Determination of the requirements

3.3.1 Design specifications for the overall system

Compared to current robot systems, a considerable amount of work has to be done for applicability and acceptance of an operational platform for single port surgery. The specifications for the system development were made on the basis of our own experience, the literature survey and the requirements that were posed by the surgeons. The following requirements can be deduced from the ongoing hardware developments:

General specification for the system components

- **Instruments:** Multifunctional and flexible end-effectors introduced passively through the manipulators into the body and provide one degree of freedom, similar to endoscopic instruments, to manipulate or dissect tissue. A multi functional tool changer, charged with several instruments (e.g. grasper, scissors, etc.) at the periphery, permits the exchange of the instruments within seconds.
- **Manipulators:** Miniaturized and precisely controllable actuators integrated into a long and flexible carrier system with a highly flexible mechanism i.e. a multiplicity of degrees of freedom. The kinematic of the manipulator should enable intuitive manipulations comparable to a human arm.
- **Carrier system:** It comprises two main manipulators for positioning the instruments and a highly flexible optic (telescope). The carrier system provides, as a unit, the independent control of the manipulators and the telescope. A flexible structure and a deflectable tip will allow the introduction and guiding of the system through natural orifices.
- **Guiding system:** A small, compact robot system to guide the carrier system in its available degrees of freedom without obstructing the operating team and allowing a simple and intuitive control.
- **Interface:** A wide range of sensor modalities (force, position, optic, etc.) are required for the registration of relevant parameters between support system and situs. A combination of a display for information presentation (visual, tactile, auditory, etc.) and sensors to detect the intended actions of the operator are required between support system and surgeon.

These integrated individual subsystems are not master-slave components with a direct connection to the operator interface. They provide equipment, which is controllable over intermediary planning entities so that the joint movement of the manipulators, carrier and guiding system results in a trajectory of the surgeon's intended movements. It is also self-evident that the subsystems have to be integrated so that they permit seamless transition into the working environment of the operating room and farther to be adapted on a workflow management system.

Specific requirements defined by surgeons

We intend to use electromagnetic position sensors for the tracking of the instruments. These sensors will be integrated into each manipulator and the platform to provide adequate control and navigation. As an additional specification, the surgeon may consider the option of using the single-port platform during imaging procedures such as MRI or CT. These additional specifications demand the placement of the motor drives at the periphery. The distance between the active actuation unit and the passive single-port platform near the patient was specified to be at least 2 m. Furthermore, the manipulators should enable enough flexibility to manage all the intended manipulations. Therefore, the instruments, including the opening and closing of the forceps, must have at least 7 DOF, to ensure the positioning in space.

Another decisive requirement that should be taken into account is the desired use of existing flexible endoscopic instruments for the single-port operations. These instruments, stored in exchangeable modular magazines, are introduced at the periphery by an automated tool changer. Consequently, the manipulators should have a hollow structure that enables the introduction of the required instruments within seconds. Besides the controllable opening and closing function of the forceps, the rotation of the instrument should be integrated either in the tool changer or at the manipulator tip.

The cholecystectomy, a standardized laparoscopic operation, was chosen as criterion for the definition of the surgical requirements. The achievable workspace of the instruments was defined in regard to an average gallbladder size: X: $\pm$50mm (Horizontal), Y: $\pm$30mm (Vertical) and Z: $\pm$30mm (In/Out). Depending on the surgical task, a force of at least 2 N should be provided at the instrument tip to achieve tissue manipulation [141]. The surgeons have also defined the preferred values of a speed higher than 50 mm/s, an accuracy better than 2 mm and the final outer diameter of less than 22 mm (for the complete flexible system that can also be applied for NOTES).

3.3.2 Design considerations and corresponding restrictions

An intuitive manipulation of the tissue demands an opposed configuration of the manipulators so that traction and counter-traction can be exerted. This calls for manipulators with high flexibility and a swiveling mechanism to access the target laterally. It has already been demonstrated that continuous bending segments provide high manipulability and the most optimal operating range [85]. The requirement of a hollow structure for the manipulator, through which the instruments are inserted, excludes many of the available joint mechanisms. Bending segments such as developed by Breedveld et al. [75] or Peirs et al. [65] can be considered for the distal articulation. From the aforementioned knowledge and available opportunities to expand the distal flexibility, we have decided to integrate an ordinary flexible, hollow endoscope deflecting for the distal part of the manipulators. This 2 DOF deflecting is actuated by 4 bowden wires and as known in the endoscopy, the wires can be actuated in a distance up to 3 m.

Cable actuated mechanisms, flexible shafts and hydraulic or pneumatic mechanisms are available options for the implementation of the flexible drive transmission over a distance of more than 2 m. Another possibility is a combination of wire mechanism with a linkage or gear mechanism. Each of these options has its advantages and disadvantages, which are described in detail in the Section A.1. Due to such things as the intended integration of the flexible endoscope deflecting, unifying the drive of the entire system and the consideration of the advantages of the bowden wire mechanism relative to the requirements, we have decided to implement the joint actuation of the platform primarily by using bowden wires.

The implementation of a single-port system with additional distal joints already induce many challenges, so that the additional consideration of a completely flexible shaft for the carrier system, right from the beginning, would go beyond the scope of this dissertation. Therefore, the first step would be the development of a semi-rigid system for laparoscopic single-port surgery that can be expanded in later phases in a completely flexible system for transluminal surgery was defined as the objective of this research.

In a first prototype, the outer diameter of the developed single-port platform was restricted to an inner diameter of 34 mm of the greatest available retrieving trocar of Ethicon. Accordingly, the outer diameter of the manipulators and the telescope was determined to achieve the best configuration in the available space of the trocar. The telescope with enhanced flexibility will be based on existing technology of flexible endoscopes. Long term development stages of the intended highly versatile telescope also stimulated us towards the parallel development of an interim solution where a conventional endoscope could be used for the evaluations.

3.4 Concept of the platform and differentiation from existing works

3.4.1 Description of the concept

Figure 3.6 shows the schematic drawing of the developed single-port platform which was designed according the defined specifications and resulting considerations. As inferred from the requirements, the overall system consists of three components:

- The platform, which carries the two manipulators and the telescope. It is separate in two units: The former is the passive unit, as shown in Figure 3.6, with the passive mechanism to actuate the manipulators and the telescope, and the latter is the active drive unit, including the motors and control unit, placed at a distance of 2 m.
- The tool changer with the exchangeable magazine that is integrated to the active unit and inserts the desired instruments through the individual manipulators.
- The guiding system for positioning of the single-port platform. This manipulator guides the platform in 4 DOF around the invariant point. A specially designed link with a quick fastener provides quick and easy dismantling of the system.

The SoloAssist telemanipulator, which was developed by the company, Aktormed, in Germany, in cooperation with the research group MITI at Klinikum rechts der Isar, was used as guiding system for the HVSPS platform. This hydraulic manipulator with 3 DOF (detailed description in the next chapter) is mainly designed for guiding a laparoscopic camera. For the application of the SoloAssist, however, an additional joint was developed for the rotation of the complete platform. This was accomplished in a particular project funded by the Bavarian research foundation (BFS).

The development of the tool changer for the HVSPS platform is being carried out within a currently ongoing thesis project at TUM. Therefore, conventional, flexible endoscopic instruments, a pair of pliers and scissors with a diameter of 2.3 mm and a length of 2.3 m, were used for the determination of requirements and evaluations of the proposed platform. The instrument channel through the manipulators extends to the active unit where it will be connected to the tool changer by a specific valve.

The passive unit of the platform includes the two manipulators and the telescope integrated in the insert with a 34 mm external diameter. Figure 3.7a shows a cross-section of the insert with

Table 3.1: Specification of the operating range of the individual joints

	q_1	q_2	q_3	q_4	q_5	q_6
Workspace	$\pm 270°$	$60mm$	$\pm 90°$	$\pm 180°$	$\pm 150°$	$\pm 90°$

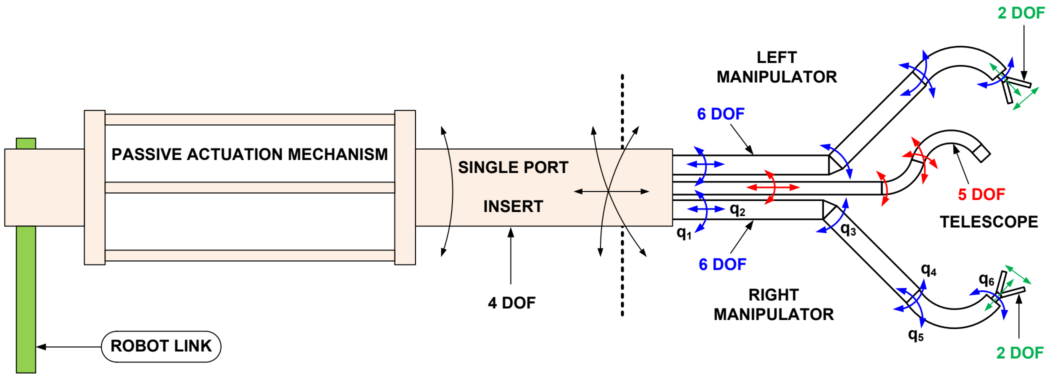

Figure 3.6: Schematic drawing of the semi-rigid single-port surgical platform: Two 6 DOF manipulators (∅12mm), a 5 DOF flexible telescope (∅10mm) and a 4 DOF robot guiding the insert (∅34mm).

the configuration of the manipulators and the telescope. The available space is used optimally, so that the greatest available distance results between both manipulators. Consequently, the manipulators are placed centrally with the minimal wall thickness close to the insert border. The greater the distance between the rigidly guided manipulators, the greater is the achievable distance and the workspace of the distal instruments. The telescope is placed centrally above both manipulators in the greatest possible distance. An additional channel for aspiration and instillation can be integrated in the lower section of the insert, opposite the telescope. It is also conceivable to integrate a third, smaller manipulator here that offers additional functionalities such as retracting tissue or holding surgical filament during suturing.

According to the requirements, a flexibility of at least 7 DOF should be provided and considered in the conceptual design of the manipulators. Furthermore, the design and kinematics of the manipulator should be based on the human arm. As shown in Figure 3.6, the conceived manipulator has 6 DOF as well as the opening and closing of the instrument. The workspace of the manipulator joints are listed on Table 3.1. The second DOF of the instrument corresponds to the instrument retraction and insertion, which is executed by the tool changer. The bendable section (deflecting) is representing the wrist that has two bending joints q_4 and q_5 at the base and an additional rotation joint q_6 of the instrument at the tip.

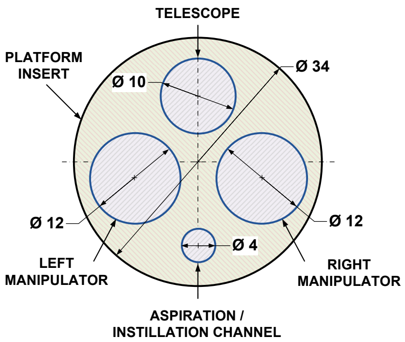

(a) Cross-section of the insert

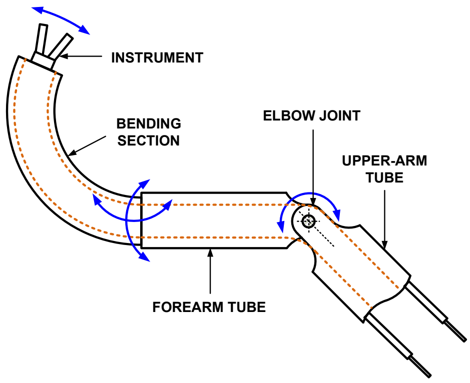

(b) Distal section of the hollow manipulator

Figure 3.7: a) Cross-section of the insert with the configuration of the manipulators and the telescope b) Distal section of the hollow manipulator with the bendable section and "elbow" articulation.

A fourth DOF for the enlarged deflection is realized with the "elbow" joint q_3, which is connected by a tube to the bending segment. The elbow joint between the upper-arm and the forearm, as represented in Figure 3.7b, has to afford the maximal possible deflection of the instrument. Corresponding to the specifications, this hollow swiveling joint should provide as one of the main challenges up to $\pm 90°$. The bowden wires for the wrist and elbow articulations, two wires for each joint and six in total, are guided through the manipulators to the actuation unit, 2 m away. They are placed circularly around the instrument channel, which is placed at the center of the manipulator. To maintain the pneumoperitoneum, the upper-arm tube of the manipulator and the telescope are guide gas-tightly in the insert. Two further articulations for each manipulator, q_1 and q_2 representing the "shoulder" joint, are integrated as subunits on the proximal part of the insert, which stays outside of the body. A passive actuation mechanism for the linear motion and rotation of the upper-arm tube is realized in this subunit, where the rotation of the motors are remotely transmitted by bowden wires into the intended motion.

The connection between the platform and the guiding system is realized at the proximal end of the platform with a specific linkage tube through which the manipulators and the telescope are introduced. Additionally, the rotation mechanism of the platform is integrated at the linkage tube. All the bowden wires are fed through flexible plastic hoses from the passive unit to the active unit of the platform. The active unit platform includes the mechanism that provides the transmission of the motor rotation into pull motion of the bowden wires. Two bowden wires for each joint are wound as a pair on a shaft axle, which is rotated by a motor.

3.4.2 Differentiation from existing works

Highly versatile single-port robotic platform for laparoscopic surgery:

Our extensive literature survey revealed that so far only a few robotic single-port systems are being developed and proposed as possible solutions specifically for laparoscopic single-port surgery. One of the important systems hereunto is the IREP, which is developed by the research group of Swanstrom et al. [68]. Another system called SPRINT robotic system is being developed by the research group of Dario et al. [108]. Both of these single-port systems differ in many points from the concept that is proposed in this study. Some of the important points are, for example, the hollow structure of the manipulators which enables the introduction of flexible instruments, the control unit including the electro-motors placed in the periphery, the highly flexible telescope providing an S-shape and the kinematic structure of the bowden wire controlled manipulators with a large workspace.

As already described in prior art, the multi-arm daVinci master-slave system was also used for single-port interventions [99]. The approach of introducing both manipulators in crossed configuration through same port is, of course, completely different from the focus here. However, Intuitive Surgical has a patent application in which they claim a new minimally invasive surgical system [106]. Up to now, there are no further details or publications available regarding this system. NOTES robots, which have been developed by Abbott et al. [132] or Phee et al. [131] have flexible platform shafts, similar to flexible endoscopes. The flexibility i.e dexterity of the instruments of these platforms is much less than intended in our concept. Furthermore, the visualization area of these platforms, with either an optics rigidly attached at the tip or solely using a conventional endoscope is, in comparison, less than the telescope designed for this study.

Joint control by bowden wires over long distance and providing the displacement of the control unit, including motors, to the periphery:

Laparoscopic instruments with distal articulations are usually controlled by motor drives that are integrated directly at the proximal part of the instrument. This includes nearly all the instruments listed in Table 2.1, as well as the single-port systems such as IREP or SPRINT and, of course, also the daVinci master-slave system. The manually controlled, single-port platform, SPIDER, or manual NOTES platforms are not considered here in relation to automated control over long distance. Instruments and the ViaCath platform for the Laprotek system, which are developed by the research group of Peine et al. [78, 132] or the NOTES robotic system, as proposed by Phee et al. [131], use bowden wires for the joint control. As mentioned above, the concepts of these two transluminal robotic systems are different from the developed system. The instruments of the proposed platforms correspond to the manipulators of our system that have a hollow structure and offer a higher flexibility in comparison.

Hollow manipulators with enhanced dexterity providing the insertion of flexible instruments:

Most of the identified manipulators with enhanced flexibility do not provide hollow structures for the insertion of the instrument. In our case, different effectors (instruments) such as pliers or scissors without further additional articulations can be exchanged quick and easily. In contrast, the majority of the laparoscopic instruments with multiple joint mechanisms, such as listed in Table 2.1, need to be exchanged as a whole which is elaborate and time consuming. Instruments with only one hollow bending section, similar to the deflecting of a flexible endoscope, as proposed by Breedveld [75] or Peirs [65], could be considered as a component of the manipulator. In general, NOTES platforms provide hollow structures. However, the instruments of these platforms correspond to the manipulators proposed in our concept. Consequently, the functionality and the flexibility of our concept is much higher than that of the NOTES platforms.

Chapter 4

The Highly Versatile Single-Port System

The developed single-port system mainly consists of the following two units: On the one hand, as shown in Figure 4.1, a multi-arm platform was developed that is inserted through a single access into the patient and remotely actuated by using a flexible drive transmission mechanism. On the other hand, a modular drive platform was developed that actuates all the articulations from 2m at the periphery . The passively controlled, highly versatile single port platform consists of two articulated hollow manipulators with 6 DOFs and a semi-rigid telescope with 5 DOFs that are combined into one unit. The bowden wire actuated manipulators and the telescope are integrated gas-tightly in the insert with ∅34mm×200mm and inserted together in

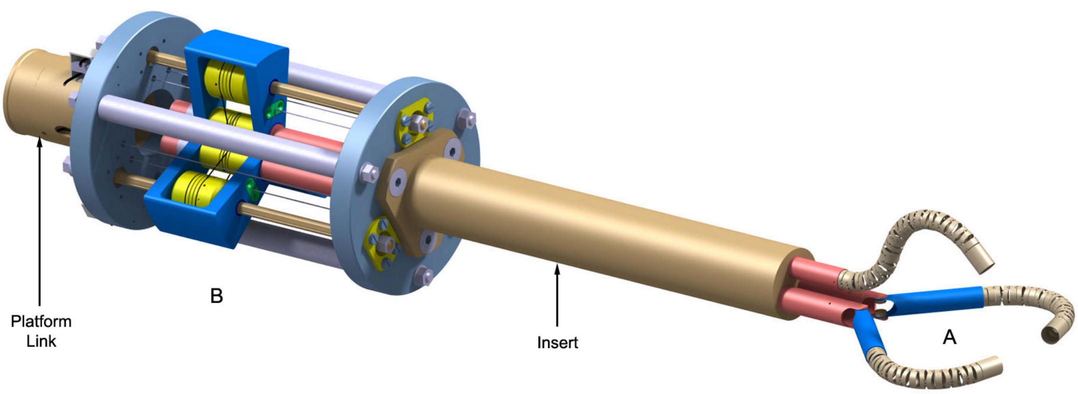

Figure 4.1: Design of the highly versatile single-port platform. A: Distal dexterity inside the body. B: Actuation mechanism for rotation and linear motion (∅100x160mm)

a straight configuration through the trocar into the abdominal cavity. The insert is mounted on the proximal unit of the passive platform in which the linear and rotary articulations are implemented. An additional joint was developed to enable the rotation of the entire platform, which is mounted on the linkage tube. As shown in Figure 4.2, the passive single-port platform is attached at the proximal flange onto the hydraulic SoloAssist telemanipulator with 3 DOFs that provides the guidance at the invariant point. In this figure, the drive units are also shown in the background, on which the flexible hoses with the bowden wires are attached.

The passive single-port platform has a distal diameter of 34mm, a proximal diameter of 100mm and a total length of 400mm from the SoloAssist link to the insert tip. The entire platform, including the rotation, is made of plastic, aluminum or stainless-steel and has a total weight of 3 kg. The working range of the individual joints of the manipulators are defined in Section 3.4.1 and the workspace of the instruments is specified to be 100x60x60 mm.

The entire single-port system, as shown in Figure 4.2, comprises the following components that are described in this chapter in detail: Manipulators with distal articulations, a double-bending telescope for enhanced visualization, a three-arm single-port constellation with additional linear and rotary articulations, rotation of the entire single-port platform, an actuation mechanism at the periphery and a telemanipulator for guiding the passive platform.

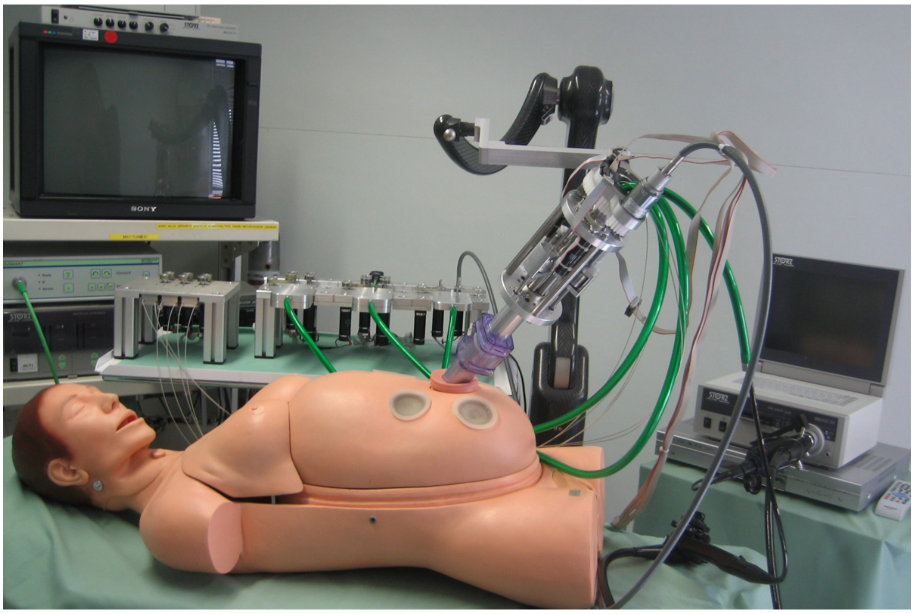

Figure 4.2: The overall highly versatile single-port system: Passive platform attached to the SoloAssist guiding system and actuated by the active drive unit at the periphery.

4.1 Manipulator with distal articulations

According to the design specifications and considerations (cf. Section 3.3), a flexible endoscope bending section is integrated for dexterity enhancement at the distal end of the manipulator. As presented in Figure 4.3, the manipulator comprises a bendable section of a gastroscope with two DOF and an elbow joint with a further DOF. An opposed configuration is illustrated in this picture, in which the bendable sections are deflected to 180° and the elbow joints are bent to 90°. There are a multitude of flexible endoscopic instruments, differing in function and size, which come into consideration for the intended application. Our preliminary studies of single-port interventions have shown that conventional endoscopic instruments do not provide high performance and load capacity for surgical procedures. The integrated gastroscope bending section, with an outer diameter of 9 mm, enables the insertion of instruments up to 4 mm by using the appropriate instrument channel. The kinematics and the corresponding dimensions of the first prototype of the manipulator were defined empirically. The individual components and their dimensions are listed below:

- Gastroscope bending section: ∅ 9 mm × 75 mm
- Forearm tube: ∅ 10 mm / ∅ 8 mm × 50 mm
- Upper-arm tube: ∅ 12 mm / ∅ 10 mm × 400 mm

The bending section that is actuated by four bowden wires is one of the important and decisive parts of the implemented design. Corresponding to the specification of the control at a distance of 2m at the periphery, it was decided to actuate the elbow joint by bowden wires as well. The assets and drawbacks of the bowden wire actuation are described in Section A.1 in detail.

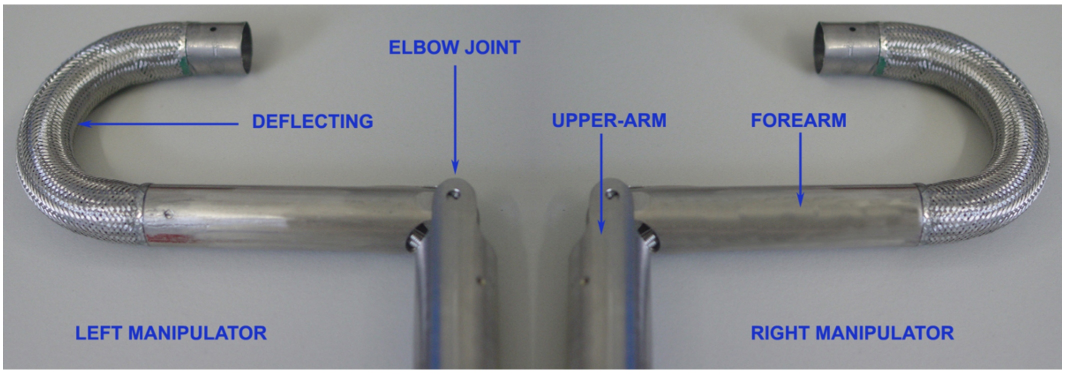

Figure 4.3: Distal section of the two single-port manipulators in opposed configuration.

4.1.1 Endoscope deflecting for high dexterity

The size of the available bending sections for endoscopy are diverse. There are very small sizes with an outer diameter of about 6mm for bronchoscopy up to large bending sections of about 13 mm in diameter for colonoscopy. The integrated bending section for the manipulators, as shown in Figure 4.4, is a conventional gastroscope deflecting, which is manufactured by Karl-Storz in Germany. This hollow-structured design provides the integration of an instrument channel for the introduction of the instruments at the periphery.

The bendable section with a diameter of 9 mm and a length of 75 mm, consists of 20 parts. The individual parts are riveted together in an irregular arrangement and the hinge distance is 3.5 mm. Figure 4.4a presents the configuration of the rivet joints. The bending section is attached at the linkage part to the forearm tube and is controlled by 4 bowden wires, which are welded on the front part and guided through lugs at each part. Each wire is in-line with the corresponding hinge axis and the outer sheath of the bowden wires are welded to the linkage part. A pair of bowden wires, which are controlled by one motor drive, enables the bending in one plane. In total, 13 hinges on the blue plane, as shown in Figure 4.4b, permit a deflection of more than ±180° and 6 hinges on the red plane, a deflection of more than ±150°.

As presented in Figure 4.3, the bending section is covered by a metalic mesh in order to permit a consistent bending over the entire structure. At the very end, a flexible rubber cover is mounted on the bending section and fixed at both ends by using a specific filament. This permits the protection of the mechanism during the sterilization procedure and the surgical intervention. The already clinically used 5 mm telescope of Olympus with a distal flexible bending section is a good example thereof [87].

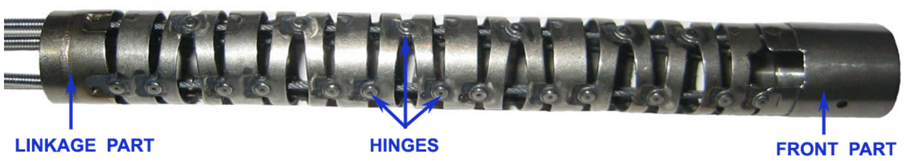

(a) Gastroscope deflecting manufactured by Karl-Storz, Germany

(b) Design of the deflecting with the corresponding bending planes.

Figure 4.4: Bending section of an endoscope integrated as distal deflecting of the manipulator

4.1.2 Hollow elbow joint actuated by bowden wire

The main challenge of the elbow joint is the hollow structure that should enable the introduction of the flexible instruments. A further challenge is the need for a deflection up to ±90° that provides an extended working range. The developed elbow joint is presented in Figure 4.5. Two pulleys with central threads are welded in a distance of 5 mm into the forearm tube which has an outer diameter of 10mm. Both tubes can be pivoted by two studs that are screwed through the pulleys. For the reduction of friction, two sliding washers are mounted between the upper-arm and the forearm tube. The outer sheath of the bowden wire is welded in-line with the pulley at the right position into the upper-arm tube and the 0.55 mm wire is wound one turn on the pulley and welded in the groove on the forearm tube.

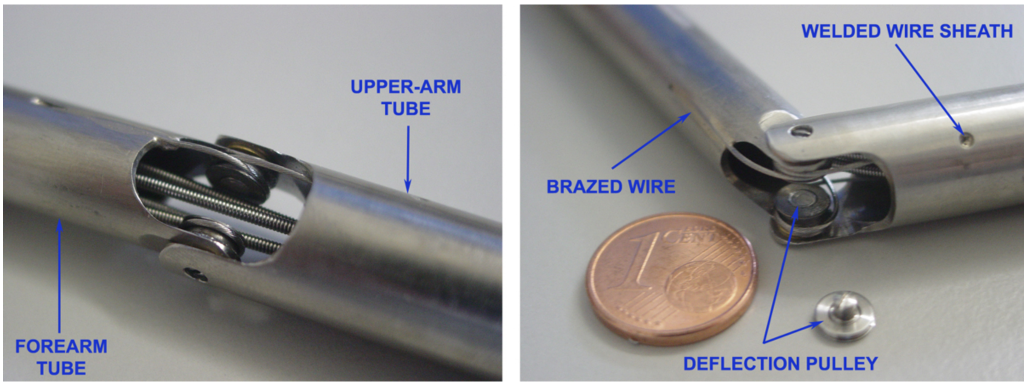

Figure 4.5: Elbow articulation of the single-port manipulator.

The advantages and disadvantages of this elbow design are listed in Table 4.1. As one of the major drawbacks, the design of this elbow joint reduces the transmittable forces due to its low force translation ratio. The following force reduction results from the given ratio of the forearm tube length l_f plus bending section length l_d relative to the pulley radius r_p.

$$i = (l_f + l_d)/r_p = 125mm/2.5mm = 50$$

Table 4.1: Assets and drawbacks of the hollow elbow articulation

Advantages	Disadvantages
hollow design permits instrument insertion deflection angle up to ±90° easy manufacturing and disassembly	high friction and inaccuracy slip-stick effect due to friction short lever arm leading to low load capacity insertable channel smaller than 5 mm

The manufacturing of the elbow joint with small and thin-walled stainless steel parts was realized by high precision machinery. First, both tubes were milled in several steps and, afterwards, the pulleys and stud screws were machined. Each pulley of the joint, with a dimension of $\varnothing 5.5 \times 1.6$ mm, was welded on one side of the entire circumference. The available width of 0.2 mm could only be accomplished by laser spot welding. This method can be used for thin-walled materials such as stainless steel with a high melting point. Spot welding of the pulleys was performed with a Nd:YAG laser with the characteristics of 5kW pulse peak capacity, 0,5-20 ms pulse length, 20 Hz pulse frequency and 0.2-2 mm spots. The following parameters were used thereby: 200 Volt, 150 ms impulse, 0.4 mm laser diameter and 1 Hz cycles. By also using the laser spot welding process, the bowden wire sheaths for the elbow joint were welded into the upper-arm tube. A special jig was designed for the radial positioning of the bowden wire in order to weld the sheath in-line with the pulleys through a radial hole.

Next, the steering wires were attached to the forearm tube. In contrast to laser welding, the fixation of the steering wire, composed of multiple small wound steel wires, on the stainless steel tube could only be realized by brazing. A silver alloy at a melting temperature of 1200° C and a hydrogen flame were used. The steering wire is brazed on a length of at least 5 mm at its end in order to provide sufficient strength. Due to the fact that the wires are brittle and break when subjected to high temperatures, the brazing of the wires at the inflection point should be avoided. Therefore, no high temperatures were applied to the wire at this point which would have changed the structure and rigidity.

Based on experience in endoscopic systems with repeated breakage of the wires, it is absolutely essential to design mechanisms that can be disassembled and repaired. The developed elbow joint can easily be disassembled by unscrewing the shafts through the pulleys. A wire replacement can be achieved by unsoldering the broken one. Preliminary tests have shown that the wound wire tends to uncouple from the pulley during assembly or by insufficient pretension. This property should be examined more in depth in further studies and, if necessary, a prevention can be achieved by welding a hinge on the pulley.

The radial orientation of the elbow joint relative to the bending section was achieved by the alignment of the bending planes. In order to afford the greatest possible horizontal workspace, the plane of the bending section with the greatest flection of ±180° was aligned with the bending plane of the elbow joint. The bending section is correspondingly attached by two stud screws to the forearm-tube and additionally secured by an adhesive.

4.2 Double-bending telescope for enhanced visualization

By the achieved experience in the hitherto performed single-port operations, there is a broad consensus among the surgeons that a single-port telescope should provide the ability to visualize the situs in different perspectives, preferably off-line from the instrument axis [95]. An optic rigidly integrated in the distal tip, as with many proposed single-port systems, is obviously not enough to meet the requirements. Initial evaluations, which we have carried out with a semi-rigid telescope comprising a distal-bending, similar to the commercially available 5mm Olympus endoscope [87], resulted in enhanced flexibility. However, the workspace was not sufficient for the visualization of the manipulators in their entire workspace. Additional flexibility is required to achieve the intended visualization. Therefore, further design evaluations of the telescope were carried out in a simulation.

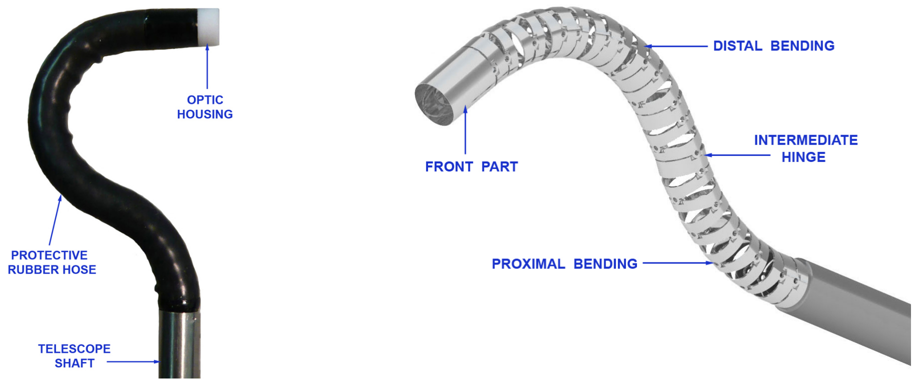

Figure 4.6: Double-bending telescope comprising two bendable sections and 3 DOFs in total.

A semi-rigid design with a distal double-bending structure that can take an S-shape, as shown in Figure 4.6, resulted in enough flexibility to visualize the manipulators in the specified workspace of 100×100×60 mm. An adequate visualization of the instruments could be achieved in almost any angles, including a retroflexed configuration. The developed telescope, with a diameter of 10 mm, comprises two bendable sections similar to the flexible endoscopes, which are covered by a metal mesh and a protective rubber hose. The optic and illumination can be integrated into the tip and the corresponding cables are guided through the telescope. A relative proportion of two-thirds for distal bending and one-third for proximal bending resulted in the largest possible workspace, which was determined by using a simulation. Accordingly, the distal bending of 70 mm length has two DOFs and the proximal bending of 36 mm length has one DOF that is aligned with the vertical plane of the distal bending.

4.3 Linear and rotary articulations of the manipulator

4.3.1 Approach of the passive actuation mechanism

According to the concept, the design of the single-port system includes two further joints, the rotation and linear motion into the body for each manipulator and the telescope that is integrated at the proximal part of the platform. One of the main challenges here is the limited space between the manipulators that restricts the possibilities of realizable actuation mechanisms. Only 1.3 mm around each manipulator remains for the integration of the rotation mechanism in the available distance of 2.7 mm between both manipulators. Drive belt, spur gears and steel wire are possible mechanisms for the transmission of the rotatory motion. Neither standard pulleys for drive belts nor standard spur gears provide such small sizes with small wall thicknesses which can be used for the intended purpose. An alternative, therefore, would be the transmission of the rotation by winding a small steel wire around a thin-walled pulley with corresponding grooves. The actuation can be realized either by an integrated motor into the platform or by a motor at the periphery with an additional drive transmission for the rotation. In contrast, spindle drives, a rack and pinion drive, hydraulic or pneumatic actuators and wire actuation are possible mechanisms for the implementation of the linear motion of the manipulators that can be actuated by direct drive or at the periphery.

Two possible combinations of the linear and rotatory motions are: i) Direct motor drive or a mechanism for the rotation that is translated with the manipulator, for example, by a spindle ii) Integration of a ball-spline providing the linear motion along the shaft as well as a torque transmission for the rotation. The former, with a built-in motor drive, could be easily implemented. However, it contradicts the defined specification of the displacement of the drives to the periphery. Furthermore, it is challenging to integrate a rotatory mechanism with cable connections which translates along the platform. On the other hand, a ball spline combines both articulations in a compact form with a straight cylindrical spline nut. The rotatory motion is achieved by rotating the ball spline shaft and the linear motion by translating the spline nut along the shaft. A ball spline was chosen for the implementation of the intended platform.

Primarily we should distinguish between the following two general actuation concepts: 1) Direct drive by integrating the motors into the platform as presented in Figure 4.7a and 2) Actuation at the periphery by means of flexible drive transmission mechanism as presented in Figure 4.7b. Although it was specified that the motor drives should be placed at the periphery, for completeness, we briefly describe possible approaches to give an overview.

I) Direct drive by using spindle and ball spline

For this approach, the linear motion is realized by a spindle (screw drive) that is linked with a guiding sleeve to the manipulator and the ball spline. The rotation is achieved by rotating the ball spline nut, which is integrated in the guiding sleeve and translated with the manipulator. A steel wire is used for drive transmission from the spline nut to the manipulator pulley. As presented in Figure 4.7a, the components are integrated between two platforms that provide the bearing of the shafts as well as the integration of the required motor drives. The rotation of the spindle and the ball spline are achieved by using drive belts. This concept of integrated motors is simple and easy to realize and involves less friction or backlash compared to the subsequent solutions. The increase in size and mass of the platform due to the motor drives and the fastening and friction of the steel wire for the rotation are the main drawbacks.

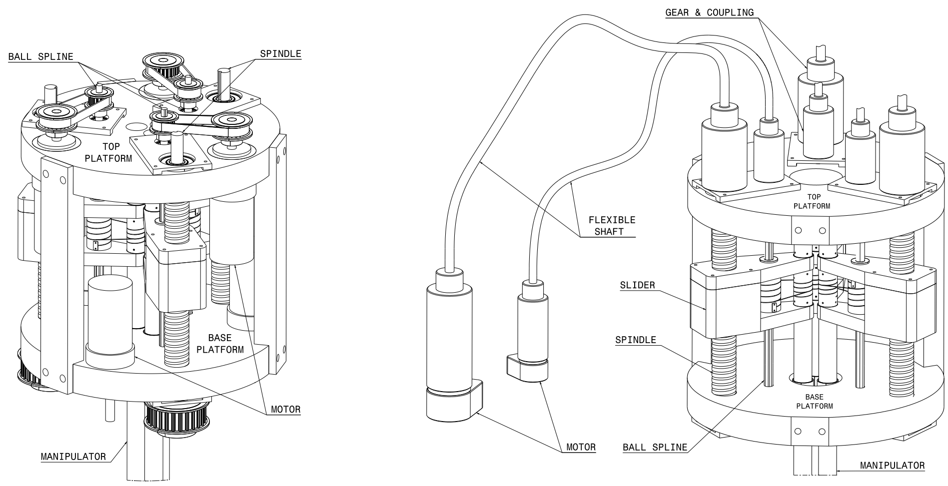

(a) Integrated motor drives (b) Actuation by flexible shafts at the periphery

Figure 4.7: Concepts of the linear and rotary joint of the manipulators: a) Direct drive by motors integrated into the platform b) Actuation of the passive platform mechanism by using flexible shafts.

II) Actuation with hydraulic or pneumatic actuators

Hydraulic or pneumatic cylinders offer easy opportunities to realize linear systems. The spindle in the previous solution could be replaced, for example, by a hydraulic piston that provides linear motion. Hydraulic or pneumatic systems enable, as an advantage, the actuation over long distances. However, the installation size of the platform would be increased thereby. Moreover, pneumatic systems are noisy and do not provide precise positioning and hydraulic systems have the risk of leakage and demand an elaborate reservoir and pumping mechanism.

III) Actuation at the periphery by using flexible shafts

Similar to the first approach, instead of integrating the motor drives into the platform, the spindle and the ball spline are actuated at the periphery by using flexible shafts. The platform near the patient can be designed, thereby, to be simple and more compact. A flexible shaft has a preferential direction of rotation and can not be equally loaded in reverse direction. Therefore, these shafts are generally used for drive mechanisms with high speeds and one direction of rotation. The flexible shaft has a large measure of torsion that makes it impossible to achieve a precise rotation or positioning. Furthermore, as presented in Figure 4.7b, gears with specific couplings should be integrated on the platform for speed reduction.

IV) Actuation at the periphery by using bowden wires

In this approach, as shown in Figure 4.8, both the rotary and the linear motion are realized by means of bowden wires. The motors can be displaced, thereby, at the periphery and two bowden wires are each used to transmit the rotation of the actuators to the joints of the platform. As with the other concepts, a ball spline is used to implement the rotation as well as the linear actuation. The rotation between the ball spline nut and the manipulator is achieved in a similar manner by using a steel wire wound around specific pulleys. Unlike the other approaches, the rotation of the ball spline shaft is realized on the top platform by a further pulley and bowden wires. The linear motion is also implemented by bowden wires that pull on each side of the slider to translate the linked manipulator along the ball spline. The lower wire is deviated by a pulley on the base platform and both bowden wire sheathes are attached to the top platform.

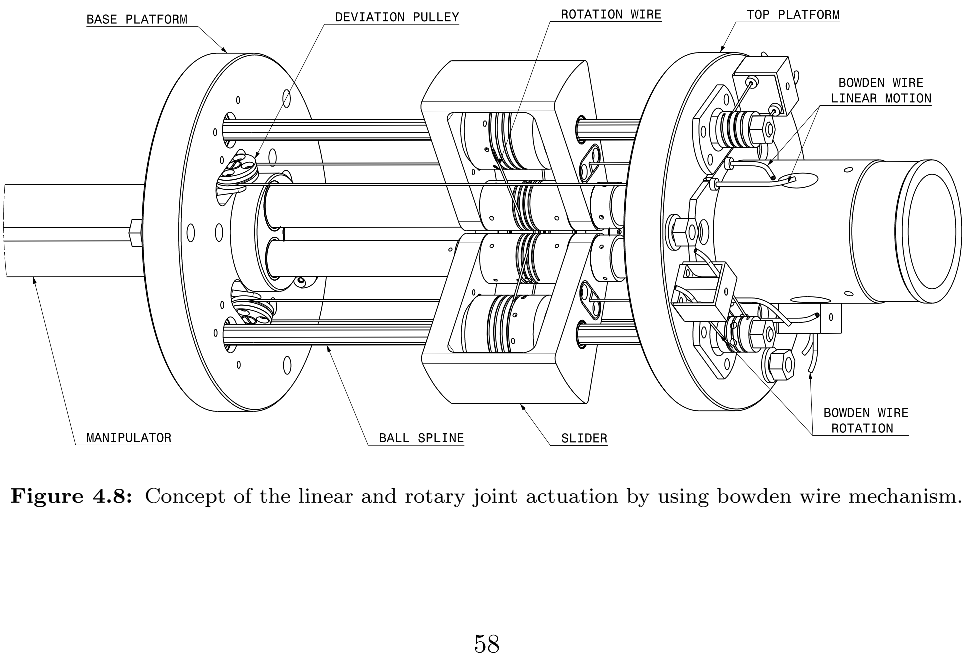

Figure 4.8: Concept of the linear and rotary joint actuation by using bowden wire mechanism.

The approach with bowden wire actuation has advantages, such as the need for a small footprint, the displacement of the electrical drives to the periphery and a simple design and manufacturing of the single-port platform. In contrast, a system with bowden wire as drive transmission mechanism also has such drawbacks as high friction and inaccuracy due to the wire actuation, the risk of wire breakage, the load dependent decrease of the required prestress, the slip-stick effect and the difficult modularization. The specified need for the displacement of the drives to the periphery as the main reason and the further advantages such as small installation size or simple design and weight were the deciding factors for the implementation of the platform according to the bowden wire approach which is described, subsequently, in detail.

4.3.2 Bowden wire actuated linear and rotary articulations

The rotation of the manipulators and the linear motion into the body are considered to be shoulder articulations. Figure 4.9 presents the proximal part of the developed single-port platform including the actuation mechanism of these two articulations. The manipulators and the telescope that are arranged circularly in an angle of 120° to each other provide 6 DOFs in total. A detailed cross-section of the mechanism for one manipulator is shown in Figure 4.10 with the description of the implemented components. The base platform and the top platform, each with a dimension of ∅100×12 mm, have a distance of 136 mm to each other in order to achieve the intended linear stroke of at least 80 mm for the manipulators. Accordingly, a total length of 200 mm resulted for the proximal unit of the single-port platform including the robot linkage. The linear and rotary articulations have been realized by using three THK LT6 ball splines [1].

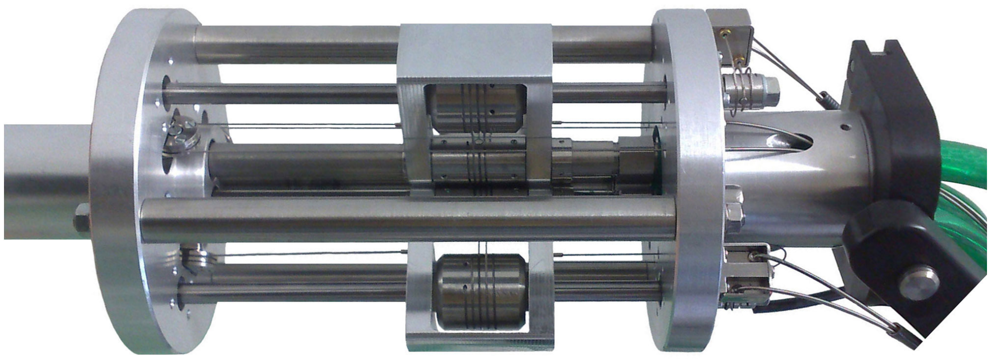

Figure 4.9: Proximal unit of the developed single-port platform including the linear and rotary articulations as well as the linkage for the guiding system.

[1] https://tech.thk.com/de/products/pdfs/de_b3_024.pdf

The ball spline shaft, with a 6 mm diameter, has a usable length of 140 mm and the ball spline nut with the specific pulley for the rotation as well as the manipulator pulley, all with a length of 25 mm, are integrated into the U-shaped slider with a total height of 41 mm. As shown in the cross-section of the platform in Figure 4.10, two double-row angular contact ball bearings in an “O” arrangement are used to mount the ball spline shaft in the base and top platform. This bearings can also support a certain amount of radial load induced by the manipulator. In order to ensure stability and to prevent unexpected loads, the upper and lower platform are supported by three spacing bolts, which are mounted circularly between the ball splines.

The insert, with a 34 mm diameter and a length of 216 mm, is screwed to the underside of the base platform. A plain bearing is integrated on each side of the bores for guidance of the manipulators and the telescope. O-Ring seals are additionally mounted into the front part to prevent air leakage. The guide bores in the base platform, with integrated plain bearings, were machined exactly according to the bore positions in the insert. For this prototype, the base and top platform and the insert are made of aluminum. It is quite conceivable to manufacture these parts in plastic, for example, by laser sintering. This would have a low dead weight.

A tube is mounted on the top platform for the connection of the single-port platform to the guiding system. This thin-walled linkage tube enables the lead-through of the flexible hoses, including the bowden wires and the instruments. The top platform, as a counterpart of the base platform, has a central bore that also enables the insertion of the manipulators. As presented in Figure 4.12a, the rotation of the ball spline shaft is implemented on the top platform. Therefore, it was necessary to mount a block in-line with the ball spline in which the bowden wire sheaths could be attached. A rotation pulley is fixed with a locknut to the end of the shaft and clamps, thereby, the inner ring of the angular contact ball bearing.

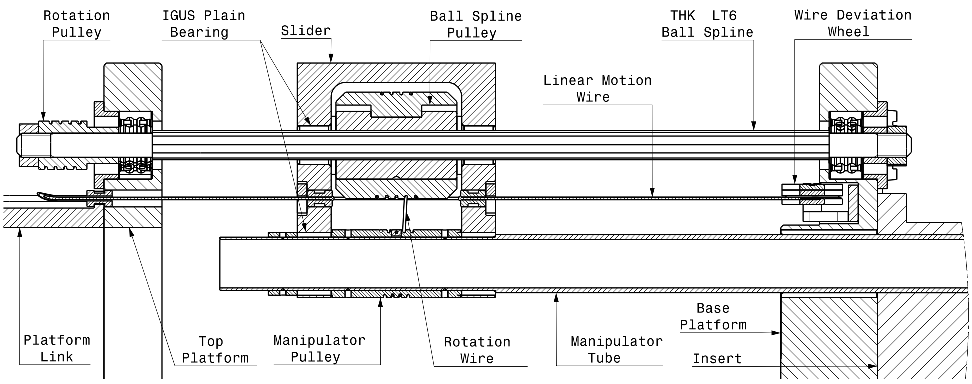

Figure 4.10: Sectional view of the linear and rotary actuation mechanism of one manipulator.

The bowden wire is wound on the grooved rotation pulley with a diameter of 9 mm and fixed radially by inserting the welded pin on the wire into the pulley. A rotation of ±180° of the ball spline shaft can be achieved with the linear pulling motion of the bowden wire. The ball spline nut rotates accordingly by the same angle and transmits the rotation to the manipulator. Due to the limited space between the manipulators, the transmission of the rotation from the ball spline to the manipulator is realized by a wire. As shown in Figure 4.11b, two specific pulleys, one for the ball spline nut and the other for the manipulator, with corresponding grooves and the smallest possible diameter, were designed. Figure 4.12c illustrates the wound wire with a small pin welded in the middle. The pin is inserted into the corresponding hole in the manipulator pulley and each end is fixed by a stud screw on the ball spline pulley after winding the wire around both pulleys. The following transmission ratio results corresponding to the realized manipulator pulley d_{mp} and the ball spline pulley d_{sp}

$$i \;=\; d_{sp}/d_{mp} \;=\; 21.4mm/13mm \;\cong\; 1.65$$

The maximal rotation angle of the manipulator is, accordingly, ±300°. Due to the limited space, as shown in the sectional view in Figure 4.11a, plain bearings are integrated in the slider to enable the rotation and the linear motion of the manipulator and the ball spline as well as the rotation of both pulleys. The pulleys are first mounted into the slider, and the manipulator and the ball spline shaft are then inserted through them. The manipulator pulley is fixed by stud screws to the manipulator and the ball spline pulley by a slot nut to the ball spline nut.

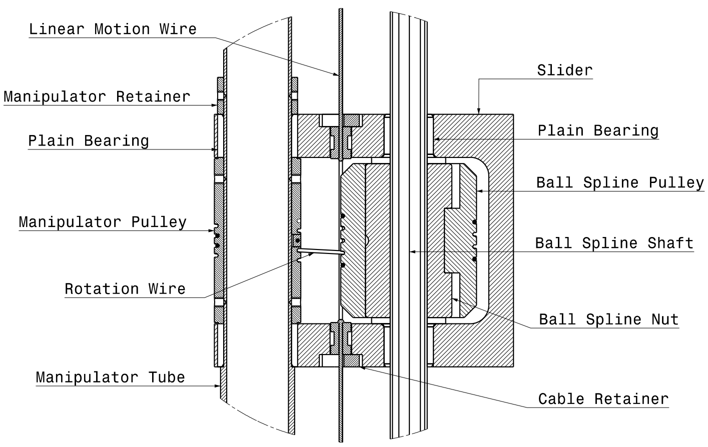

(a) Sectional view of the slider and the rotary mechanism

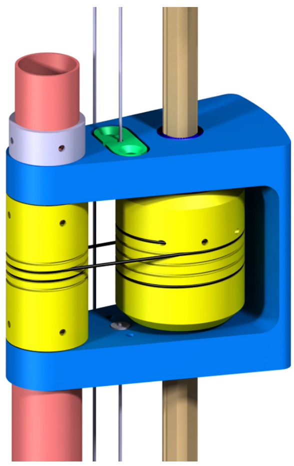

(b) Design of the rotation

Figure 4.11: Design of the rotation mechanism: a) Sectional view illustrating the implemented components b) 3D view of the rotation mechanism of one manipulator

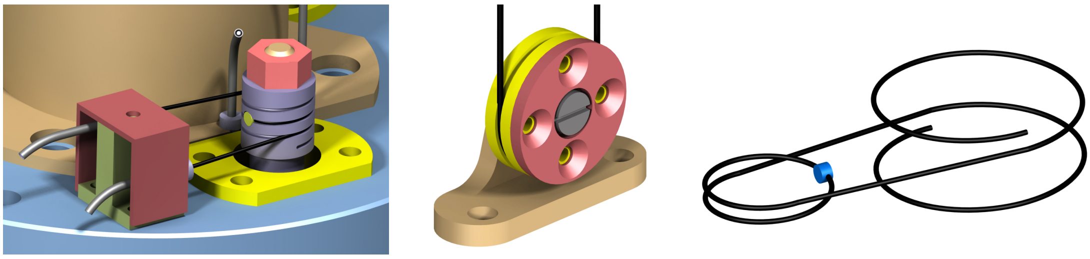

(a) Bowden wire actuated rotation (b) Wire deviation wheel (c) Wound rotation wire with welded pin

Figure 4.12: Detailed views of the wire actuation: a) Design of the drive transmission to the ball spline shaft b) Design of the wire deviation wheel c) Wound wire for the rotation transmission to the manipulator

The linear motion of the manipulator is implemented by attaching a bowden wire on both end faces of the slider. The welded pin on the wire is fixed by a cable retainer and enables the pulling of the slider in both directions. A translation of the manipulator is achieved by the manipulator pulley that is clamped in the slider and fixed by stud screws on the manipulator. Two possibilities have been considered for the fixation of the bowden wire sheaths. One possibility would be the fastening of the upper wire on the top platform and the lower wire on the base platform. Another possibility, as shown in Figure 4.13, would be the attachment of both wire sheaths on the top platform, which is, in terms of cable routing, better suited for an easy and compact guidance of the wires away from the patient. The latter demands an appropriate wire deviation mechanism for the lower wire. Therefore, as shown in Figure 4.12b, a wire deviation wheel with a miniature ball-bearing was designed, which is mounted on the base platform. After attaching the bowden wire sheaths to the platform link, the appropriate tension of the wire is set in the actuation mechanism at the periphery. The maximal achievable linear range of motion is 87 mm.

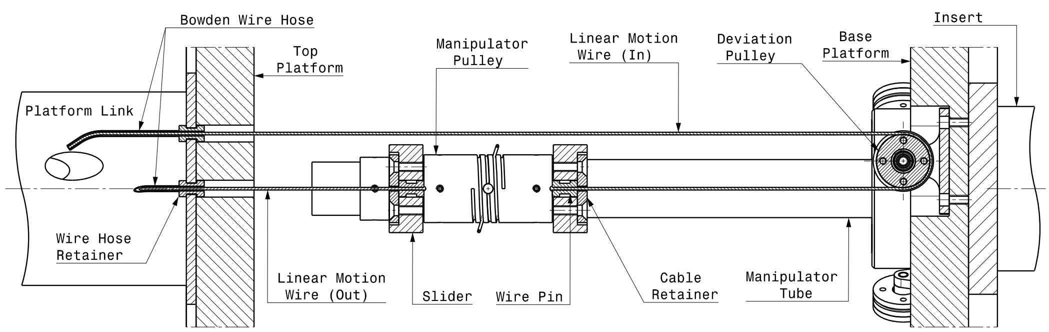

Figure 4.13: Sectional view illustrating the linear actuation mechanism of the manipulator

4.4 Connection and rotation of the single-port platform at the guiding system

The development of the rotary joint for the single-port platform was accomplished in cooperation with the company, Aktormed, in Germany, who have also developed the SoloAssist hydraulic guiding system. This small project, “Interface between the SoloAssist and a single-port system”, was funded by the Bavarian Research Foundation (BFS). Furthermore, this project also involved an investigation into whether or not the camera guiding system SoloAssist (description in Section 4.6) is, in principle, suitable to carry and guide such a multifunctional single-port system instead of a telescope.

4.4.1 Requirements and concept of the rotary joint for the platform

First, the requirements for the interface were identified. The SoloAssist should allow a tilting of up to 60° to the vertical axis and a complete turn at the invariant point to reach all quadrants of the abdomen. A rotation of at least ±180° is necessary for the platform that should be achieved in a velocity below 1 rad/s. The zoom function should enable, in a range of 80 mm, the insertion of the platform into the body. In contrast to a conventional light-weight telescope, the SoloAssist should carry the platform with a total weight of 3 kg including the weight of the rotary mechanism. Last but not least, the system should provide a quick-release fastener for the simple and quick dismantling of the system.

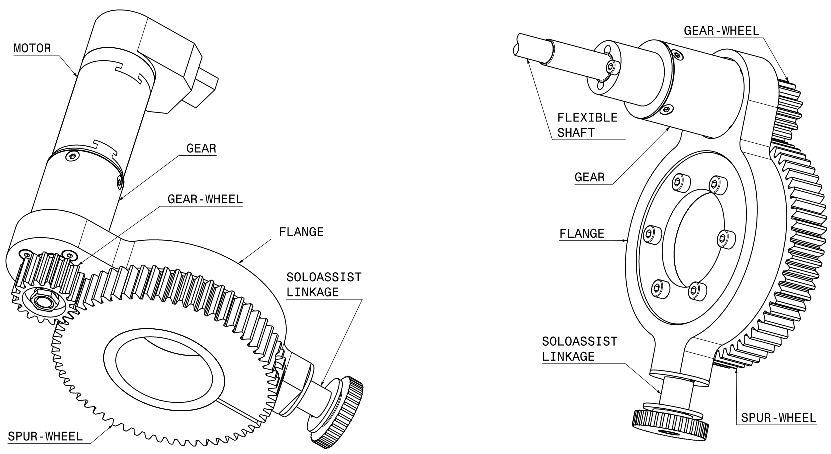

(a) Motor mounted on the flange (b) Actuation by flexible shaft

Figure 4.14: Concepts of the rotation for the single-port platform: a) Direct drive by attaching the motor on the flange b) Actuation at the periphery by using a flexible shaft

Two concepts have been considered for the realization of the rotary articulation. In the first concept, as shown in Figure 4.14a, the rotation is realized by attaching the motor directly on a flange that is mounted on the platform. The spur-wheel is fixed, thereby, with a screw on the platform link and rotated by the gear-wheel relative to the flange. A thin-walled angular ball bearing is integrated between both components. The second concept, as shown in Figure 4.14b, is, in principle, similar to the first one. It differs only in that the drive is placed at the periphery and a plain bearing is used instead of the angular ball bearing.

Similar to the implementation of the entire platform, the intention of the second concept was the displacement of the electrical drive to the periphery in order to meet the specification and to profit from the same advantages. In contrast, due to the required higher torques, the drive transmission is realized by means of a flexible shaft. The main reason for using a plain bearing is that the angular ball bearing in the necessary size is too bulky and heavy. The drawbacks of the second concept are, in comparison, the inaccuracy resulting from the torsion of the flexible shaft and the friction of the plain bearing. The displacement of the drives to the periphery and the realization of a compact, lightweight platform were the decisive factors for the implementation of the second concept, which is described subsequently in detail.

4.4.2 Rotation of the single-port platform by means of a flexible shaft

Figure 4.15 shows the implemented solution of rotary unit for the single-port platform. The components are made of aluminum or plastic, in order to reduce the weight of the passive platform. A quick-release fastening of the rotary unit is provided by the simple attachment of the SoloAssist link on the flange by means of a knurled nut.

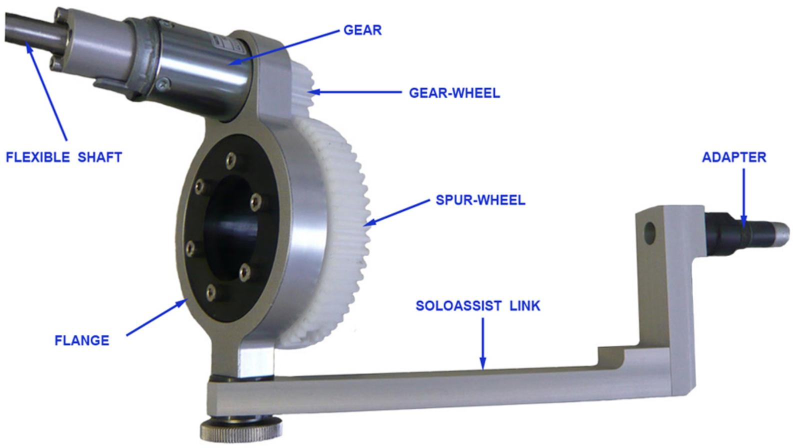

Figure 4.15: Rotary drive unit of the single-port platform attached to the SoloAssist link.

As shown in the sectional view in Figure 4.16, the bearing of the rotation consists of a plain bearing inner ring that supports the aluminum flange radially and axially. The plain bearing as well as the spur-wheel are slotted and clamped together by a radial screw on the platform link. On the other hand, the gear-wheel is clamped directly on the gear shaft and the gear is mounted at a distance of 57 mm from the axis of the platform on the flange. A transmission ratio of $i_z = 3.75$ results from the ratio of the teeth numbers (60/16) of the gear wheels.

The rotation of the gear-wheel is achieved from 2 m in the distance by a DC motor. A flexible shaft with a diameter of 3.2 mm and a protective hose are used for the drive transmission. The planetary gear on the flange reduces, in addition, the high speed of the flexible shaft by a transmission ratio of $i_g = 162$. The torsion of the flexible shaft is thereby reduced as well that in turn leads to a decrease of the inaccuracy. Furthermore, a specific coupling was designed on the motor as well as the gear for the connection of both ends of the flexible shaft. On the motor side, the flexible shaft is inserted into a sleeve on the shaft and on the gear side into an additional implemented drive shaft. In the last assembly step, the protective hose that axially holds the flexible shaft, is attached on both ends. The following speed and torque of the platform can be calculated from the given values of the motor and the drive transmission.

$$n_p \;=\; n_m/(i_g \cdot i_z) \;=\; 8050\ 1/min/(162 \cdot 3.75) \;=\; 13.25\ 1/min \;=\; 79.5°/s$$

$$\tau_p \;=\; \tau_m \cdot i_g \cdot \eta_g \cdot i_z \cdot \eta_z \;=\; 8.5\ Ncm \cdot 162 \cdot 0.73 \cdot 3.75 \cdot 0.9 \;=\; 33.92\ Nm$$

Torsion and efficiency of the flexible shaft has not been taken into account in these calculations!

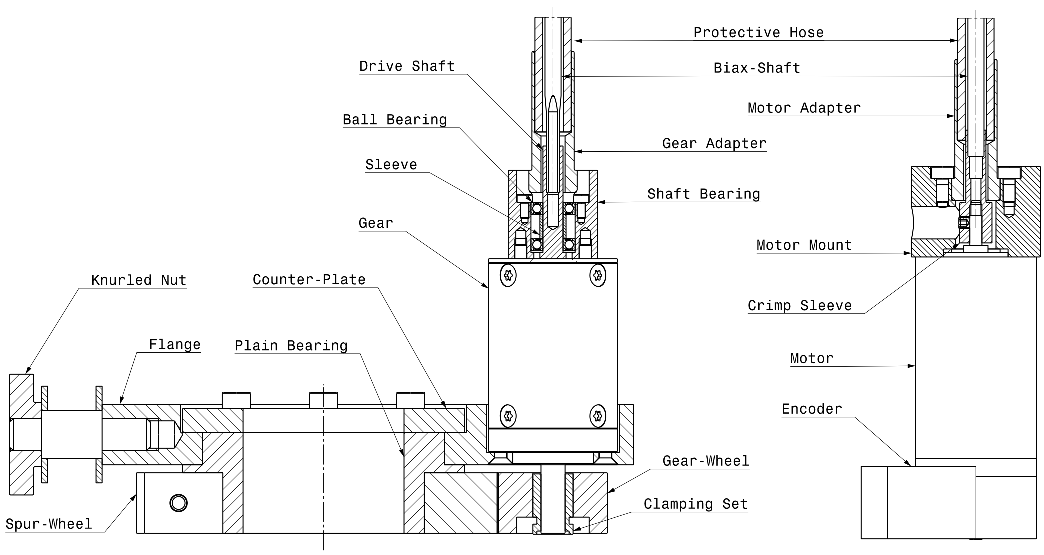

Figure 4.16: Sectional view of the rotary drive mechanism including the coupling of the shaft.

4.5 Actuation mechanism at the periphery

The main focus for the implementation of the drive mechanism at the periphery was primarily not set on the size and compactness, but rather a simple and functional drive unit was designed to determine and evaluate the feasibility and requirements of the single-port system. A modular and function-related actuation was built up depending on the pulling length of the bowden wires in individual subunits. Distal articulations, the bending section and the elbow joint, as well as the rotation of the manipulators with a pulling length of up to 15 mm were implemented equally. An additional unit was designed for the linear motion with a pulling length of 40mm.

4.5.1 Actuation unit for the deflecting and the elbow joint

Figure 4.17a shows the assembled platform comprising the three subunits for the actuation of the distal joints of the manipulators and the telescope. Conventional endoscope mechanisms have been used which are usually built into the handhold of an endoscope and operated manually by two handwheels. As shown in Figure 4.17b, two Karl-Storz endoscope steering mechanisms, each enabling the control of 2 DOFs, were mounted underneath each subunit. Each of the three distal joints and a total of 9 DOFs are controlled thereby. A further equal unit with 3 DOFs was used to control the rotation of the manipulators and the telescope.

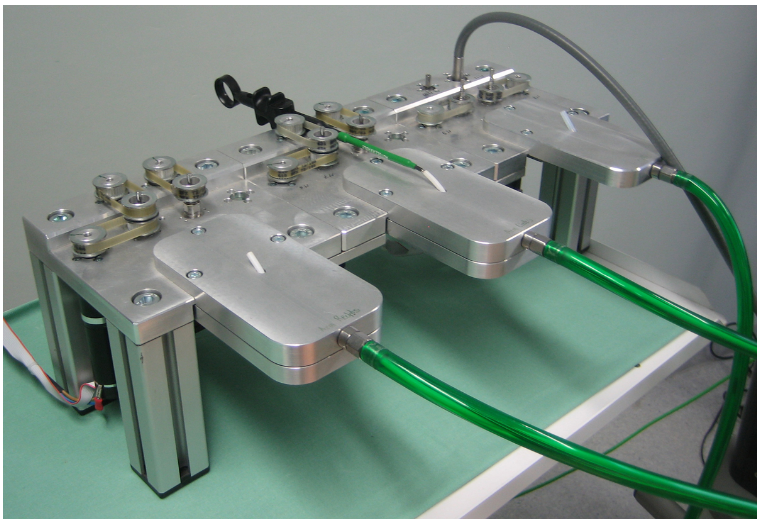

(a) Actuation unit for the deflecting and elbow joint of the manipulators

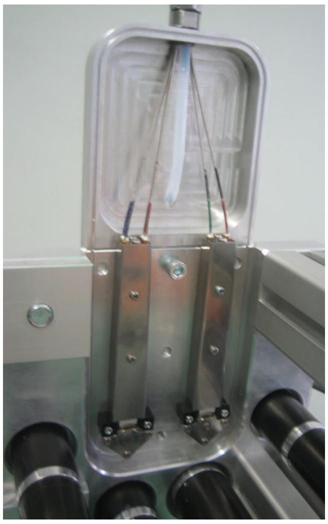

(b) Steering mechanism

Figure 4.17: Platform of the actuation mechanism including the drives of the deflectings and the elbow joints of the manipulators and the telescope (9 DOF)

In order to ensure gas tightness, a flexible plastic hose is attached on the manipulators and through them the bowden wires and the instrument channel are guided and mounted gastightly to the control unit. Therefore, a quick fastener coupling with integrated O-ring sealing was implemented on both ends of the plastic hose. Moreover, the bowden wire mechanism is covered by two plates with a seal in between. Each plate is mounted from one side on the platform, and the instrument channel is conducted through the top plate outward. A specific plug valve is foreseen as an intermediate solution for the introduction of the flexible instruments.

Figure 4.18 shows the sectional view through the middle of the drive mechanism. The Karl-Storz steering unit is realized by implementing a quill drive mechanism that provides the control of both joints on the same axis and from the same side. Both handwheels were replaced by two specific pulleys for the intended drive. The upper pulley on the inner shaft actuates the lower bowden wire and the lower pulley on the outer shaft actuates the upper bowden wire. Both motor drives are placed in 40 mm distance, 90° to each other and drive belts are used for the drive transmission in a ratio of 1:1.

A wire with a linkage part at both ends is wound one turn onto the underside of the outer and the inner shaft and firmly welded on the middle. The linkage parts of the steering mechanism are routed alongside a fixation block, where the controlled wires with the counterparts are attached. The bowden wire hoses are mounted, thereby, in the corresponding slots on the fixation block. A tension of the wires is achieved by screwing both ends of the linkage parts. The maximum possible motion length of ±15mm is determined by the length of the fixation block minus the length of the linkage and it can be reduced or adjusted by screwing a further part on the linkage.

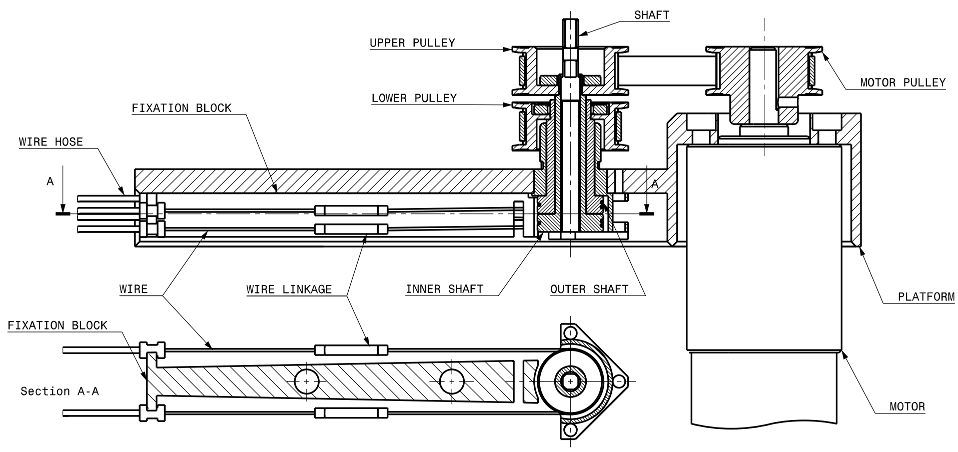

Figure 4.18: Sectional view of the drive unit and bowden wire mechanism for distal articulations

4.5.2 Actuation unit for the linear motion of the manipulators

The conventional steering of the Karl-Storz endoscope with a maximal pulling length of ±15mm is not sufficient for the control of the linear motion of the manipulators. Therefore, an additional platform was developed to translate the manipulators in the required working range of ±40mm. As can be seen in the sectional view in Figure 4.19a, the drive mechanism of the linear motion is implemented similar to the Karl-Storz steering. Instead of the implementation of a quill drive mechanism, a pair of bowden wires for one joint are controlled by one steering unit. A shaft for the wire-pulley with a diameter of 27mm is mounted by means of a ball bearing on the platform. The wire with the linkage on both ends is wound on the pulley and the welded pin at the middle of the wire is inserted into the corresponding hole in the pulley. The attachment of the wires and their adjustment is implemented in the same way as the Karl-Storz endoscope steering. After mounting the wires, the fixation block with the wires is covered by a sheet metal part. Figure 4.19b shows the platform from below with the three steering mechanisms that have been implemented parallel to each other.

The Maxon motor RE25 and the gear GP26 with the following characteristics was used for the drive of the linear motion: $n_m = 9550rpm$, $\tau_m = 26,7mNm$, $i_g = 128$, $\eta_g = 0.59$. The torque and speed on the gear shaft amounts: $n_g = 62,5rpm$, $\tau_g = 1,3Nm$. The provided force and speed for the linear motion of the manipulators is accordingly:

$$F_s = \tau_g/r = 1.3Nm/0.0132m = 98.5N$$

$$v_s = 2\pi \cdot r \cdot (n_g/60) = 2\pi \cdot 13.2mm \cdot (62.5/60)1/s = 86.4mm/s$$

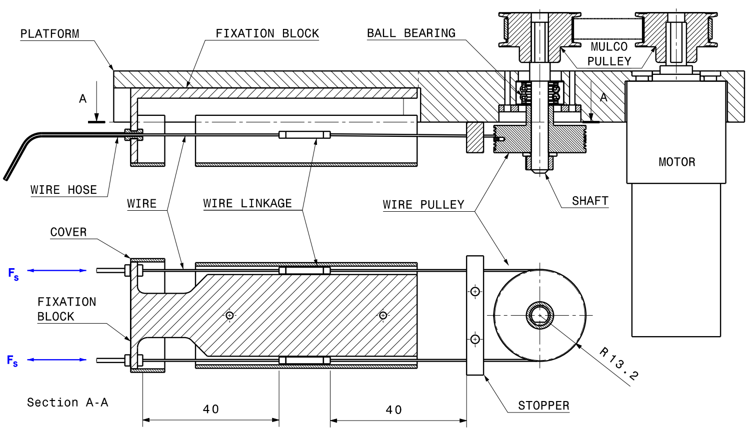

(a) Sectional view of the linear actuation mechanism

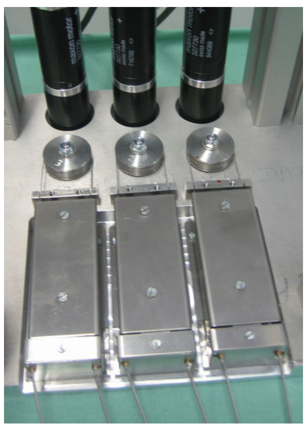

(b) Linear actuation unit

Figure 4.19: Platform for the linear motion of the manipulators and the telescope (3 DOF)

4.6 Hydraulic SoloAssist telemanipulator for guiding the single-port platform

SoloAssist is a mechatronic positioning system with fluid actuation that allows enhanced power transmission and positioning compared to other technologies (Figure 4.20b). The system was developed by the company, Aktormed, in cooperation with the research group MITI, Klinikum rechts der Isar, in Germany. Integrated pressure sensors for each actuation of the robot permit the manual pushing of the system at any time out of the operating field, which is a significant feature for patient safety. The implementation of nonmetallic materials such as carbon fiber in the upper part of the system with low level artifact allows intra-operative imaging. The manipulator resembles a human arm and has a working range of 360° in both directions of the base joint, an inclination up to 80° and penetration depth of 250 mm into the body. The system, with a weight of 18 kg, is simple to dock in various rail positions at the operating table and can be dismantled quick and easily.

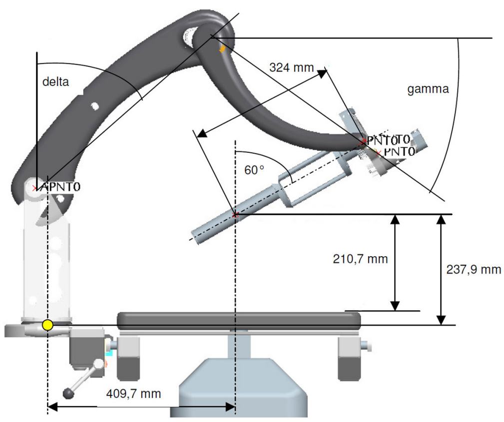

(a) Workspace analysis of the guiding system

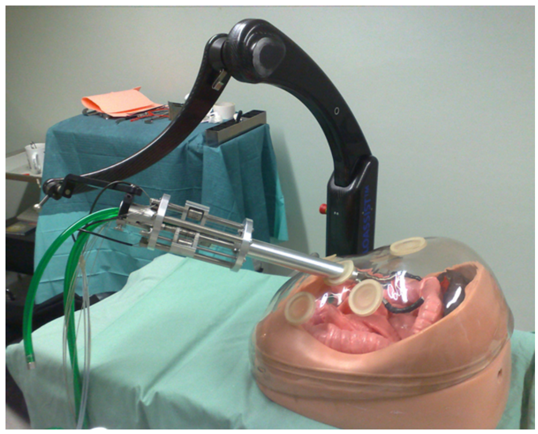

(b) SoloAssist guiding the single-port platform

Figure 4.20: SoloAssist hydraulic telemanipulator for guiding the single-port platform

For an optimal positioning, the SoloAssist system is calibrated at the trocar point which serves as a pivot. The defined invariant point allows the calculation of individual axial movements for tilting the telescope and performing circular motion. The system offers two control modes: Cartesian control, which is usually used to set the trocar point, and the invariant point control, where the X and Y-axis are replaced by tilting and circular motion referring to the invariant point and the Z-axis corresponds to zoom in and out function of the platform. A change between both modes can be achieved by means of a push-button on the control unit.

A joystick integrated on a laparoscopic handhold with exchangeable instruments, a small hand panel and a foot pedal are proposed input devices so far. For this research an UDP interface was set up to control the system by speech control [142]. The defined commands for the speech control are listed in the Table 4.2.

Table 4.2: Definition of the speech commands for the SoloAssist robot and its relation to Cartesian and invariant point control.

Command	left	right	forward	backward	down	up
Cartesian	x-	x+	y-	y+	z-	z+
Inv. point	tilt-	tilt+	cw. rot.	ccw. rot.	zoom+	zoom-

In a preliminary study, it was determined that the working range offered by the SoloAssist robot is sufficient to guide the single-port platform in the intended workspace (4.20a). However, as mentioned in Section 4.4, the SoloAssist had to be adjusted in order to carry the platform with a total weight of at least 3 kg instead of a light-weight telescope. An increase of the load capacity can be achieved by adjusting the pressure limiter of the hydraulic cylinders. The base joint provides enough force and was, therefore, not changed. In the standard configuration, the pressures for both of the other joints amounts to less than 20 bar and the system can carry loads up to 1 kg. The adjusting screw of the pressure limiter increases the pressure by 6.5 bar in one revolution (1mm). Both screws for lowering the system were screwed by further 5.9 revolutions to a final depth of 10 mm that corresponds to a pressure of approximately 57 bar and a load capacity of 3 kg.

Chapter 5

Kinematics and Control of the Single-Port System

This chapter presents the implemented kinematics of the bending section and the single-port manipulator. The programmed simulation for the evaluation of the system and kinematic analysis is also presented. Finally, the implemented solution of the low-level control is described. In the presented concept, our approach was to control the manipulators and the telescope independent of the guiding system. Therefore, the platform with the manipulators is guided first to the region of interest and then the surgery is accomplished with both manipulators. We accomplished the kinematic analysis of the system according to this approach. The distal tip of the platform inside the abdominal cavity is controlled with the described kinematic solution of the SoloAssist in Section A.2 that also includes the invariant point restriction. The determined manipulator kinematics enables a velocity-based task-space control of the instruments.

A distributed, modular control architecture, as shown in Figure 5.1, was conceived to control the single-port system. The high-level control forms the central control unit for all the modules. It gets, for example, the reference position from the master console and provides, after a path planning, the desired position and control mode for the low-level control. The real tool or joint position from the low-level control is the provided interface for the robot simulation. Furthermore, the high-level control also processes the GUI commands from the simulation as well as sensor and image data. The open source robotics library "cisst", developed at the John Hopkins University, is one possible solution for the implementation of such architectures [143]. An example for a distributed software framework for robotic surgery that uses the cisst library is published in [144]. The implemented low-level control and the simulation of the platform can

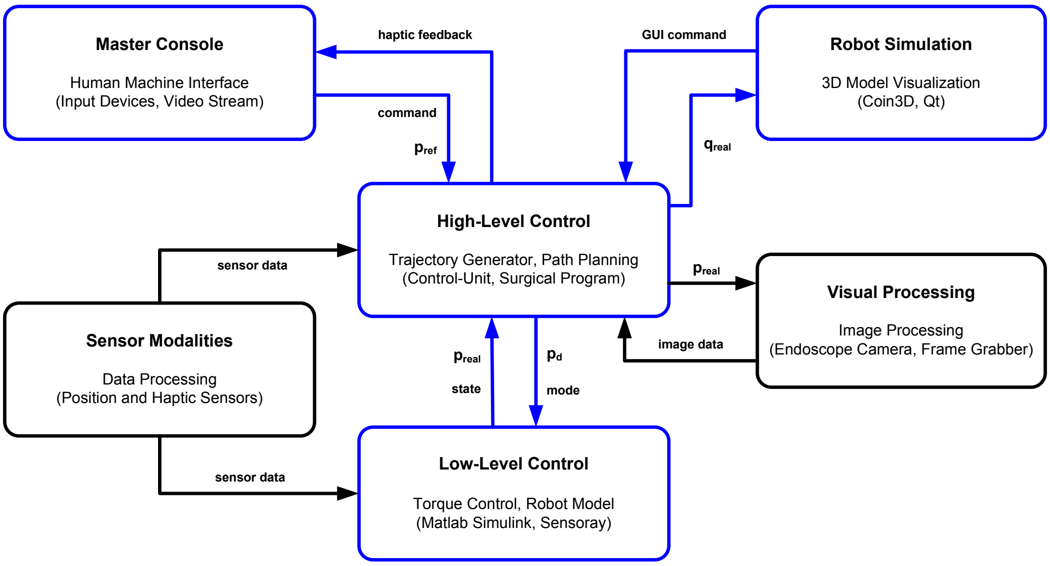

Figure 5.1: Concept of the control architecture for the single-port system. The high-level control forms the central control unit for all the modules. The provided and required interfaces p_{ref}, p_d and p_{real} are the reference, desired and real tool positions.

be integrated as modules in a similar architecture. By implementing the appropriate interfaces, the manipulators can be controlled over a higher-level control entity that provides the desired tool position. The simulation enables the visualization of a simplified 3D model of the platform that can also be integrated into the overall system.

5.1 Kinematics of the flexible bending section

The kinematics of the implemented bending section is required to determine the kinematics of the manipulator and the single-port system. The bending section of the Karl-Storz gastroscope with 2 DOFs consists of 20 parts. All of them are riveted together in a periodic arrangement and the distance between the hinges is 3.5mm. Figure 5.2 presents the configuration of the riveted joints. The bending section is mounted at the linkage part to the fore-arm tube and the deflection is realized by four bowden wires. Each of them is welded at the front part and guided through lugs in the parts. The bending of the 13 Z-hinges by ϑ permits a deflection of more than $\pm180°$ in the horizontal plane, and the bending of the 6 Y-hinges by ϕ, a deflection of more than $\pm150°$ in the vertical plane. A deflection in each plane is realized by two bowden wires, i.e. the hinges are not actuated individually.

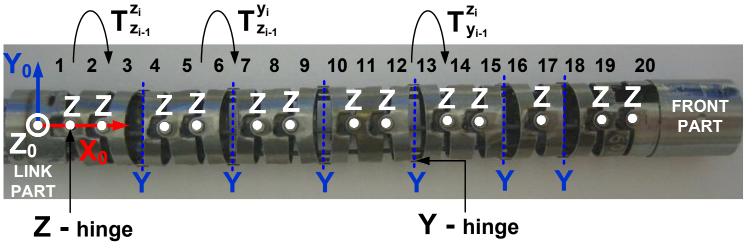

Figure 5.2: Bending section of the Karl-Storz gastroscope illustrating the configuration of the hinges and their orientations. The bending section comprises the three different "passive" joints Tzz, Tyz and Tzy.

There are different ways to describe the kinematics of bending sections [55]. The bending section of an endoscope has a quasi-constant curvature. In order to describe the kinematics close to the physical system, we used the approach published by Lipkin et al. [145]. For the determination of the instantaneous kinematics, we first consider the hinges as independent joints and then sum them up at the end in the two directions. The rotation angles of the tool tip in relation to the base frame results from the sum of all the ϑ_i angles about the Z_i hinges and the sum of all the ϕ_i angles about the Y_i hinges. The kinematics for the Karl-Storz bending section with $n = 19$ hinges is proposed subsequently. In these calculations, friction is overlooked and it is assumed that the individual hinges are bent in equal measure. The DH parameters for $i = 1, 2, \ldots, 19$ (hinge/joint number) are: $a_i = 3.5mm$, $d_i = 0$ and

$$\alpha_i = \begin{cases} 0 & for \quad i = \{1,2,5,8,11,14,19\} \\ \pi/2 & for \quad i = \{3,6,9,12,15,17\} \\ -\pi/2 & for \quad i = \{4,7,10,13,16,18\} \end{cases} \tag{5.1}$$

Using these three cases results in the following three transformation matrices between the frames.

$$T^{i}_{i-1} = \begin{cases} T^{z_i}_{z_{i-1}} = \begin{bmatrix} \cos(\vartheta) & -\sin(\vartheta) & 0 & a \\ \sin(\vartheta) & \cos(\vartheta) & 0 & 0 \\ 0 & 0 & 1 & 0 \\ 0 & 0 & 0 & 1 \end{bmatrix} & \text{for} \quad \alpha_i = 0 \\ T^{z_i}_{y_{i-1}} = \begin{bmatrix} \cos(\phi) & -\sin(\phi) & 0 & a \\ 0 & 0 & -1 & 0 \\ \sin(\phi) & \cos(\phi) & 0 & 0 \\ 0 & 0 & 0 & 1 \end{bmatrix} & \text{for} \quad \alpha_i = \frac{\pi}{2} \\ T^{y_i}_{z_{i-1}} = \begin{bmatrix} \cos(\vartheta) & -\sin(\vartheta) & 0 & a \\ 0 & 0 & 1 & 0 \\ -\sin(\vartheta) & -\cos(\vartheta) & 0 & 0 \\ 0 & 0 & 0 & 1 \end{bmatrix} & \text{for} \quad \alpha_i = -\frac{\pi}{2} \end{cases} \tag{5.2}$$

T_{i-1}^{i} represents the homogeneous transformation matrix from joint $\{i-1\}$ to $\{i\}$. With the given individual transformation matrices, the forward kinematics is calculated as follows:

$$T_0^{19} = T_{z_0}^{z_1} \cdot T_{z_1}^{z_{18}} \cdot T_{z_{18}}^{z_{19}} \quad \text{where} \quad T_{z_1}^{z_{18}} = T_{z_1}^{z_2} \cdot T_{z_2}^{y_3} \cdot T_{y_3}^{z_4} \cdot \ldots \ldots T_{y_{15}}^{z_{16}} \cdot T_{z_{16}}^{y_{17}} \cdot T_{y_{17}}^{z_{18}} \tag{5.3}$$

For the determination of the bending kinematics, which is integrated into a kinematic chain (see Section 5.2.1), the transformation matrix $T_{z_1}^{z_{18}}$ remains the same. The twist velocity of the bending section at the end frame relative to the base frame can be calculated using the $6 \times n$ Jacobian matrix J_d and the $n \times 1$ vector $\dot{\theta}_d$ with the hinge angle rates.

$$t_0^n = \begin{bmatrix} v_0^n \\ w_0^n \end{bmatrix} = J_d \cdot \dot{\theta}_d \quad \text{where} \quad \dot{\theta}_d = \begin{bmatrix} \dot{\vartheta} & \dot{\vartheta} & \dot{\phi} & \ldots & \dot{\vartheta} \end{bmatrix}^T \quad \text{and} \tag{5.4}$$

$$J_d = \begin{bmatrix} z_0 \times p_0^n & \ldots & z_i \times p_i^n & \ldots & z_n \times p_n^n \\ z_0 & \ldots & z_i & \ldots & z_n \end{bmatrix} \tag{5.5}$$

t_0^n is the twist of the bending section from the joint $\{0\}$ to $\{n\}$ and p_i^n is the position vector from the joint $\{i\}$ to $\{n\}$. Grouping all the partial velocities into the specific directions z or y reduces the twist equation to:

$$t_0^n = \dot{\vartheta} \cdot \sum_{i=j} \begin{bmatrix} z_i \times p_i^n \\ z_i \end{bmatrix} + \dot{\phi} \cdot \sum_{i=k} \begin{bmatrix} z_i \times p_i^n \\ z_i \end{bmatrix} \quad \text{where} \quad \begin{aligned} j &= 1, 2, 4, 5, 7, 8, 10, 11, 13, 14, 16, 18, 19 \\ k &= 3, 6, 9, 12, 15, 17 \end{aligned} \tag{5.6}$$

For the calculation of the twist relative to the bending section tip, all the partial velocities are expressed in the end frame n. The vector z_i can be expressed in the frame n as follows:

$${}_n z_i = T_n^i \cdot {}_i z_i = (T_i^n)^T \cdot {}_i z_i \qquad \text{where} \qquad {}_i z_i = \begin{bmatrix} 0 \ 0 \ 1 \end{bmatrix}^T \tag{5.7}$$

The angular velocities of the axis z_n and y_n that are of interest to determine the two unknown angles ϑ and ϕ of the bending section, can be expressed in the end frame n as:

$$\begin{bmatrix} ({}_n w_0^n)_{y_n} \\ ({}_n w_0^n)_{z_n} \end{bmatrix} = \begin{bmatrix} \sum_{i=k(y)} {}_n z_i & \sum_{i=j(z)} {}_n z_i \\ \sum_{i=k(y)} {}_n z_i & \sum_{i=j(z)} {}_n z_i \end{bmatrix} \cdot \begin{bmatrix} \dot{\phi} \\ \dot{\vartheta} \end{bmatrix} \tag{5.8}$$

Grouping all the velocity indices of both angles results in a 2×2 matrix that can be easily inverted to calculate the velocity of the 2 DOF bending section at the tip.

5.2 Kinematics of the single-port manipulator

The kinematics of the developed single-port manipulator with 6 DOFs in total, including the rotation of the instruments, is calculated using the described kinematics of the bending section. Furthermore, the instantaneous kinematics is determined to achieve a velocity based control of the tool tip, since the inverse kinematics of the manipulator has no unique solution.

Figure 5.3 illustrates the implemented kinematics of the manipulator with the individual joints. The kinematics of the bending section is determined, first, relative to the base of the bending section {3} and then mapped to the platform base {0}, which is placed at the middle of the distal tip of the platform. All the hinges of the bending section are considered as independent joints and reduced at the end to the joints θ_4/θ_5 of the manipulator. The sum of all the partial angles, ϑ_i, results in the joint, θ_4, and the sum of all the partial angles, ϕ_i, in the joint, θ_5. A rotation of the flexible instruments is represented by θ_6.

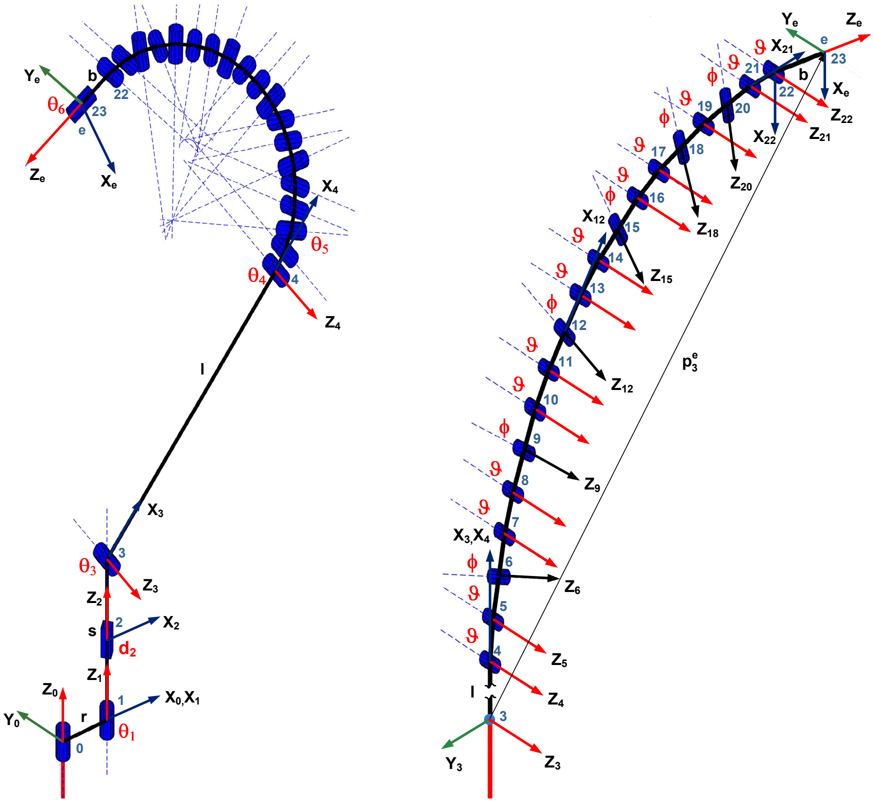

(a) Kinematics of the manipulator

(b) Kinematics of the bending section

Figure 5.3: Schematic drawing of the manipulator and the bendable section kinematics generated with the robotic toolbox in Matlab [146]. It illustrates the individual joints and the used coordinate axis.

The DH table of the manipulator is presented in Table 5.1. The passive hinges of the bending section are represented by joints 4 to 22. A complete joint data of the periodic hinge configuration of the bending section has already been presented in the previous section. The distances between the joint frames are:

$$r = 9mm \qquad l = 54.5mm \qquad a = 3.5mm \qquad b = 7.5mm$$

Table 5.1: DH table of the single-port manipulator: Joints 4 to 22 represent the hinges of the bending section that correspond to θ_4/θ_5 and joint 23 corresponds to θ_6 of the manipulator.

i	1	2	3	4	5	6	...	20	21	22	23 (e)
α_i	0	0	$\pi/2$	0	0	$\pi/2$	...	$\pi/2$	$-\pi/2$	0	$\pi/2$
a_i	r	0	0	l	a	a	...	a	a	a	0
d_i	0	$d_2 + s$	0	0	0	0	...	0	0	0	b
θ_i	θ_1	0	$\theta_3 + \pi/2$	ϑ	ϑ	ϕ	...	ϕ	ϑ	$\vartheta - \pi/2$	θ_6

5.2.1 Forward kinematics

The forward kinematics of the single-port manipulator T_0^e is computed using the transformation matrix T_0^3 for the first three joints, T_3^{22} for the two joints of the bending section and T_{22}^e for the rotation joint of the instrument. The transformation matrix from base $\{0\}$ to the joint $\{3\}$ is:

$$T_0^3 = \begin{bmatrix} -\cos(\theta_1)\sin(\theta_3) & -\cos(\theta_1)\cos(\theta_3) & \sin(\theta_1) & r \\ -\sin(\theta_1)\sin(\theta_3) & -\sin(\theta_1)\cos(\theta_3) & -\cos(\theta_1) & 0 \\ \cos(\theta_3) & -\sin(\theta_3) & 0 & d2+s \\ 0 & 0 & 0 & 1 \end{bmatrix} \tag{5.9}$$

The transformation matrix T_3^{22}, comprising the 19 passive joints of the bending section, is:

$$T_3^{22} = T_{z_3}^{z_4} \cdot T_{z_4}^{z_{21}} \cdot T_{z_{21}}^{z_{22}} \tag{5.10}$$

The transformation matrix $T_{z_4}^{z_{21}}$ is equal to the transformation matrix $T_{z_1}^{z_{18}}$ in the equation 5.3 and the fist and last transformation matrix of the bending section are:

$$T_{z_3}^{z_4} = \begin{bmatrix} \cos(\vartheta) & -\sin(\vartheta) & 0 & l \\ \sin(\vartheta) & \cos(\vartheta) & 0 & 0 \\ 0 & 0 & 1 & 0 \\ 0 & 0 & 0 & 1 \end{bmatrix} \qquad T_{z_{21}}^{z_{22}} = \begin{bmatrix} \sin(\vartheta) & \cos(\vartheta) & 0 & a \\ -\cos(\vartheta) & \sin(\vartheta) & 0 & 0 \\ 0 & 0 & 1 & 0 \\ 0 & 0 & 0 & 1 \end{bmatrix} \tag{5.11}$$

The transformation from the last hinge of the bending section to the instrument (e) is:

$$T_{22}^{e} = \begin{bmatrix} \cos(\theta_6) & -\sin(\theta_6) & 1 & 0 \\ 0 & 0 & 0 & b \\ -\sin(\theta_6) & -\cos(\theta_6) & 0 & 0 \\ 0 & 0 & 0 & 1 \end{bmatrix} \tag{5.12}$$

Accordingly, the forward kinematics of the manipulator is computed as follows:

$$T_0^e = T_0^3 \cdot T_{z_3}^{z_4} \cdot T_{z_4}^{z_{21}} \cdot T_{z_{21}}^{z_{22}} \cdot T_{22}^e \tag{5.13}$$

5.2.2 Instantaneous kinematics

The following notation is used for the calculation of the end-effector twist: ${}_0t_i^e$ is the twist of joint {i} with respect to joint {e} expressed in joint {0}. The twist of the developed single-port manipulator is accordingly:

$${}_0t_0^e = {}_0t_0^3 + {}_0t_3^{22} + {}_0t_{22}^e \tag{5.14}$$

The twist resulting from the first three joints of the manipulator is computed as follow:

$$J_1 = \begin{bmatrix} z_1 \times (p_0^e - p_0^1) \\ z_1 \end{bmatrix} \qquad J_2 = \begin{bmatrix} z_2 \\ 0 \end{bmatrix} \qquad J_3 = \begin{bmatrix} z_3 \times (p_0^e - p_0^3) \\ z_3 \end{bmatrix} \tag{5.15}$$

$${}_0t_0^3 = \begin{bmatrix} {}_0v_0^3 \\ {}_0w_0^3 \end{bmatrix} = \begin{bmatrix} J_1 & J_2 & J_3 \end{bmatrix} \cdot \begin{bmatrix} \dot{\theta}_1 & \dot{d}_2 & \dot{\theta}_3 \end{bmatrix}^T \tag{5.16}$$

The twist of the bending section with respect to the joint {3} is given by the equation 5.4. By using this equation, the twist of the bending section with respect to the joint {0} is:

$${}_0t_3^{22} = \begin{bmatrix} {}_0v_3^{22} \\ {}_0w_3^{22} \end{bmatrix} = E \cdot {}_3t_3^{22} = E \cdot J_d \cdot \dot{\theta}_d \qquad \text{with} \qquad E = \begin{bmatrix} R_0^3 & 0 \\ 0 & R_0^3 \end{bmatrix} \tag{5.17}$$

According to the definition of the equation 5.6, by summing up the partial angles, the twist of the bending section with respect to the manipulator base is:

$${}_0t_3^{22} = \dot{\vartheta} \cdot E \cdot \sum_{i=j} \begin{bmatrix} z_i \times p_i^e \\ z_i \end{bmatrix} + \dot{\phi} \cdot E \cdot \sum_{i=k} \begin{bmatrix} z_i \times p_i^e \\ z_i \end{bmatrix} \tag{5.18}$$

$$j = 4, 5, 7, 8, 10, 11, 13, 14, 16, 17, 19, 21, 22 \qquad \text{and} \qquad k = 6, 9, 12, 15, 18, 20$$

This results for the two individual joints θ_4/θ_5 of the manipulator the following Jacobians:

$$J_4 = E \cdot \sum_{i=j} \begin{bmatrix} z_i \times p_i^e \\ z_i \end{bmatrix} \quad \text{and} \quad J_5 = E \cdot \sum_{i=k} \begin{bmatrix} z_i \times p_i^e \\ z_i \end{bmatrix} \tag{5.19}$$

The twist of the bending section mapped to the manipulator base is consequently:

$$ {}_0t_3^{22} = \begin{bmatrix} J_4 & J_5 \end{bmatrix} \cdot \begin{bmatrix} \dot\theta_4 & \dot\theta_5 \end{bmatrix}^T \tag{5.20}$$

The twist of the last joint (rotation of the instrument) is computed as follow:

$$ J_6 = \begin{bmatrix} z_e \times (p_e - p_e) \\ z_e \end{bmatrix} = \begin{bmatrix} 0 \\ z_e \end{bmatrix} = \begin{bmatrix} 0 \\ R_0^e \cdot \hat e_3 \end{bmatrix} \qquad \text{with} \qquad \hat e_3 = \begin{bmatrix} 0 & 0 & 1 \end{bmatrix}^T \tag{5.21}$$

$$ {}_0t_{22}^e = J_6 \cdot \dot\theta_6 \tag{5.22}$$

The twist of the manipulator is given by the sum of the partial twists of the equations 5.16, 5.20 and 5.22.

$$ {}_0t_0^e = \begin{bmatrix} J_v \\ J_w \end{bmatrix} \cdot \dot\theta = J_m \cdot \dot\theta \qquad \text{with} \qquad \dot\theta = \begin{bmatrix} \dot\theta_1 & \dot d_2 & \dot\theta_3 & \dot\theta_4 & \dot\theta_5 & \dot\theta_6 \end{bmatrix}^T \tag{5.23}$$

$$ J_m = \begin{bmatrix} z_1 \times p_1^e & z_2 & z_3 \times p_3^e & E \cdot \sum_{i=j} z_i \times p_i^e & E \cdot \sum_{i=k} z_i \times p_i^e & 0 \\ z_1 & 0 & z_3 & E \cdot \sum_{i=j} z_i & E \cdot \sum_{i=k} z_i & R_0^e \cdot \hat e_3 \end{bmatrix} \tag{5.24}$$

The 6×6 Jacobian J_m of the manipulator can be inverted to calculate the joint velocities $\dot\theta$ by a given twist of the end-effector.

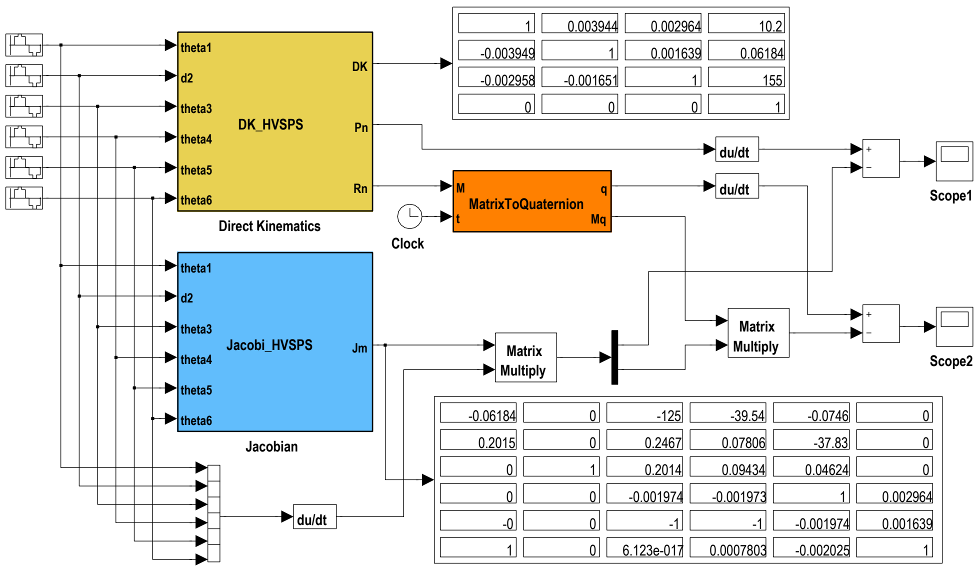

Figure 5.4: Matlab-Simulik program for the numeric verification of the Jacobian. DK_HVSPS computes the forward kinematics and Jacobi_HVSPS the Jacobian of the manipulator. In MatrixToQuaterenion, the quaternions q and the matrix M_q are determined from the rotation matrix R_e

5.2.3 Numeric verification of the Jacobian

Because the inverse kinematics of the manipulator can not be determined, a numerical approach was chosen to verify the Jacobian. For the verification of the Jacobian J_m, the computed twist with the Jacobian was subtracted from the twist that was computed with the forward kinematics. As shown in Figure 5.4, the verification of the Jacobian, i.e. the equation 5.23, was implemented in Matlab-Simulink. Sine waves with the maximal workspace of the individual joint as amplitude, a frequency of $\pi/5\ rad/s$ and a sampling time of $5\ ms$ was used as input. First the linear velocity of the tool tip was computed and verified with the following equation:

$$\frac{d}{dt}p_e - J_v \cdot \frac{d}{dt}\theta = \delta \qquad \text{and} \qquad \lim_{\Delta t \to 0} \delta = 0 \tag{5.25}$$

θ is the vector of the joint angles and p_e the vector of the tool tip position that is determined with the forward kinematics. δ is the error and depends on the sampling time. The plot of the linear velocity error (Scope1) of the tool tip is shown in Figure 5.5. The error is reduced by decreasing the sampling time and at a sampling time of $5\ ms$, the error is below $\pm\ 2.1\ mm/s$.

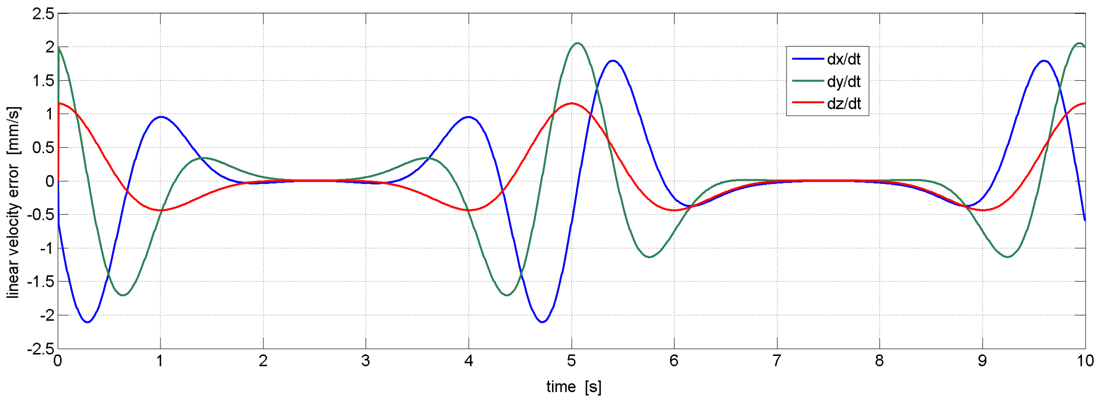

Figure 5.5: Error plot of the linear velocity of the tool tip.

We used quaternions for the verification of the angular velocity, since the calculation with Euler angles are not defined at all angles (singular configuration). Therefore, the quaternions were determined with the forward kinematics and compared with the calculated angular velocity. The time derivative of the quaternion ϵ can be related to the angular velocity vector w as:

$$\frac{d}{dt}\epsilon - M_\epsilon \cdot \begin{bmatrix} \omega_x \\ \omega_y \\ \omega_z \end{bmatrix} = \delta \qquad \text{with} \qquad M_\epsilon = \frac{1}{2} \cdot \begin{bmatrix} -\epsilon_1 & -\epsilon_2 & -\epsilon_3 \\ \epsilon_0 & \epsilon_3 & -\epsilon_2 \\ -\epsilon_3 & \epsilon_0 & -\epsilon_1 \\ \epsilon_2 & -\epsilon_1 & -\epsilon_0 \end{bmatrix} \tag{5.26}$$

The plot of the angular velocity error (Scope2) of the tool tip is shown in Figure 5.6. Similar to the error of the linear velocity, the angular velocity error is decreasing by reducing the sampling time. As shown in the figure, at a sampling time of 5 ms, the angular velocity error in quaternions is below $\pm$ 0.02 $1/s$.

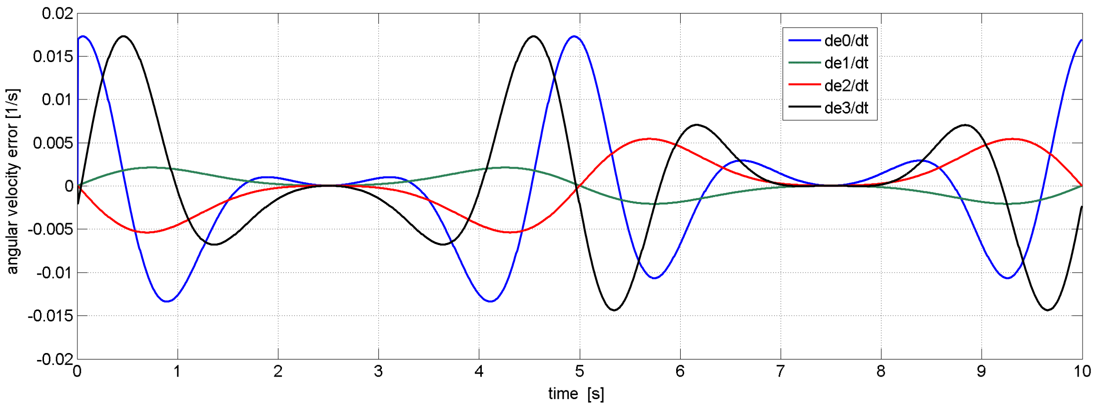

Figure 5.6: Error plot of the angular velocity of the tool tip in quaternions.

5.3 Simulation and kinematic analysis of the system

The simulation of the single-port manipulator was programmed in regards to the parallel evaluation of the hardware development, system functionalities and teaching facilities. This program was integrated on an independent, stand-alone computer to provide the visualization of the controlled platform and the intended interaction by using a GUI. The main reasons for this simulation are:

- Evaluation and optimization of the platform design
- Development of new surgical instruments and kinematics
- Identification of appropriate man-machine interfaces
- User training for the physicians

The simulation of the complete surgical scenario, with the single-port manipulator attached to the SoloAssist and mounted on an operating table, was implemented using the Coin3D open source library. As shown in Figure 5.7a, the model of the single-port platform comprises a simplified one-to-one replica of the physical system. The simulation of the bowden wires and their friction is not implemented in the current version. A collision of the manipulators in the implemented simulation is avoided by using the provided collision detection in the Coin3D library. This feature is also used, for example, for the detection of the interaction between the instruments and the spheres as shown in Figure 5.7b. The workspace of the manipulators, kinematic structure of the platform and motion modalities were evaluated with this simulation.

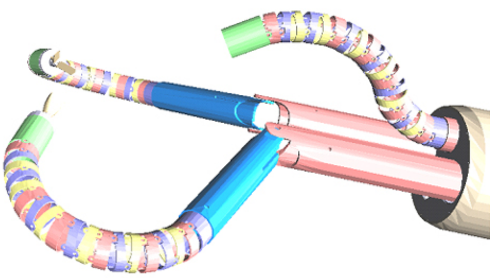

(a) Distal view of the simulated platform

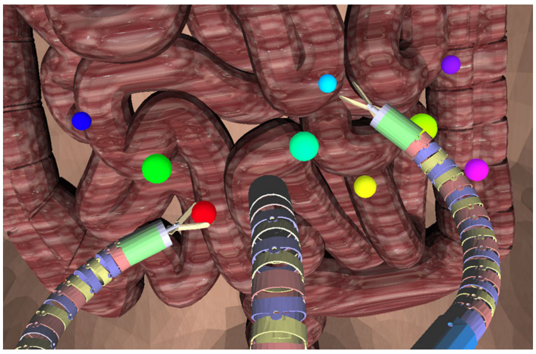

(b) Evaluation scenario of the simulation

Figure 5.7: Simulation environment for the evaluation of the platform and the kinematics.

Moreover, a pick-and-place scenario was programmed for the purpose of training and teaching the physicians. In this training exercise, surgeons had to grasp spheres with the instruments and place them at a predefined position. The kinematic model of the manipulator, as defined in Section 5.2, was implemented and evaluated in this simulation. A common velocity-based control, as shown in Figure 5.8, was implemented in a model-view-controller paradigm to evaluate the task-space control of the instruments. The 6 DOF position and orientation of the instrument tip and the grasping function are operated by using a SpaceNavigator from 3Dconnexion. At the moment, the simulation works independent to the hardware. It is planned to integrate them together in order to also enable an on-line visualization of the physical system.

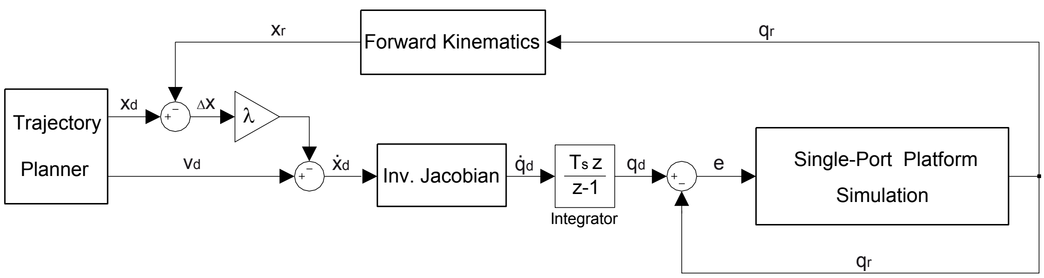

Figure 5.8: Velocity-based control of the single-port manipulator. A basic velocity profile is used to control the simulation of the platform.

5.4 Low-level control of the single-port platform

The low-level control of the system was implemented in cooperation with the Institute of Automatic Control Engineering at the Technische Universität München. As a stand-alone unit, it provides the real-time control of the integrated Maxon motors of the single-port platform. An existing system environment of a Linux kernel with RTAI real-time application is used for the implementation of the control. Moreover, Matlab-Simulink is used to realize the closed-loop control of the individual motor drives. The implemented low-level control of the manipulators was evaluated with two joysticks as input devices.

5.4.1 Structure of the control hardware

Figure 5.9a shows the realized control hardware of the platform. In its current state, the entire system provides the control of 16 motor drives in total. A PC with the real-time Linux kernel and 4 integrated Sensoray 626 PCI I/O boards, 16 ADS 50/5 Maxon 4Q-DC servo-amplifiers and a Statron 3256.1 ($0-36\ VDC/0-40\ A$) DC power supply are integrated in a 19-inch rack. Each Sensoray board enables the control of 4 motors. The encoder signals of the motors are fed directly over these cards to the computer, and a current control is realized with the Maxon servo-amplifiers. A schematic design of the control structure with four motor drives is shown in Figure 5.10. The servo-amplifiers are run in current mode and the input voltage from -10V to 10V is controlled over the DAC output of the Sensoray board.

5.4.2 Joint-space control of the manipulators with two joysticks.

As shown in Figure 5.10, we implemented and evaluated a joint-space control of both manipulators by using two joysticks as input devices. The implemented Matlab-Simulink program with a closed-loop control of one motor is shown in Figure 5.11. A PD controller is used for the motors and the values of $k_p = 10$ and $k_d = 800$ were determined as optimal for the control of the manipulators without load. The joystick with a USB interface delivers a signal of -1. . . 1 that is multiplied with a conversion factor to limit the range according to the joint space.

The friction and backlash resulting from the bowden wires and the load dependency of the manipulator are not considered in the implemented control. A velocity-based task-space control of the manipulators with the kinematic model, as described in Section 5.3, can be achieved by implementing an adequate interface in Matlab-Simulink. We plan to determine a dynamic model comprising the friction and load dependency close to the physical system.

(a) Control hardware integrated in a 19-inch rack

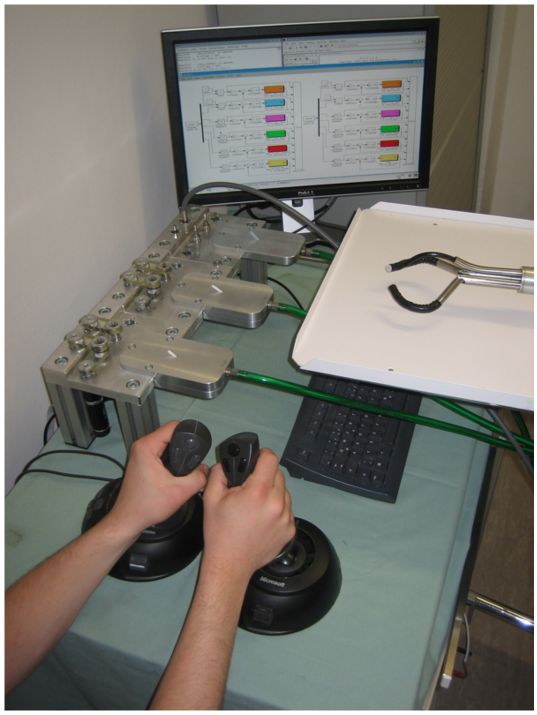

(b) Control of the manipulators with two joysticks

Figure 5.9: Control hardware of the single-port platform and evaluation of the control with two joysticks.

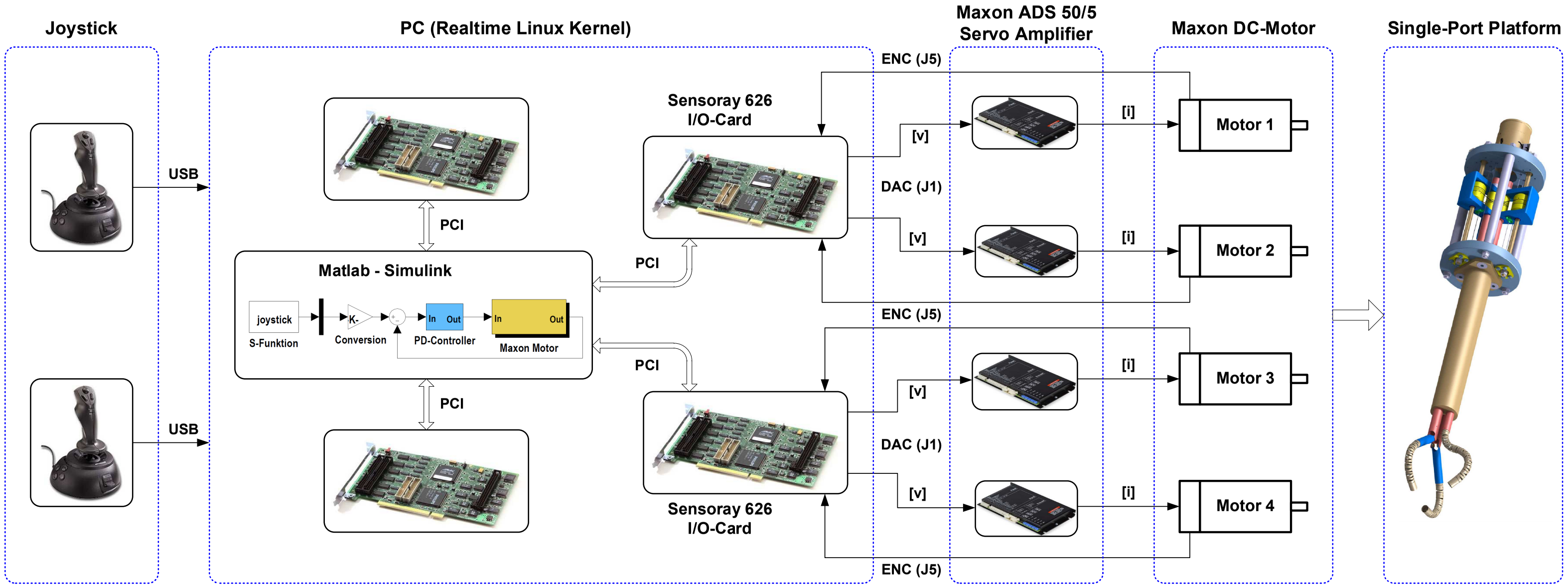

Figure 5.10: Schematic design of the realized low-level control of the single-port platform.

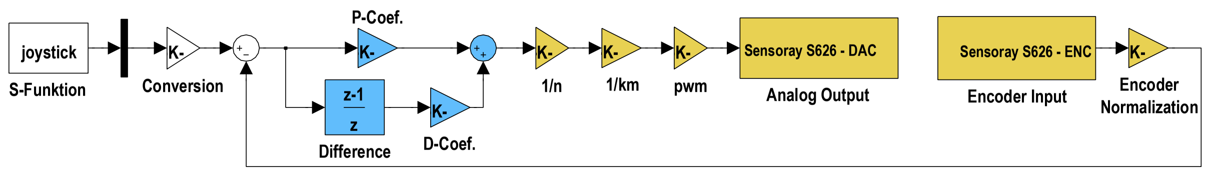

Figure 5.11: Matlab-Simulink program of the implemented closed-loop control for one motor that is actuated by a joystick.

Chapter 6

Evaluations

6.1 Measurement of the working range

The working range of the manipulators can be defined by means of the kinematic structure; however, there is some uncertainty due to the bowden wire actuation of the joints and, in particular, the bendable section with multiple hinges. Therefore, the working range of the manipulators was determined first theoretically and, thereafter, individual measurements were carried out in order to identify the deviations of the bendable section or the elbow joint. In these measurements, we focused mainly on the distal three degrees of freedom that are crucial for the workspace of the system and, respectively, on the intervention in the abdominal cavity. Since the manipulators have the same kinematic structure, the measurements were only carried out on one manipulator.

6.1.1 Set-up of the measurement

The Aurora electormagnetic tracking system (NDI, Canada) was used to carry out the workspace measurements of the manipulator. The 5 DOF sensors of this system, each with a diameter of 2mm, were small enough to mount into the manipulator. A magnetic field generator generates a cubic field with a side length of 50 cm at the front in which the measurements are taking place. According to the specification of the manufacturer, the accuracy of the tracking system is less than 1mm. The magnetic sensors are connected over the sensor interface (signal amplifier) to the system control unit. The tracing system is controlled over a PC, where the measured data are simultaneously written in a text file and evaluated thereafter.

Two sensors were required to measure the working range of the manipulators. One sensor was mounted through the manipulator at the tip of the bendable section in order to measure the motions in relation to the second sensor, which was defined as a reference and mounted on the upper-arm tube (Figure 6.1). The center of the hollow "elbow" joint was defined as the origin for the working range and the motions were analyzed in relation to it. The measured points were vertically displaced by 7mm (6mm radius of upper-arm tube plus 1mm radius of the sensor), because the sensor could not be mounted into the articulated "elbow" joint. This displacement was considered in the analysis of measured data. The origin of the cylindrical sensor is located in the middle of the radial coil. For the determination of the origin in the length, we held two sensors against each other and measured a distance of 12mm. Consequently, the origin is located 6mm from the tip and the sensors were mounted accordingly.

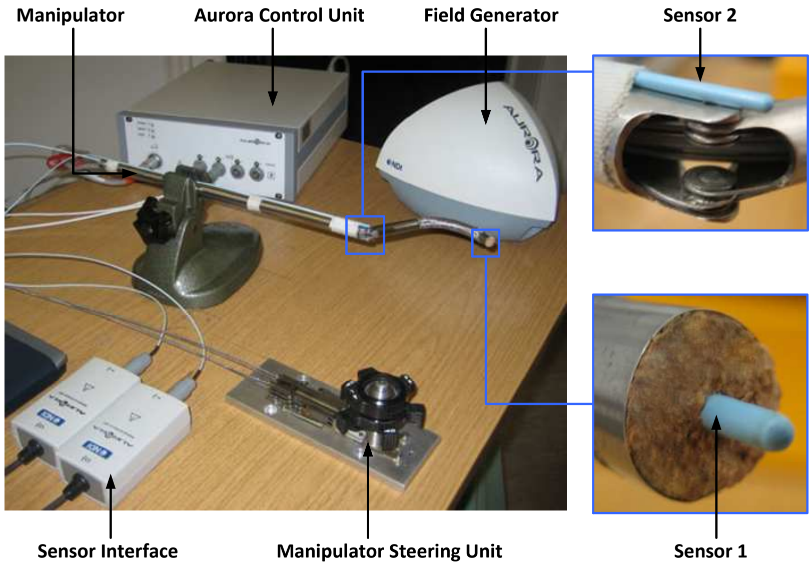

Figure 6.1: Electromagnetic tracking set-up for the workspace measurements.

Five series of measurements have been carried out for this evaluation. In the first measurements, the working range of the bending section was measured in the horizontal as well as in the vertical plane. Thereafter, the maximum workspace of the tool tip was measured in the horizontal plane by the actuation of the elbow joint together with the bending section. Finally, a grid of the maximal working range and the surface of the tool tip by motion of the three distal joints was measured to generate a polygon mesh of the workspace. The measurements with the largest deviations are described, subsequently, in comparison to the theoretical workspace.

6.1.2 Workspace of the bending section

The theoretical workspace of the gastroscope bending section (Karl-Sorz, Germany) is determined according to its kinematics. As described in Section 4.1.1 the bending section has 13 hinges in the horizontal and 6 hinges in the vertical plane that enable a bending of at least ±180° horizontally and ±150° vertically. The hinges lie 3.5mm from each other and the total length of the bending section is 75mm, including the front and base part. For the theoretical workspace, it was assumed that individual hinges bend in an equal angle by pulling the bowden wire attached on the front part. Figure 6.3a shows the bending curves of the bending section in the horizontal (XZ) and the vertical (YZ) plane and Figure 6.3b shows the entire workspace of the bending section that can be attained with the tool tip.

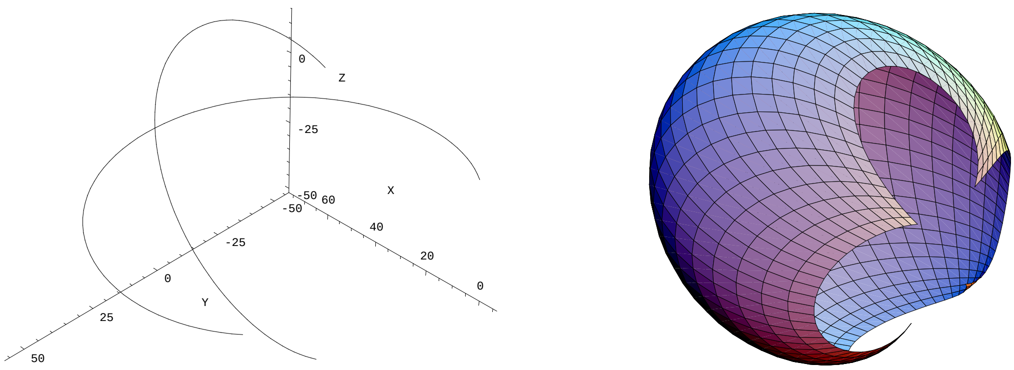

(a) Bending curves in the XZ/YZ-plane

(b) Surface of the entire workspace

Figure 6.2: Theoretical workspace of the gastroscope bending section.

In order to achieve a quantifiable comparison, we measured the trajectory of the deflecting tip in the horizontal and vertical plane and evaluated the deviation to the theoretical curves. Figure 6.3a presents the measurement in the horizontal plane. Apart from the two larger deviations, 3.5mm at the maximum on the left and 2.7mm on the right side, the measured trajectory is fairly accurate. As it can be seen in the figure, the deflectings could be bent up to ±200°, which is by far more than the specified value of ±180°. The equivalent measurement in the vertical plane is presented in Figure 6.3b. The larger deviations are here, at the two ends of the workspace and the measured trajectory deviates by 4.9mm at the upper end and 2.8mm at the lower end. A larger deflection, 180° upwards and 165° downwards, could be also achieved at this plane, however, a bending of more than ±150° deviates significantly from the theoretical curve.

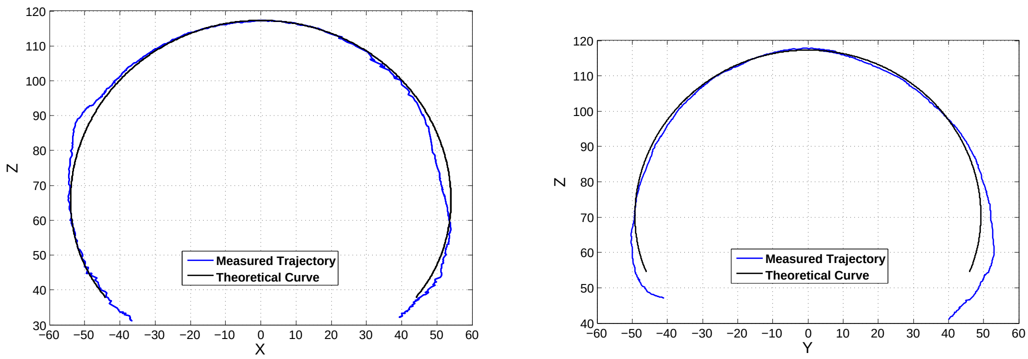

(a) Workspace in the horizontal plane

(b) Workspace in the vertical plane

Figure 6.3: Measured workspace of the bending section in the horizontal and vertical planes.

6.1.3 Workspace of the single-port manipulator

For the determination of the theoretical workspace of the manipulator, the maximal achievable bending angle of the bending section was adapted according to the measured values. The workspace that is obtained with the bending of the elbow joint by ±90° and the bending section by ±200° in the horizontal plane is presented in Figure 6.4a. The tridimensional workspace of the three distal DOFs, as shown in Figure 6.4b, is obtained by including the deflection of the bending section in the vertical plane. The illustrated surface is determined by the combination of three partial surfaces that presents the individual maximum working ranges. This includes the surface, which is achieved by horizontal deflection of the elbow joint by ±90° and vertical deflection of the bending section by +180°/-165°, as well as both surfaces achieved by the deflection of the bending section vertically by +180°/-165° and horizontally by +200° on the left side and -200° on the right side.

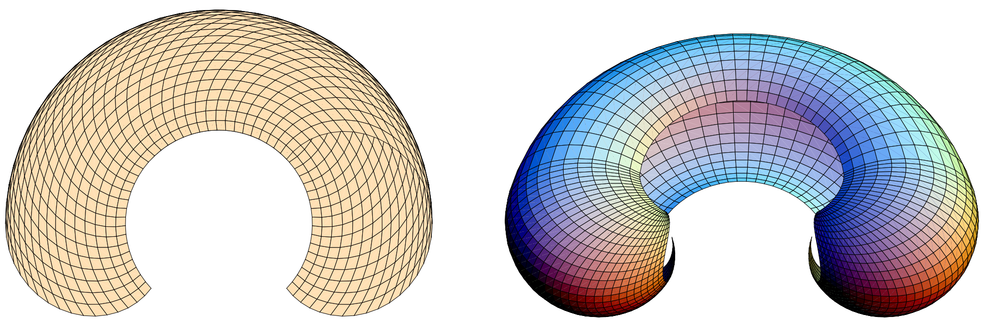

(a) Horizontal workspace of the manipulator

(b) Surface of the theoretical workspace

Figure 6.4: Surfaces of the theoretical workspace of the manipulator determined with the kinematics

With the measurements performed here, the trajectory of the manipulator tip at the outer border of the working range was determined in the horizontal plane and compared with the theoretical workspace. The red hatched surface in Figure 6.5 presents the crescent shaped workspace that is determined by the assumption of 122mm length for the upper-arm tube including the bending section. The blue line illustrates the spline curve of the measured trajectory. The maximum operation range of the manipulator is presented by the outer line and the inner curve presents the range of motion of the bending section. The large deviation of 11mm at the top of the crescent can be deduced from the inconstant movement of the bending section. This inaccuracy occurs mainly at a deflection of more than 90°. With the exception of the large deviation at the crescent tip, the measured points, with a maximum deviation of 4.9mm, can be considered as fairly accurate.

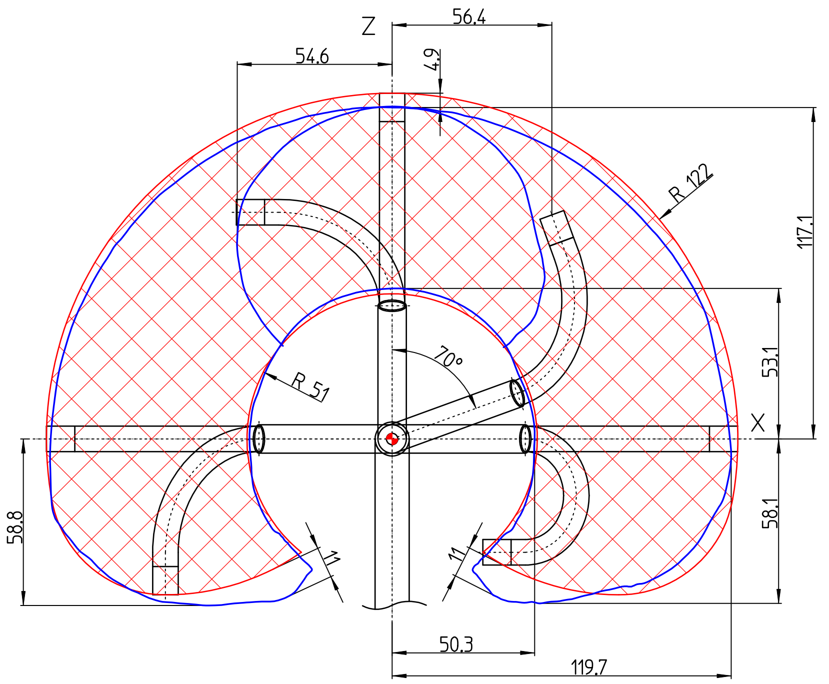

Figure 6.5: Workspace evaluation of the distal dexterity of the manipulator in the horizontal plane: Red hatched surface presents the theoretical workspace and the blue lines present the measured trajectories.

The further two DOFs of the manipulator expand the workspace so that the presented crescent is rotated by 360° about the Z-axis and moved 80mm in the Z direction into the body. At an angle of 70°, as shown in Figure 6.5, the horizontal distance of the instrument is 56.4mm to the center of the manipulator and 63.8mm to the center of the insert. By the vertical deflection of the bending section, this distance can be additionally reached in a vertical height of ±50 mm.

In the fourth measurement series, several trajectories of the manipulator were measured by the motion of all the three distal DOFs. Figure 6.6 presents the polygon mesh of the measured workspace. These measurements were carried out in order to illustrate the tridimensional workspace and to visually identify areas with larger deviations to the theoretical workspace. Upon closer examination of individual curves it can be noted that this measurement shows similar deviations in comparison to previous measurements.

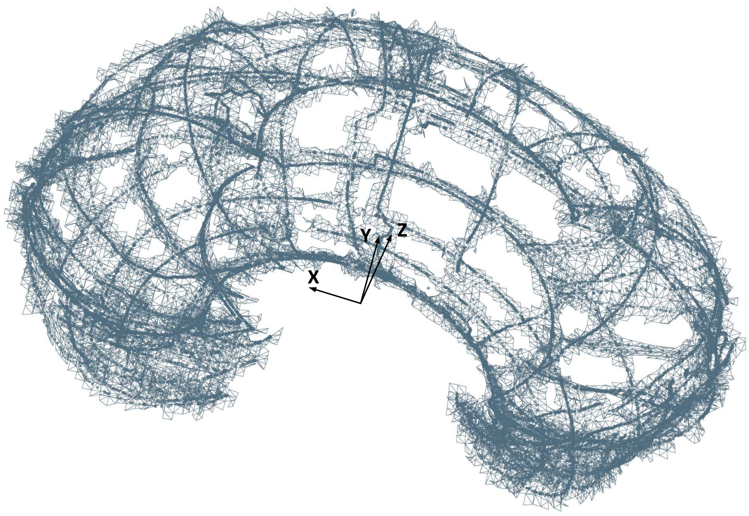

Figure 6.6: Polygon mesh of the measured workspace.

6.1.4 Discussion

According to our data, it can be shown that the required workspace of $100 \times 100 \times 60$ mm can be achieved with the developed single-port platform. Individual workspace measurements also enabled the identification of the deviations regarding the theoretically determined workspace. Except at the end of the bending section, it can be assumed that the workspace deviations are less than 5mm. However, these inaccuracies should not be equated with the positioning accuracy, which can be improved by integrating sensor modalities.

Extensive measurements will be accomplished after the integration of adequate position sensors into the manipulators in order to identify the position accuracy of the instruments. While evaluating the measurements of the workspace, it was also identified that the motion behavior of the bending section changes considerably with the application of load on the tool tip. This behavior should be examined more closely in further studies.

6.2 Evaluation of the forces on the manipulator

The amount of the achievable forces on the instruments is a crucial criterion for the applicability of the developed system. The manipulators should provide a certain amount of force in order to perform the intended laparoscopic single-port interventions. Therefore, the applicable forces on the manipulator were measured in this evaluation and verified according to the specifications.

6.2.1 Materials and Methods

The force gauge FH500 (Sauter, Germany) was used to determine the achievable forces of the individual joints of the manipulator. The device was mounted horizontally on a test rig that can run a continuous traction or pressure motion by pressing a button. Forces up to 500N with a resolution of 0.01N can be measured with this device. The force gauge is connected to the PC, where the measured values are continuously stored in a frequency of 10 Hz. Measured forces in the direction of the device are defined positive (pressure) and away from it negative (traction). Five different measurement series were carried out in this evaluation to determine the achievable forces of each manipulator joint.

In the first measurements, as presented in Figure 6.7, the generated forces by the bending section perpendicular to the manipulator tip are measured at different bending angles of the bending section. The measurements were carried out in a straight configuration and at a horizontal deflection of 45° and 90° respectively. This allows the determination of the dependence of the forces with respect to the bending angle of the bending section. In the three specific angles, the bending section is bent 3 times against the measuring device and away from it to determine the average pressure or traction. In a similar set-up, by the rotation of the manipulator by 90°, the vertical bending force of the bending section was measured in a second series of measurements.

Figure 6.7: Measurement of the forces applied by the bending section on the manipulator tip at different bending angles of the deflecting: a) straight configuration b) deflecting at 45° c) deflecting at 90°

Another series of measurements was conducted to determine the achievable forces at the manipulator tip by bending the elbow joint. As shown in Figure 6.8, the forces were measured in the straight configuration and at an elbow deflection of 50° and 80° respectively. The bendable section was held in a straight form to measure the worst case with the greatest leverage to the elbow joint. In each of the three measurements, the average pressure and traction forces perpendicular to the manipulator tip were determined by the horizontal deflection of the joint.

Figure 6.8: Measurement of the forces applied by the elbow joint on the manipulator tip at different bending angles of the elbow joint: a) straight configuration b) elbow bent to 50° c) elbow bent to 80°

The linear force of the prismatic joint and the torque of the rotational joint of the manipulator were determined in the last two series of measurements. As shown in Figure 6.9a, the pulling force was primarily measured with the manipulator in a straight form. Thereafter, the pushing force of the prismatic joint was measured at the upper-arm tube after deflecting the elbow joint (see Figure 6.9b). It should be noted, however, that the pushing of the tissue, compared to pulling, is an action that is rarely performed in laparoscopic surgery. In the last measurement, as shown in Figure 6.9c, the elbow was deflected to 90° and the perpendicular force at the wrist was, thereby, measured by the rotation of the manipulator. Three measurements were carried out in each case to determine the average forces.

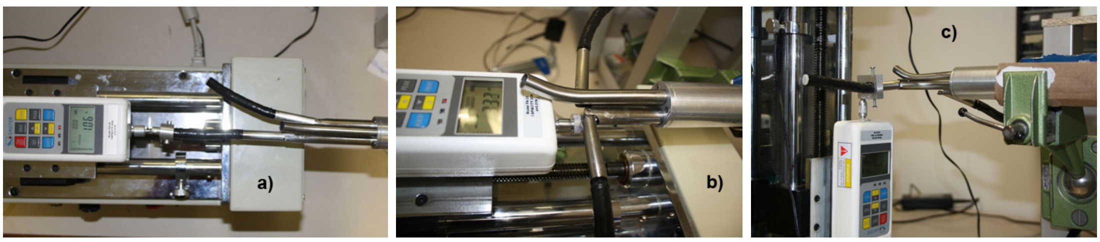

Figure 6.9: Linear force measurement of the prismatic joint and torque measurement of the rotational joint: a) pulling in straight form b) pushing with the upper-arm tube c) rotation force at the wrist

6.2.2 Results of the force measurements

The results of the first measurements, comprising the measured forces at the manipulator tip by horizontal deflection of the bending section, are shown in Figure 6.10. The force dependence of the bending angle with the respective pressure and traction forces are illustrated by clustered box plots. At each cluster, the pressure forces are presented by the lower blue boxes and the traction forces by the upper green boxes. Furthermore, the mean values of the measurements are indicated below each box.

On average, a pressure force of 1.83N and a traction force of 1.75N was achieved by horizontal deflection of the bending section. As it is apparent from the box plot, both the pressure as well as the traction forces increase with an increase in the angle. The reasons for this are, for example, the increase of the bowden wire tension or the taut structure that reduces the backlash and enables a better transmission of the force. While the measurements were being made, it was also observed that the elbow tends to decline slightly in the straight form, which additionally reduces the achievable force. This behavior diminishes with the increase of the bending angle. Moreover, it can be noted from the results that in a difference of less than 0.2N, the pressure and traction forces behave in a similar manner. The differences between the measured forces can be inferred from the pretension of the bowden wires and the friction.

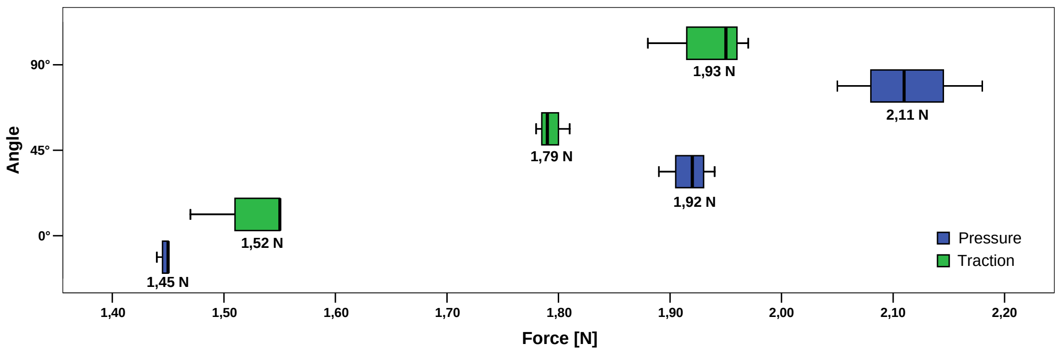

Figure 6.10: Results of the force measurements by horizontal deflection of the bending section

The results of the vertical deflection of the bending section, as shown in Figure 6.11, are a little bit different in comparison to the horizontal forces. On average, a pressure force of 1.87N and a traction force of 2.38N was achieved in these measurements. In the vertical direction, the pressure and traction forces increase similar to the horizontal forces with the increase of the bending angle. However, the traction forces here are between 0,4N and 0.6N higher than the pressure forces. On the one hand, the pretension of the bowden wires and the friction are reasons that could explain this difference in part. On the other hand, as an important system behavior, the reason for this can be inferred by the inconstant stiffness of the flexible bending section. The load dependent curvature of the bending section behaves, in relation to the bending angle, in a different manner. While the curvature is constant during tensile loads, the bending section tends to buckle at large bending angles and under high pressure loads.

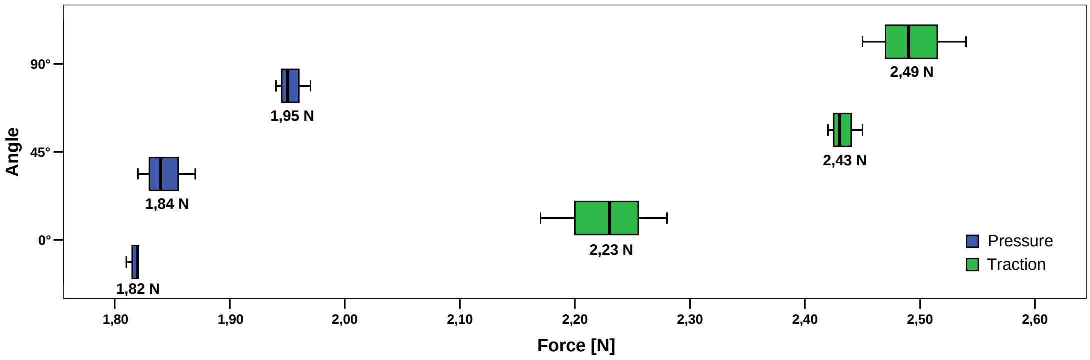

Figure 6.11: Results of the force measurements by vertical deflection of the bending section

As presented in Figure 6.12, the results of the force measurements that were achieved with the bending of the elbow joint are due to the large lever arm not being as high as the deflecting forces. On average, a pressure force of 0.72N and a traction force of 0.53N was achieved by the bending of the elbow joint. The pressure force increases with the increase of the bending angle and, in contrast, the achievable traction force decreases. On average, the forces are equal at 0°, but the traction force at 90° is about 0.4N lower than the pressure force. This difference can be inferred by the diminishing residual rotation at an increased bending angle. Because of the pretension and backlash of the bowden wire, the low pulling length generates a lower force.

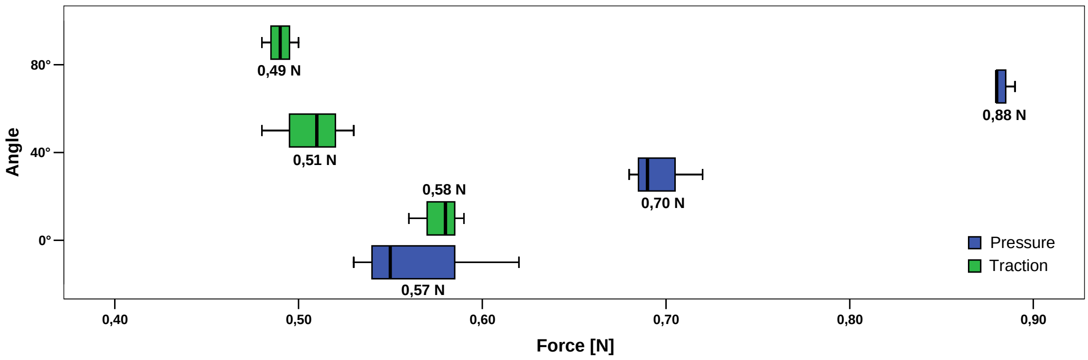

Figure 6.12: Results of the horizontal force measurements by bending the elbow joint

The results of the two last series of measurements are shown in Figure 6.13. On average, the pressure force of the prismatic joint amounts to 11.5N and the traction force to 10.6N. The difference between these forces can be inferred from the friction of the bowden wires and the friction of the manipulator. Initial force measurements by the rotation of the manipulator have shown that with the achievable force of the rotational joint just the friction of the bowden wires and the manipulator could be overcome. A rotation of the manipulator was achieved by higher pretension of the bowden wires and by increasing the pulling length at the control mechanism; however, the motions were jerky and could not be controlled well. Therefore, it was decided to integrate, as an interim solution, small motor drives into the platform in order to provide higher rotational forces for the intended clinical evaluations. The intermittently permissible theoretical torque at the gear output of the integrated Maxon motors with ∅16mm is 0.3Nm and a drive belt is additionally used for the transmission of the rotation. As shown in the right plot, an average force of 3.4N was measured by the rotation of the manipulator. The rotational force was measured at the wrist with a lever arm of 50mm. Thus, the upper-arm tube of the manipulator achieves a torque of 0.17Nm, which results in a transfer efficiency of 0.57.

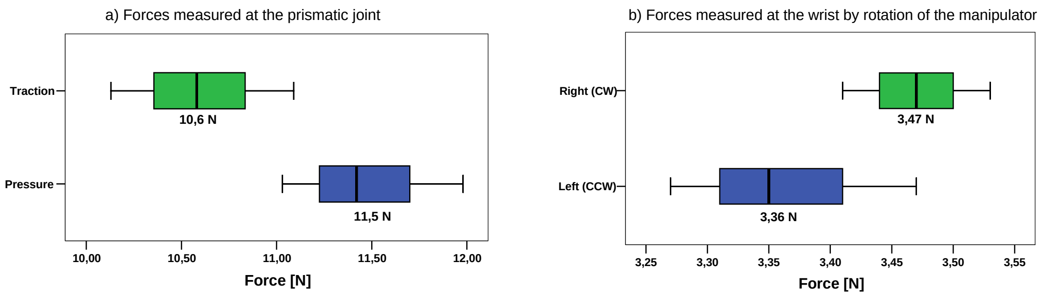

Figure 6.13: Results of the measured forces with the prismatic and rotational joints

The achievable average forces with the manipulator are presented in summary in Figure 6.14.

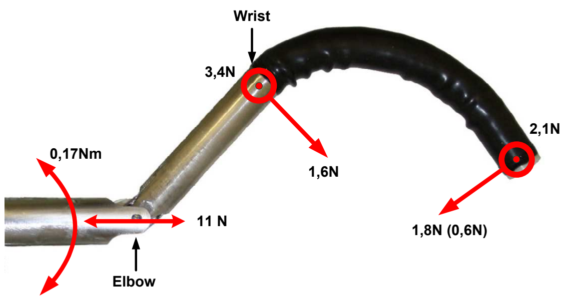

q_1	0.17 Nm
q_2	11 N
q_3	0.6 N
q_4	2.1 N
q_5	1.8 N

Figure 6.14: Applicable average forces on the single-port manipulator

6.2.3 Discussion

The measurements have shown that by a horizontal deflection of the bending section an average force of 1.8N can be achieved on the manipulator tip. By the tensile load in the vertical direction, even a force of more than 2N could be applied. These forces partially meet the required minimum force of 2N or are slightly below it. Although the integrated motor drives have been dimensioned to at least three times the required forces, it was demonstrated by these measurements that a large part of the force gets lost due to the friction of the bowden wires. However, as one of the great advantages of the developed system, the motors at the periphery can be dimensioned bigger in order to increase the required forces at the manipulator tip.

The results of the elbow forces, 0.6N on average, were rather small in comparison to the deflecting forces. The large lever arm of 125mm to the manipulator tip and correspondingly a transmission ratio of 50, is the main reason for the low forces that were achieved by bending the elbow joint. The measured forces represent the worst case and are higher in application (bended/opposed) configuration. Furthermore, in the first instance, it is not intended to manipulate loads at the manipulator tip by bending only the elbow joint. The application of forces on the instrument is achieved by the entire kinematic chain of the manipulator. Theoretically, the achieved forces with the bending section and the elbow joint can be summed up for a lateral pulling of tissue. Nevertheless, there is potential and need for optimization to achieve a higher load capacity of the manipulators. One possibility would be the reduction of the lever arm by a shorter bending section and forearm tube which also reduces, in contrast, the achievable workspace of the manipulator. Another solution is the reduction of the bowden wire length by integrating the motors at the proximal part of the platform or the redesign of the elbow joint.

An high force of 11N on average was measured, in contrast, at the prismatic joint. Despite the friction of the bowden wires and the manipulator, a sufficient force is provided in order to ensure the necessary force at the manipulator tip. A loop formation of the bowden wires could be prevented which would significantly reduce the achievable forces due to the increased friction. Furthermore, the friction of the plain bearings and the integrated O-ring seals results in a high static friction and a slip-stick effect at the beginning of the motion which can be reduced by the integration of tailored bearings and seals.

The torque of 0.17Nm at the rotary joint, which was achieved with the integrated motors, is sufficient for the intended applications. The specified force of 2N is guaranteed up to a lever arm of 85mm, which covers a working range of at least 100×100mm. However, a new concept should be developed for the realization of the requested drive at the periphery. One solution, therefore, is the enlargement of the pulley diameter as well as the use of a larger motor. Another solution is the realization of the rotation by using flexible shafts similar to the rotation of the entire platform, which is described in Section 4.4.2. However, it should be considered that due to the torsion of the shaft this drive transmission is significantly less accurate compared to bowden wire actuation.

It can be concluded that the measured forces with the manipulator are satisfactory, despite the a priori known disadvantage of the high friction of the bowden wires. The forces can be increased by adequate optimization steps, as mentioned above. These have to be investigated individually to provide a more robust system. Force measurements in these evaluations were conducted under optimal conditions. Therefore, the investigation of the load capacity, depending on deployment and wear, would provide additional information about the system's behavior. Furthermore, an extensive force measurement can be performed after the integration of suitable force sensors. A property that should be examined, thereby, is the position dependent load capacity of the manipulators.

6.3 Performing laparoscopic cholecystectomy

The following evaluations were carried out to assess the developed single-port system clinically.

- Evaluation of the single-port platform on a human mock-up trainer
- Performing laparoscopic in-vivo cholecystectomy in animal experiments

First, technical aspects such as the working range and the forces were qualitatively evaluated in three experiments for the distal dexterity and subsequently simple surgical tasks were simulated on the human mock-up ELITE trainer. After getting the required skills for handling and control of the system on the in-vitro trainer as well as the specifically programmed simulation environment, three animal experiments were carried out to resect the gallbladder through a single access. The results of these evaluations were published in [147, 148, 149].

6.3.1 Material and Methods

The "Highly Versatile Single Port System" (HVSPS)

As shown in Figure 6.15, the developed platform with two manipulators and a flexible endoscope is used to perform these evaluations. Due to the lack of the designed double-bending telescope (under development), it was decided to first realize the visualization by using a commercial endoscope with an outer diameter of 6mm that is inserted through a 10mm tube with a distal deflection of 30° and controlled manually. As described in Section 6.2, the rotation of the manipulators is realized by integrated motors to provide the required torque. The manipulators are controlled in joint space by using two joysticks as input devices and the overall platform is held and guided by the SoloAssist, which is operated by foot pedals. Furthermore, the flexible instruments are inserted through the manipulators and operated manually as well.

Figure 6.15: The Highly Versatile Single Port Platform

Experimental set-up for the in-vitro evaluations

The in-vitro evaluations on the ELITE trainer, as shown in Figure 6.16a, were accomplished in the experimental operating room of the research group MITI. The ELITE trainer is a replica of a human female torso with a highly immersive reconstruction of the abdominal cavity to train laparoscopic surgery and NOTES techniques [150]. The model is made of different latex compounds and provides gas-tight laparoscopic incisions to perform the intended interventions. The platform is inserted through the umbilical access into the abdominal cavity. Primarily, the reachable workspace of the developed platform as well as the SoloAssist was verified in this evaluation. Subsequently, the resection of a gastric and intestinal tumor was simulated. Finally, the gallbladder was resected on the ELITE trainer under conditions that were close to real.

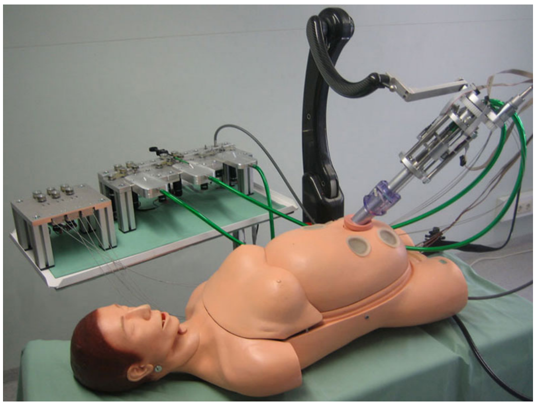

(a) In-vitro evaluation on the ELITE trainer

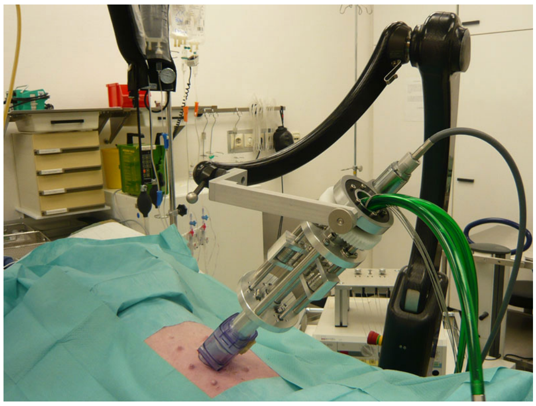

(b) In-vivo evaluation in animal experiment

Figure 6.16: Set-up of the laparoscopic in-vitro and in-vivo evaluations of the single-port system

Evaluation set-up and scenario of the laparoscopic in-vivo cholecystectomy

The laparoscopic gallbladder resections in the animal study, as shown in Figure 6.16b, were performed in the experimental operating room of the Klinikum rechts der Isar. Three surgeries were accomplished on pigs under general anesthesia by the same surgical team. A surgeon controlled both manipulators with two joysticks, a gastroenterologist manually operated the flexible endoscope and the instruments were controlled and exchanged manually by an assistant. The entire surgical intervention was managed by the commands of the surgeon who controlled the manipulators. According to the previous results from the in-vitro evaluations, the liver was retained by a retractor, which was introduced through an auxiliary incision, out of the operating range.

6.3.2 Results

Experimental in-vitro evaluation on the ELITE trainer

The guidance of the platform by the SoloAssist was verified in the first evaluation. A pivoting angle of more than 60° was achieved at the invariant point in any direction. Thus, all the quadrants of the abdomen could be reached through the umbilical access. The total weight of 3kg of the platform lies at the upper limit of the load capacity and resulted occasionally in jerky movements. The 80mm penetration depth of the manipulators is rather deeper than necessary and a depth of 50-60mm would be fully sufficient. These evaluations have also shown that the workspace of the manipulators, especially their opposite configuration, was adequate to accomplish the intended intervention on the gastric tract or the resection of the gallbladder. However, in an opposed configuration of the manipulators with an elbow distance of more than 100mm, a lateral collision or obstruction could not always be prevented.

Figure 6.17a shows the overview of the distal part of the platform during the intervention on the gastric tract. Grasping, cutting and ligation tasks could be performed successfully during a partial resection of the intestine. The achievable force was sufficient to accomplish these interventions; however, it was not enough to move or retract the liver out of the operating field. In addition to these evaluations, which intended to assess function and verify the requirements, a cholecystectomy was performed in a further experiment. The dissection of the gallbladder was achieved in 135 minutes. The interdisciplinary training was indispensable for the intended in-vivo cholecystectomy in the subsequent animal experiments.

(a) Evaluation of the platform in the ELITE

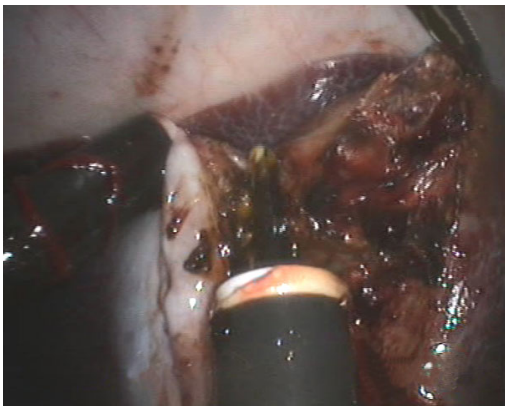

(b) Endoscopic view of the in-vivo intervention

Figure 6.17: Laparoscopic evaluation of the platform: a) Close view of the manipulators during in-vitro evaluation b) Endoscopic view of the in-vivo evaluation during the resection of the gallbladder

Accomplishment of in-vivo cholecystectomy in animal experiments

All three gallbladder resections were accomplished successfully. The complete surgical intervention, without technical set-up, took between 95-130 minutes.

After insufflation of the peritoneum with a Verres needle, the HVSPS platform was inserted through an incision in the middle of the abdomen into the abdominal cavity. The manipulators with the protruding flexible endoscope were in a straight configuration during the introduction and afterwards folded out in the peritoneal cavity. The endoscopist inspected the situs after the introduction and helped the surgeon to guide the platform to focus the gallbladder.

Two flexible instruments (a pair of pliers and scissors) were introduced afterwards through the manipulators, which were exchanged within seconds according to the task. After the ligation of the cystic duct and cystic artery with coagulation current, dissection of the gallbladder was achieved by using grasping and cutting instruments. Figure 6.17b shows how the gallbladder is held with a grasper by the left manipulator and dissected by using a TT knife introduced through the right one. Afterwards, the gallbladder was recovered through the main incision. In order to do this, the manipulators were steered to the straight position to pull the gallbladder together with the platform out of the abdominal cavity. Finally, both incisions were sutured.

The opposition of the manipulators was indispensable for an intuitive and efficient operation. Moreover, the coordination of the physicians was essential and decisive for the performance and quality of the interventions. With increasing experience of the physicians, the operations were performed consistently in less time.

6.3.3 Discussion

With this evaluation, it was shown that laparoscopic cholecystectomy is feasible by using the developed single-port system. The workspace and the forces of the manipulators were sufficient to resect the gallbladder or to perform a partial resection of the gastrointestinal tract. In comparison to the conventional laparoscopic cholecystectomy, the performed single-port surgeries lasted significantly longer. This results from the demanding control of the various degrees of freedom in joint space and the coordination of the individual actions of the physicians. This extended time can be reduced by task space control of the manipulators, an adequate human-machine interface and an integrated simulation and planning environment.

During the surgeries, the instruments were usually in the visual field of the camera; however, it was not always clear exactly how the structure of the manipulator arms was positioned and whether a lateral collision or restriction was present or not. Therefore, the integration of position sensors in the manipulators as well as the navigation of the system is inevitable for the accomplishment of such demanding single-port interventions.

The achievable forces with the manipulators and the specified requirement of 2N (also by other research groups such as [107]) was not sufficient for the retraction of the liver. Therefore, a retractor was inserted through an auxiliary incision to keep the liver out of the operating field. A conceptional question that should be answered by further developments and evaluations in cooperation with the physicians is: Can the manipulators be designed to achieve higher force for the retraction of the liver or should the additional incision for the retractor be considered as an alternative?

The large working range of the manipulators as well as the semirigid telescope enables the accomplishment of interventions in retroflexion. There are four different scenarios which were simulated in the in-vitro evaluations: 1) both, the manipulators and the telescope are operated in prograde direction 2) the manipulators are in retroflexion and the visualization is in prograde direction 3) the telescope is in retroflexion and the manipulators are operated in prograde direction and 4) both, the manipulators and the telescope are operated in retroflexion. These opportunities should be investigated in further evaluations to identify the surgical impact and the technical challenges such as the control and the operation of the manipulators.

6.4 Performing in-vitro NOTES cholecystectomy

The developed single-port platform as described in Chapter 4, which has been conceived to perform laparoscopic single-port interventions, was used here to evaluate the potential role of mechatronic systems for NOTES procedures. In this study, the platform was used to simulate transanal NOTES procedures and to assess the practical applicability and the prospects of facilitating transluminal surgery. Three cholecystectomies were performed for "manual" as well as mechatronically supported NOTES. The primary intent of these surgical interventions was the evaluation of the distal dexterity of the platform. Hence, the limited flexibility due to the access, which can be overcome by the development of a fully flexible system, is not considered here in detail. The results of this evaluation were partially published in [113].

6.4.1 Material and Methods

The "Highly Versatile Single Port System" (HVSPS)

The HVSPS with two manipulators and a flexible endoscope was used to perform this evaluation. Due to the lack of the designed telescope (under development), the visualization was first realized by using a commercial endoscope with an outer diameter of 6mm that was inserted through a 10mm tube with a distal deflection of 30°. Figure 6.18 shows schematically the set-up of the platform and the intervention. The platform was introduced through the transanal access of the human mock-up ELITE trainer, which was created by the ISSA instrument set (detailed description subsequently). The SoloAssist telemanipulator held and guided the platform at the proximal linkage part. Similar to the performed in-vivo evaluation, the manipulators were controlled in joint space by using two joysticks as input devices. The flexible instruments were inserted through the manipulators and operated manually.

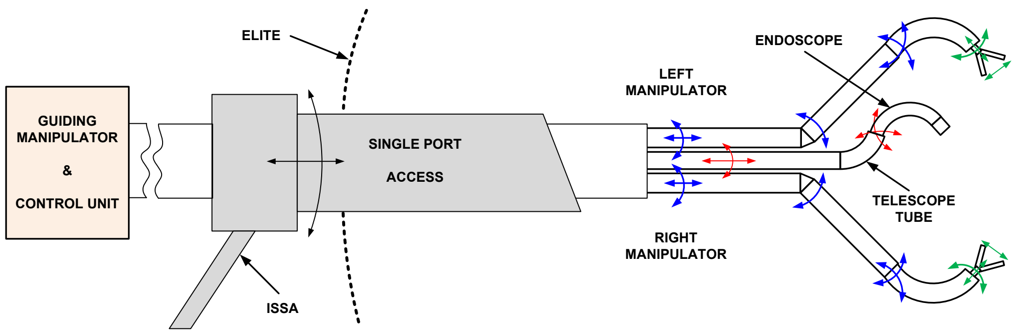

Figure 6.18: Schematic drawing of the evaluation set-up for the transanal NOTES intervention

The "Endoscopic - Laparoscopic Interdisciplinary Training Entity" (ELITE)

The ELITE trainer is an ex-vivo model offering a highly immersive reconstruction of the abdominal cavity to train laparoscopic surgery and NOTES techniques. This new training model, which was developed by the research group MITI (Klinikum rechts der Isar, Germany) is a one-to-one replica of a human female torso. It consists of an abdominal wall providing gas-tight laparoscopic incisions and an abdominal cavity with an adjustable pressure. All the intraabdominal organs are produced from different latex compounds with different characteristics and colors to provide a realistic mock-up of the intraabdominal anatomy. The ELITE system is validated for NOTES cholecystectomy and appendectomy [150] and it is suitable to compare "manual" NOTES with the mechatronically supported NOTES. For this study, the transanal access was chosen to perform the cholecystectomy with the semi-rigid single-port platform.

The "Innovative, safe and Sterile Sigmoid Access" (ISSA)

Since the transgastric approach could not prevail due to the long and difficult access route, the transcolonic surgical approach was developed to enhance the potential of transluminal surgery. Therefore, a new set of instruments comprising an endoscopic trocar, a flexible obturator and a modified transanal endoscopic microsurgery device was designed to enable sterile sigmoid access for transcolonic surgery. The developed instruments were published in [112] and the first prototype was manufactured in cooperation with Karl-Storz, Germany. The set of instruments has already been successfully evaluated in a survival animal study that confirmed safety and sterility as objectives during surgical intervention [111]. This instrument set was used to perform the evaluations through the transanal access on the ELITE trainer.

Setup of the surgical intervention and the experimental environment

For "manual" NOTES cholecystectomy, a flexible standard endoscope (13806PKS, Karl-Storz or CF-2T160L/I, Olympus) was introduced via the opening in the rectosigmoid and positioned in the right upper quadrant of the abdomen. The gallbladder and the infundibulum were localized first. The use of an additional 2 mm forceps, inserted through the navel, enhanced the exposure of the operative situs (in particular of the cystic duct). The cystic duct had to be occluded with 3 endoscopic clips and subsequently severed. Then, 20 to 50 ml of 0.9% saline solution was instillated using the endoscopic injection needle into the layer between the gallbladder and the liver. The gallbladder was excised by means of the IT or TT knife (Olympus, Japan). Transmural forceps had to be used to create sufficient counter-traction. Finally, the gallbladder was pulled out using standard endoscopic grasping forceps.

To perform the identical procedure with the developed single-port platform, the HVSPS was, as demonstrated in Figure 6.19a, introduced through the transanal access. The manipulators were in a straight position during introduction and expanded in the peritoneal cavity. The gastroenterologist, controlling the flexible endoscope, observed the situs after the introduction and helped guide the manipulators to face the gallbladder. Two flexible instruments (grasper, scissors or needle knife) were introduced through the manipulators, which could be exchanged within seconds for different tasks. Comparable to the real circumstances of a cholecystectomy, the layer between the gallbladder and liver could be dissected using grasping and cutting instruments. The opposition of the manipulators, as a key function of the system, was essential for an intuitive working experience. The gallbladder could be held with a grasper through the left manipulator and dissected by using a TT knife introduced through the right (Figure 6.19b).

(a) Overall view (abdominal wall removed) (b) Endoscopic view

Figure 6.19: First application of the HVSPS for NOTES on the ELITE trainer performing a cholecystectomy using the transanal ISSA approach

6.4.2 Results

"Manual" NOTES cholecystectomy

The NOTES cholecystectomies could be successfully performed on the ELITE trainer within 37 to 75 minutes, depending on the expertise of the endoscopist. The interventions were accomplished with the help of two further assistants. One of them managed the flexible instruments, while the other supported the intervention with the help of additional forceps. The use of the additional transmural instruments was indispensable for the performance of the NOTES cholecystectomy. Sufficient exposure of difficult regions could be achieved herewith, to perform the necessary operative manipulation with the conventional two channel endoscope.

NOTES cholecystectomy using the HVSPS

The gallbladder resections on the ELITE trainer with the HVSPS through the transanal access were also accomplished successfully. In all cases the complete system had to be operated by a team composed of two physicians and two assistants. One physician controlled the manipulators with two joysticks, an assistant manually controlled the flexible instruments guided through both manipulators, a second physician guided and manually controlled the flexible endoscope and a second assistant operated the manipulators' remaining degrees of freedom.

While verbal commands between the staff were sufficient for the accomplishment of the manual NOTES cholecystectomy, the HVSPS NOTES intervention demanded, in contrast, a far more intuitive cooperation between the team members. Nevertheless, the precise positioning of the system, the endoscope and manipulators is difficult and time consuming, resulting in a total operation time of more than 3 hours.

On the other hand, the possibilities of exerting traction and counter-traction and enabling a visualization independent to both manipulators have significantly improved the dexterity and the range of the manipulations. Precise and targeted motions could be applied with the dominant hand (right manipulator) after the exposure of the anatomical structure with the second hand (left manipulator). Moreover, any surgical action could be observed under the appropriate angle of view; however, it took additional time to coordinate and to position the instruments and the flexible telescope.

6.4.3 Discussion

Multifunctional robotic platforms are currently assumed to be the key to make more advanced NOTES procedures feasible and, perhaps, even mature for clinical use. Many research institutes are developing new types of instruments with additional intraabdominal flexibility for single port surgery, mainly for laparoscopy, and some of them are also suitable for NOTES (see Table **??**). Incisionless Operating Platform (Transport) [126], Endo-Samurai [127], Direct Drive Endoscopic System (DDES) [123] and Anubis Scope [128] are manually operated platforms proposed for NOTES. Meanwhile, there are also some robot systems such as the MASTER, developed by Phee et al., or the ViaCath system, developed by Abbott et al. However, little is known about how much these devices really contribute to improve the NOTES technique. This may differ between the various designs, but, nevertheless, it is interesting to consider this question in principle. Since only a few prototypes of these platforms exist worldwide, it was impossible to evaluate and compare several of them in the same simulator - the ELITE.

Accordingly, we used the so called HVSPS platform to simulate NOTES under lab conditions. Admittedly, the HVSPS design differs in several regards from systems such as the Transport, the DDES or the Endo-Samurai, in particular concerning the diameter, the semi-rigid concept and the quality of the man-machine interface. However, the main features, especially the distal dexterity, are similar enough that some experience and information gained with this platform is of general importance.

This first evaluation of a mechatronically supported NOTES procedure in comparison to the same "manual" NOTES operation in the same simulation environment has at least demonstrated some interesting facts. The option of triangulation considerably facilitates targeted, highly precise surgical actions such as dissection, clipping, etc. - as soon as both instruments are brought to the desired position. The quality of surgery is further enhanced by the flexible visualization, making pure NOTES possible, as shown in this preliminary trials. The accomplished interventions have also shown that the achievable workspace and forces of the manipulators were sufficient to resect the gallbladder. As an advantage of the developed semi-rigid platform, the rigid proximal part of the platform and stiffness of the manipulators was of crucial importance in order to apply the intended motions and forces precisely at the target site.

However, the surgical interventions are currently very time-consuming because of difficulties in controlling various degrees of freedom of the system and the essential coordination of the individual actions of the team members. Although the cholecystectomy could be performed successfully with the semi-rigid platform in the prograde direction, a complete flexible platform with a reinforcible structure is required to perform NOTES interventions from different directions and positions. As specified in the requirements, the platform should have a maximum outer diameter of 22mm to also enable transgastric access. Besides the hardware development of adequate platforms, the operation and control of such demanding systems are major problems that must be solved. Thereby questions arise regarding the man-machine interface, navigation and surgical workflow. One lesson learned during the introduction of laparoscopic surgery is the fact that some ostensibly crucial technologies (like 3D visualization) become superfluous with increased dexterity and experience. Whether comparable phenomena will occur in NOTES, as well, is unclear.

Chapter 7

Conclusion

7.1 Summary

This thesis presents the design, implementation, control and evaluation of a platform for laparoscopic single-port procedures. First of all, the problems and requirements of single-port surgery regarding surgical as well as technical aspects were investigated through preliminary experiments in close cooperation with the physicians and described in this work. The design specifications and considerations regarding the instruments, manipulators and guiding system that meet the requirements of a single-port system were identified and described in detail. Accordingly, the overall concept of the developed platform, comprising two articulated manipulators and a semi-rigid telescope, was worked out. Apart from the specifically implemented approaches, the following issues constitute the focus and difference of this work: A highly versatile, single-port robotic platform for laparoscopic abdominal surgery, joint control by bowden wires over long distance providing the displacement of the control unit, including motors, to the periphery and hollow manipulators with enhanced dexterity providing the insertion of flexible endoscopic instruments.

The design and the first prototype of the developed system as well as the individual hardware components are presented. The bowden wire actuated, hollow manipulators with a distal bending section of an endoscope and an elbow joint extend the intraabdominal flexibility and enable intuitive and precise manipulations with the instruments in an opposed configuration. Endoscopic instruments can be introduced through the manipulators and exchanged according to the surgical task. The design of the double-bending telescope enables the visualization of both manipulators in their entire workspace. Both manipulators and the telescope are combined gas-tightly into one unit with a 34 mm diameter, which can be inserted through a single incision into the abdominal cavity. Two additional joints for each manipulator are implemented in the proximal part of the platform and enable a linear and rotary motion of the manipulators. The entire passive platform is held and guided at the proximal flange by the hydraulic SoloAssist telemanipulator. All the joints of the platform are controlled from 2 m distance at the periphery. Thereby, the bulky and heavy construction as well as the electromagnetic interference caused by having the motors near the patient, is avoided. An additionally designed rotary joint enables, furthermore, the rotation of the entire platform by means of a flexible shaft from the periphery. The control mechanism and the motors for the actuation of the bowden wires are integrated in modular platforms.

This work also presents the kinematics of the bending section and the manipulator that was determined according to the physical system. The implemented kinematics was verified and analyzed in a simulation with a simplified 3D model of the single-port platform. Our approach in this work was to control the manipulators and the telescope independent of the guiding system. This approach was realized in a simulation in which we implemented a velocity-based, task-space control of the instrument for the kinematic analysis. A space mouse was used as the input device to operate both manipulators. In addition, an evaluation scenario with a pick-and-place task was implemented in the simulation for the training of the physicians. Moreover, this work presents the implemented low-level control for the actuation of the manipulator in joint-space that was evaluated by two joysticks as the input device. By implementing an appropriate interface, the manipulators can also be controlled over a higher-level control entity that provides the desired joint positions.

Four experiments were carried out to evaluate the developed prototype and verify the specified requirements. Through the accomplished workspace measurements of a manipulator, it was shown that the attainable operating range is sufficient to perform a gallbladder resection. Moreover, the force measurements also revealed that the specified force of about 2N at the instruments can be achieved by the deflection of the bendable section. The feasibility of the laparoscopic cholecystectomy in an in-vitro human mock-up trainer as well as in an in-vivo animal experiment was shown. Furthermore, with the accomplished transluminal cholecystectomies with the human mock-up trainer, the potential role of mechatronic systems were determined for NOTES procedures.

7.2 Limitations and outlook

Although the first animal experiments were performed successfully with the developed single-port platform, a variety of further developments are necessary to enable a clinical application. One of the major disadvantages of the developed platform is the friction, inaccuracy and the slip-stick effect that is caused by the bowden wires. The load dependent position accuracy should be evaluated after the integration of adequate sensor modalities. By the implementation of appropriate control models, the disadvantages of the bowden wires can be reduced to some extent. These models should also comprise the friction of the bowden wires as well as the load depended motion of the bending section. The efficiency of the bowden wires is very small due to the high friction. Therefore, the integrated motors should be dimensioned bigger in order to achieve higher forces. Particularly, the rotation of the manipulators must be resized thereby.

The developed platform, with a 34 mm diameter, is an initial prototype and can be reduced in size. An external diameter of 22 mm can be achieved by the use of small-sized bending segments and thin-walled materials. It should be noted that the sterilization of the platform is not dealt with in this work in detail. The connection of the manipulators should be modular in design to allow for the individual sterilization of the components. Besides the optimization of the aforementioned limitations and drawbacks, future work will include the following topics:

- Investigation of the load dependent friction and inaccuracy of the bowden wires. Modeling of an appropriate control for the compensation of these inaccuracies.
- Implementation of a control architecture that enables a task-space control of the manipulators by using two 6 DOF teleoperators as the input device.
- Development of a tool changer with modular magazines for the introduction of the flexible endoscopic instruments through the hollow manipulators.
- Integration of different sensor modalities to enable tracking, navigation and force feedback of the instruments and the manipulators.
- Development of an adequate human-machine interface for an intuitive operation of the entire system by a single surgeon.

The development of a fully flexible system, as shown in Figure 7.1, would be ideal for performing enhanced transluminal surgery. Due to its flexible structure, such a system would also enable interventions in and through the gastric tract. The results of this work and the intended research can be used for the development of such a platform. As a result, however, the flexible structure as well as the distal workspace should be drastically reduced in size. As shown in the schematic figure, the distal dexterity of this platform will be similar, to some extent, to the developed platform. The linear motion and rotation of the manipulators could be implemented at the periphery. The use of a flexible drive transmission, such as bowden wires, shows its advantages in the implementation of such fully flexible platforms. Manipulators with two or more bending sections (snake-like structures) can be used to achieve the required dexterity. The flexible carrier could provide reinforcement at the target for controlled and precise manipulations.

Figure 7.1: Schematic drawing of a fully flexible single-port platform for transluminal surgery.

Appendix A

Appendix

A.1 Comparison of drive transmission mechanisms over long distances

A direct drive, without intermediate components for drive transmission, certainly offers advantages such as low friction, high efficiency and a reliable control. However, for surgical applications in which manipulators with distal articulations are inserted through small incisions into the body, it is difficult to realize direct drive mechanisms due to their drawbacks. Large installation size and correspondingly low forces, security aspects due to insertion of electrical power into body and, last but not least, aspects such as difficult sterilization or maintenance are some of the main disadvantages. Therefore, it is aspired to integrate the electrical drives in short distances outside the body, and transmit the motion to the joints into the body by different drive transmission mechanisms. Linkages, gears, wire routing by using pulleys, bowden wires or flexible elements such as NiTi, which also provide shape memory properties, are some of the possible mechanisms that can be considered for this purpose. Each of them has, in comparison, its advantages and disadvantages, which are not discussed here in detail. In general, by implementing these mechanisms important disadvantages of the actuation by direct drive can be overcome while other disadvantages, such as inaccuracy, friction and challenging drive transmission can be put up with.

New single-port systems such as the developed platform with many additional degrees of freedom, pose high demands for the integration of all drives above the patient. Such a design, with more than 15 high-power motors for the distal dexterity, is too bulky and would restrict the access to the patient. Furthermore, it is challenging to manipulate such a heavy drive unit with an adequate guiding system. Another limitation arises with the use of medical imaging modalities or electromagnetic tracking systems that are affected by electric drives. One crucial goal of this research is, therefore, the integration of the motor drives in a unit at the periphery and the control of the joints by using flexible drive transmission. A flexible drive transmission is, in addition, mandatory for the realization of a single-port system for transluminal surgery. Bowden wires, flexible shafts, hydraulic or pneumatic mechanisms are some of the possibilities for the flexible drive transmission. Some of the important assets and drawbacks of these mechanisms are listed in Table A.1.

A precise positioning without fixed stops can not be realized by using pneumatic mechanisms due to the high compressibility of air. In addition, pneumatic actuators are too loud and do not provide enough force and efficiency for small sized manipulators. Although, hydraulic mechanisms provide high forces and torques, they involve similar disadvantages such as inaccuracy due to the compressibility of the fluid, challenging control and, more importantly, the risk of leakage. Flexible shafts are generally used for the transmission of high speeds. Thus, a gear should be integrated on the output side in order to reduce the rotational speed. The great disadvantage of flexible shafts is the inaccuracy that results from the torsion of the shaft. Another important disadvantage is the backlash at change of direction, which mainly results due to the torsion of the shaft. For the realization of small systems and manipulators, as the intended developments here, bowden wires are the most appropriate drive transmission mech-

Table A.1: Comparison of different actuation mechanisms with flexible routing over long distances.

Actuation Mechanism	**Advantages**	**Disadvantages**
bowden wire	simple design and control small installation size cheap and simple to replace	risk of wire breakage friction and inaccuracy low power and load capacity
flexible shaft	high speeds transferable high forces and torques	inaccuracy due to torsion high backlash and hysteresis reduction gear near application
hydraulic	high forces and torques high power density simple technical components	inaccuracy due to compression risk of leaks temperature dependency
pneumatic	simple design and control safety and storage high velocity	high compression no precise positioning low power and efficiency

anism. They provide a simple design and control of the manipulators in small installation size. Wire breakage is the main disadvantage of the bowden wires that has to be considered in safety aspects and maintenance. As with the other mechanisms, the bowden wires also involve friction and have a certain amount of inaccuracy.

A.2 Kinematics of the SoloAssist guiding system

The SoloAssist camera guiding system has three active and two passive joints. The additional rotational joint at the linkage of the single-port platform, as described in Section 4.4 was implemented as the sixth joint of the SoloAssist manipulator. Figure A.1 shows the manipulator with a detailed labeling of the individual joints and their frames. A Cartesian positioning of the tool tip is achieved with the first three active joints ($\theta_1, \theta_2, \theta_3$). The rotation of both passive joints (θ_4, θ_5) results from the restriction of the invariant point. While in the real system this rotation is automatically deduced from the restriction and the force at the invariant point, the complete kinematics, including the rotation of the passive joints, was determined for the implementation of the simulation.

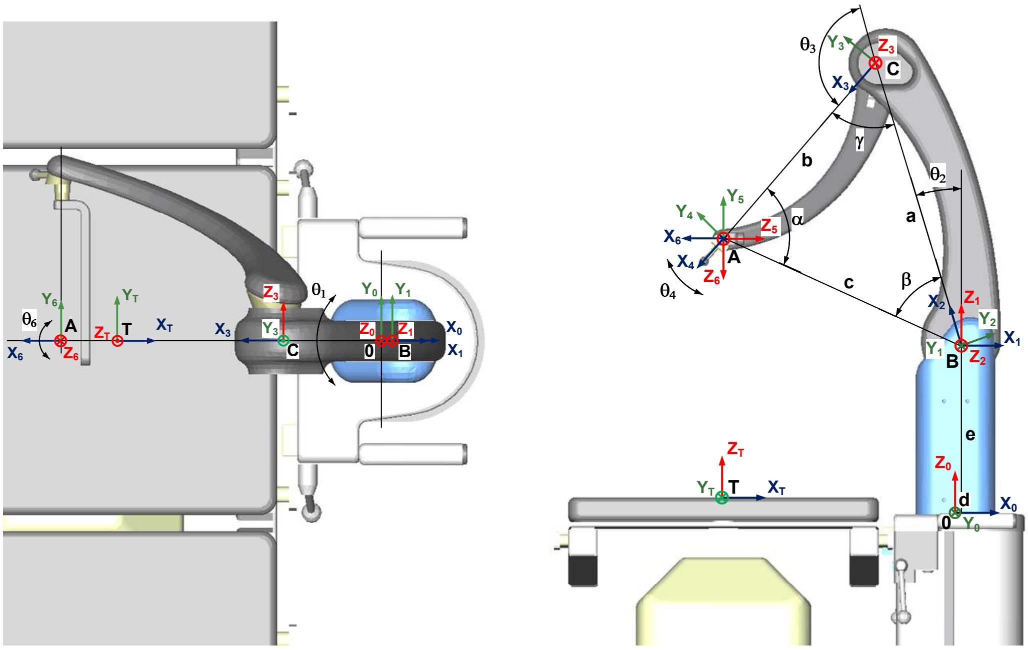

(a) Top view of the manipulator

(b) Side view of the manipulator

Figure A.1: Design of the SoloAssist telemanipulator attached to the operating table. All the joints and frames are indicated and labeled.

Table A.2 shows the DH table of the SoloAssist manipulator. θ_6 in this table corresponds to the active rotation joint for the single-port platform. The distances between the SoloAssist joints are: $a = 500mm$, $b = 400mm$, $d = 25mm$ and $e = 296.5mm$.

Table A.2: DH table of the hydraulic SoloAssist telemanipulator

i	α_i	a_i	d_i	θ_i
1	0	d	e	θ_1
2	$-\pi/2$	0	0	$\theta_2 - \pi/2$
3	0	a	0	θ_3
4	0	b	0	θ_4
5	$\pi/2$	0	0	$\theta_5 + \pi/2$
6	$\pi/2$	0	0	$\theta_6 - \pi/2$

The forward kinematics of the SoloAssist manipulator is determined by the multiplication of the six transformation matrices.

$$T_0^6 = T_0^1 \cdot T_1^2 \cdot T_2^3 \cdot T_3^4 \cdot T_4^5 \cdot T_5^6 = \begin{bmatrix} R_0^6 & p_0^6 \\ 0 & 1 \end{bmatrix} \qquad \text{where} \qquad p_0^6 = p_0^A \tag{A.1}$$

The position vector of the SoloAssist tip, where the proximal part of the platform is linked, is:

$$p_0^A = \begin{bmatrix} A_x \\ A_y \\ A_z \end{bmatrix} = \begin{bmatrix} d + \cos(\theta_1) \cdot (a \cdot \sin(\theta_2) + b \cdot \sin(\theta_2 + \theta_3)) \\ \sin(\theta_1) \cdot (a \cdot \sin(\theta_2) + b \cdot \sin(\theta_2 + \theta_3)) \\ e + a \cdot \cos(\theta_2) + b \cdot \cos(\theta_2 + \theta_3) \end{bmatrix} \tag{A.2}$$

A rotation of the tool tip A, by the first 3 joints, relative to the base 0 is determined as follows:

$$R_0^3 = R_0^A = \begin{bmatrix} \cos(\theta_1) \cdot \sin(\theta_2 + \theta_3) & -\sin(\theta_1) & -\cos(\theta_1) \cdot \cos(\theta_2 + \theta_3) \\ \sin(\theta_1) \cdot \sin(\theta_2 + \theta_3) & \cos(\theta_1) & -\sin(\theta_1) \cdot \cos(\theta_2 + \theta_3) \\ \cos(\theta_2 + \theta_3) & 0 & \sin(\theta_2 + \theta_3) \end{bmatrix} \tag{A.3}$$

When it is assumed that $\theta_4 = 0$, the transformation matrix to the tool tip A is given by the equations A.2 and A.3:

$$T_0^A = \begin{bmatrix} R_0^A & p_0^A \\ 0 & 1 \end{bmatrix} \tag{A.4}$$

Similar to other existing systems, the first three joints are used for positioning of the tool tip and the last three joints for the orientation of the tool. A geometric approach is used to determine the inverse kinematics of the SoloAssist. The distance c between the points A and B is:

$$c = \overline{AB} = \sqrt{(A_x - B_x)^2 + (A_y - B_y)^2 + (A_z - B_z)^2} \qquad \text{with} \qquad B = \begin{bmatrix} d & 0 & e \end{bmatrix}^T \tag{A.5}$$

After the determination of the required position A and the distance c, the three active joint angles of the SoloAssist can be calculated by using the cosine theorem:

$$\begin{bmatrix}\theta_1\\\theta_2\\\theta_3\end{bmatrix} = \begin{bmatrix}\arctan(\frac{A_y-B_y}{A_x-B_x})\\ \pi/2-\arccos(\frac{b^2-a^2-c^2}{-2\cdot a\cdot c})-\arcsin(\frac{A_z-B_z}{c})\\ \pi-\arccos(\frac{c^2-a^2-b^2}{-2\cdot a\cdot b})\end{bmatrix} \tag{A.6}$$

The tool tip A of the SoloAssist is determined with the defined distal tip position of the single-port platform p_0^I the length of the platform l_p and the invariant (trocar) point p_0^T:

$$p_0^A = p_0^I + \frac{p_0^T - p_0^I}{|p_0^T - p_0^I|} \cdot l_p \tag{A.7}$$

By the given positions of the platform tip and the SoloAssist tip, the orientation of the platform can be determined as follows [151]: First, the rotation matrix of the platform is determined by using the Z-Y-(X) Euler angles. The platform is rotated by ϑ about Z-axis, tilted by φ about Y-axis and the rotation about X-axis (platform) is zero. Consequently, the rotation matrix of the platform and the SoloAssist tip is:

$$R_0^6 = \begin{bmatrix}\cos(\vartheta)\cdot\cos(\varphi) & -\sin(\vartheta) & \cos(\vartheta)\cdot\sin(\varphi)\\ \sin(\vartheta)\cdot\cos(\varphi) & \cos(\vartheta) & -\sin(\vartheta)\cdot\sin(\varphi)\\ -\sin(\varphi) & 0 & \cos(\varphi)\end{bmatrix} \tag{A.8}$$

The rotation matrix of the last three joint of the SoloAssist $(\theta_4, \theta_5, \theta_6)$ can be determined with the defined rotation matrix of the SoloAssist tip and the rotation matrix of the first three joints:

$$R_3^6 = \begin{bmatrix}r_{11} & r_{12} & r_{13}\\ r_{21} & r_{22} & r_{23}\\ r_{31} & r_{32} & r_{33}\end{bmatrix} = (R_0^3)^T \cdot R_0^6 = R_3^0 \cdot R_0^6 \tag{A.9}$$

After determination of the rotation matrix, the orientation angles can be defined finally by using the Z-Y-Z Euler angles:

$$\begin{aligned}\theta_4 &= atan2(r_{23}, r_{13})\\ \theta_5 &= atan2(\pm\sqrt{1-(r_{33})^2}, r_{33})\\ \theta_6 &= atan2(r_{32}, -r_{31})\end{aligned} \tag{A.10}$$

References

[1] H. Feussner and JR Siewert. **Reduktion des Zugangstraumas: gesicherte Vorteile**. *Der Chirurg*, **72**(3):236–244, 2001. 1

[2] A. Tittel and V. Schumpelick. **Laparoskopische Chirurgie: Erwartungen und Realitaet**. *Der Chirurg*, **72**(3):227–235, 2001. 1

[3] R. Taylor. **Robots as surgical assistants: where we are, wither we are tending, and how to get there**. *Artificial Intelligence in Medicine*, pages 1–11, 1997. 2

[4] R.M. Satava. **Emerging technologies for surgery in the 21st century**. *Archives of Surgery*, **134**(11):1197, 1999. 2

[5] D. Stoianovici. **Robotic surgery**. *World Journal of Urology*, **18**(4):289–295, 2000. 9

[6] R.H. Taylor and D. Stoianovici. **Medical robotics in computer-integrated surgery**. *IEEE transactions on robotics and automation*, **19**(5):765–781, 2003. 9

[7] R.D. Howe and Y. Matsuoka. **Robotics for surgery**. *Annual Review of Biomedical Engineering*, **1**(1):211–240, 1999. 9

[8] D.B. Camarillo, T.M. Krummel, J.K. Salisbury, et al. **Robotic technology in surgery: past, present, and future**. *The American Journal of Surgery*, **188**:2–15, 2004. 9

[9] R. Englehardt. **German patients as experimental rabbits. Spiegel Magazine reports on implantation of hip endoprostheses with ROBODOC**. *Zeitschrift fuer Orthopaedie und ihre Grenzgebiete*, **141**(1):21, 2003. 10

[10] D.H. Boehm, H. Reichenspurner, H. Gulbins, C. Detter, B. Meiser, P. Brenner, H. Habazettl, and B. Reichart. **Early experience with robotic technology for coronary artery surgery**. *The Annals of thoracic surgery*, **68**(4):1542, 1999. 10

[11] G.B. Cadiere, J. Himpens, O. Germay, R. Izizaw, M. Degueldre, J. Vandromme, E. Capelluto, and J. Bruyns. **Feasibility of robotic laparoscopic surgery: 146 cases**. *World journal of surgery*, **25**(11):1467–1477, 2001. 10

[12] GH Ballantyne. **Robotic surgery, telerobotic surgery, telepresence, and telementoring**. *Surgical Endoscopy*, **16**(10):1389–1402, 2002. 10, 11

[13] B.P. Jacob and M. Gagner. **Robotics and general surgery**. *The Surgical clinics of North America*, **83**(6), 2003. 10

[14] JM Sackier and Y. Wang. **Robotically assisted laparoscopic surgery**. *Surgical endoscopy*, **8**(1):63–66, 1994. 10

[15] L. Mettler, M. Ibrahim, and W. Jonat. **One year of experience working with the aid of a robotic assistant (the voice-controlled optic holder AESOP) in gynaecological endoscopic surgery.** *Human Reproduction*, **13**(10):2748, 1998. 10

[16] BM Kraft, C. Jaeger, K. Kraft, BJ Leibl, and R. Bittner. **The AESOP robot system in laparoscopic surgery: Increased risk or advantage for surgeon and patient?** *Surgical endoscopy*, **18**(8):1216–1223, 2004. 10

[17] P. Hourlay. **How to maintain the quality of laparoscopic surgery in the era of lack of hands?** *Acta Chirurgica Belgica*, **106**(1):22, 2006. 10

[18] S.S. Kommu, P. Rimington, C. Anderson, and A. Rane. **Initial experience with the EndoAssist camera-holding robot in laparoscopic urological surgery**. *Journal of Robotic Surgery*, **1**(2):133–137, 2007. 10

[19] A.A. Gumbs, F. Crovari, C. Vidal, P. Henri, and B. Gayet. **Modified robotic lightweight endoscope (ViKY) validation in vivo in a porcine model**. *Surgical Innovation*, **14**(4):261, 2007. 10

[20] PA Finlay. **A New Miniature Manipulator for Laparoscopic Camera Control**. In *World Congress on Medical Physics and Biomedical Engineering, September 7-12, 2009, Munich, Germany*, pages 124–127. Springer, 2009. 10

[21] MO Schurr, G. Buess, H. Rininsland, E. Holler, B. Neisius, and U. Voges. **Artemis–Manipulatorsystem fuer die endoskopische Chirurgie**. *Endoskopie heute*, **9**:245–251, 1996. 10

[22] H. Rininsland. **ARTEMIS. A telemanipulator for cardiac surgery**. *European Journal of Cardio-Thoracic Surgery*, **16**(Supplement 2):S106, 1999. 10

[23] A.J. Madhani, G. Niemeyer, and J.K. Salisbury Jr. **The black falcon: a teleoperated surgical instrument for minimally invasive surgery**. In *Intelligent Robots and Systems, 1998. Proceedings., 1998 IEEE/RSJ International Conference on*, **2**, pages 936–944. IEEE, 1998. 10, 13, 14

[24] G.S. Guthart and J.K. Salisbury. **The IntuitiveTM telesurgery system: Overview and application**. In *IEEE International Conference on Robotics and Automation*, **1**, pages 618–621. San Francisco, CA. USA, 2000. 10, 11, 13, 14, 15, 16

[25] J. Marescaux, J. Leroy, M. Gagner, F. Rubino, D. Mutter, M. Vix, S.E. Butner, and M.K. Smith. **Transatlantic robot-assisted telesurgery**. *Nature*, **413**(6854):379–380, 2001. 10

[26] W.H.H. Chapman III, R.J. Albrecht, V.B. Kim, J.A. Young, and W.R. Chitwood Jr. **Computer-Assisted Laparoscopic Splenectomy with the da Vinci Surgical Robot**. *Journal of Laparoendoscopic & Advanced Surgical Techniques*, **12**(3):155–159, 2002. 11

[27] J. Bodner, H. Wykypiel, G. Wetscher, and T. Schmid. **First experiences with the da VinciTM operating robot in thoracic surgery**. *European Journal of Cardio-thoracic surgery*, **25**(5):844, 2004. 11

[28] M.T. Gettman, M.L. Blute, G.K. Chow, R. Neururer, G. Bartsch, and R. Peschel. **Robotic-assisted laparoscopic partial nephrectomy: technique and initial clinical experience with DaVinci robotic system**. *Urology*, **64**(5):914–918, 2004. 11

[29] E.J. Hanly and M.A. Talamini. **Robotic abdominal surgery**. *The American Journal of Surgery*, **188**:19–26, 2004. 11

[30] R. Berryhill Jr, J. Jhaveri, R. Yadav, R. Leung, S. Rao, A. El-Hakim, and A. Tewari. **Robotic prostatectomy: a review of outcomes compared with laparoscopic and open approaches**. *Urology*, **72**(1):15–23, 2008. 11

[31] M.P. Lowe, D.H. Chamberlain, S.A. Kamelle, P.R. Johnson, and T.D. Tillmanns. **A multi-institutional experience with robotic-assisted radical hysterectomy for early stage cervical cancer**. *Gynecologic oncology*, **113**(2):191–194, 2009. 11

[32] J. Binder, R. Braeutigam, D. Jonas, and W. Bentas. **Robotic surgery in urology: fact or fantasy?** *BJU international*, **94**(8):1183–1187, 2004. 11

[33] J. Bodner, F. Augustin, H. Wykypiel, J. Fish, G. Muehlmann, G. Wetscher, and T. Schmid. **The da Vinci robotic system for general surgical applications: a critical interim appraisal**. *Swiss Medical Weekly*, **135**(45/46):674, 2005. 11

[34] CN Gutt, T. Oniu, A. Mehrabi, A. Kashfi, P. Schemmer, and MW Buechler. **Robot-assisted abdominal surgery**. *British Journal of Surgery*, **91**(11):1390–1397, 2004. 11

[35] M. Hashizume and K. Tsugawa. **Robotic surgery and cancer: the present state, problems and future vision**. *Japanese Journal of Clinical Oncology*, **34**(5):227, 2004. 11

[36] U. Hagn, M. Nickl, S. Joerg, G. Passig, T. Bahls, A. Nothhelfer, F. Hacker, L. Le-Tien, A. Albu-Schaeffer, R. Konietschke, et al. **The DLR MIRO: a versatile lightweight robot for surgical applications**. *Industrial Robot: An International Journal*, **35**(4):324–336, 2008. 11

[37] U. Hagn, R. Konietschke, A. Tobergte, M. Nickl, S. Joerg, B. Kuebler, G. Passig, M. Groeger, F. Froehlich, U. Seibold, et al. **DLR MiroSurge: a versatile system for research in endoscopic telesurgery**. *International journal of computer assisted radiology and surgery*, **5**(2):183–193, 2010. 11, 13, 14, 15

[38] A. Tobergte, R. Konietschke, and G. Hirzinger. **Planning and control of a teleoperation system for research in minimally invasive robotic surgery**. In *Robotics and Automation, 2009. ICRA'09. IEEE International Conference on*, pages 4225–4232. IEEE, 2009. 12

[39] M. Mitsuishi, J. Arata, K. Tanaka, M. Miyamoto, T. Yoshidome, S. Iwata, M. Hashizume, and S. Warisawa. **Development of a remote minimally-invasive surgical system with operational environment transmission capability**. In *Robotics and Automation, 2003. Proceedings. ICRA'03. IEEE International Conference on*, **2**, pages 2663–2670. IEEE, 2003. 12

[40] J. Arata, M. Mitsuishi, S. Warisawa, K. Tanaka, T. Yoshizawa, and M. Hashizume. **Development of a dexterous minimally-invasive surgical system with augmented force feedback capability**. In *Intelligent Robots and Systems, 2005.(IROS 2005). 2005 IEEE/RSJ International Conference on*, pages 3207–3212. IEEE, 2005. 12, 13, 14, 15, 16

[41] M. Mitsuishi. **Medical Robot and Master Slave System for Minimally Invasive Surgery**. In *Complex Medical Engineering, 2007. CME 2007. IEEE/ICME International Conference on*, pages 8–13. IEEE, 2007. 12

[42] J. Arata, H. Takahashi, P. Pitakwatchara, S. Warisawa, K. Konishi, K. Tanoue, S. Ieiri, S. Shimizu, N. Nakashima, K. Okamura, et al. **A remote surgery experiment between japan-korea using the minimally invasive surgical system**. In *Robotics and Automation, 2006. ICRA 2006. Proceedings 2006 IEEE International Conference on*, pages 257–262. IEEE, 2006. 12

[43] M.C. Cavusoglu, W. Williams, F. Tendick, and S.S. Sastry. **Robotics for telesurgery: Second generation Berkeley/UCSF laparoscopic telesurgical workstation and looking towards the future applications**. *Industrial Robot: An International Journal*, **30**(1):22–29, 2003. 12, 13, 14

[44] H. Mayer, I. Nagy, A. Knoll, E.U. Schirmbeck, and R. Bauernschmitt. **The Endo[PA]R system for minimally invasive robotic surgery**. In *Intelligent Robots and Systems, 2004.(IROS 2004). Proceedings. 2004 IEEE/RSJ International Conference on*, **4**, pages 3637–3642. IEEE, 2005. 12

[45] H. Mayer, I. Nagy, A. Knoll, EU Braun, R. Lange, and R. Bauernschmitt. **Adaptive control for human-robot skilltransfer: Trajectory planning based on fluid dynamics**. In *Robotics and Automation, 2007 IEEE International Conference on*, pages 1800–1807. IEEE, 2007. 12

[46] J. Kim, Y.J. Lee, S.Y. Ko, D.S. Kwon, and W.J. Lee. **Compact camera assistant robot for minimally invasive surgery: KaLAR**. In *Intelligent Robots and Systems, 2004.(IROS 2004). Proceedings. 2004 IEEE/RSJ International Conference on*, **3**, pages 2587–2592. IEEE, 2005. 12

[47] S.K. Kim, W.H. Shin, S.Y. Ko, J. Kim, and D.S. Kwon. **Design of a compact 5-DOF surgical robot of a spherical mechanism: CURES**. In *Advanced Intelligent Mechatronics, 2008. AIM 2008. IEEE/ASME International Conference on*, pages 990–995. IEEE, 2008. 12

[48] M.J.H. Lum, J. Rosen, M.N. Sinanan, and B. Hannaford. **Optimization of a spherical mechanism for a minimally invasive surgical robot: theoretical and experimental approaches**. *Biomedical Engineering, IEEE Transactions on*, **53**(7):1440–1445, 2006. 12

[49] M.J.H. Lum, D.C.W. Friedman, G. Sankaranarayanan, H. King, K. Fodero, R. Leuschke, B. Hannaford, J. Rosen, and M.N. Sinanan. **The RAVEN: Design and Validation of a Telesurgery System**. *The International Journal of Robotics Research*, **28**(9):1183, 2009. 12

[50] J. Rosen, J.D. Brown, L. Chang, M. Barreca, M. Sinanan, and B. Hannaford. **The BlueDRAGON-a system for measuring the kinematics and dynamics of minimally invasive surgical tools in-vivo**. In *Robotics and Automation, 2002. Proceedings. ICRA'02. IEEE International Conference on*, **2**, pages 1876–1881. IEEE, 2002. 13

[51] S. Charles. **Dexterity enhancement for surgery**. In *Computer Integrated Surgery: Technology and Clinical Applications*, pages 467–471. MIT Press, 1996. 13

[52] P.S. Schenker, EC Barlow, CD Boswell, H. Das, S. Lee, TR Ohm, ED Paljug, G. Rodriguez, and ST Charles. **Development of a telemanipulator for dexterity enhanced microsurgery**. In *Proc. 2nd Intl. Symp. Med. Robot. Comput. Assist. Surg*, pages 81–88, 1995. 13, 14, 15

[53] MO Schurr, G. Buess, B. Neisius, and U. Voges. **Robotics and telemanipulation technologies for endoscopic surgery**. *Surgical endoscopy*, **14**(4):375–381, 2000. 13, 14

[54] N. Simaan, R.H. Taylor, A. Hillef, and P. Flint. **Minimally Invasive Surgery of the Upper Airways: Addressing the Challenges of Dexterity Enhancement in Confined Spaces**. In Russell A. Faust, editor, *Robotics in Surgery: history, current and future applications*, pages 261–280. Nova Science Pub Inc, 2007. 13

[55] R.J. Webster and B.A. Jones. **Design and kinematic modeling of constant curvature continuum robots: A review**. *The International Journal of Robotics Research*, **29**(13):1661, 2010. 13, 73

[56] R. Nakamura, E. Kobayashi, K. Masamune, I. Sakuma, T. Dohi, N. Yahagi, T. Tsuji, D. Hashimoto, M. Shimada, and M. Hashizume. **Multi-DOF forceps manipulator system for laparoscopic surgery**. In *Medical Image Computing and Computer-Assisted Intervention–MICCAI 2000*. Springer, 2000. 13, 14, 15

[57] H. Yamashita, D. Kim, N. Hata, and T. Dohi. **Multi-slider linkage mechanism for endoscopic forceps manipulator**. In *Intelligent Robots and Systems, 2003.(IROS 2003). Proceedings. 2003 IEEE/RSJ International Conference on*, **3**, pages 2577–2582. IEEE, 2003. 13, 14

[58] C. Reboulet and S. Durand-Leguay. **Optimal design of redundant parallel mechanism for endoscopic surgery**. In *Intelligent Robots and Systems, 1999. IROS'99. Proceedings. 1999 IEEE/RSJ International Conference on*, **3**, pages 1432–1437. IEEE, 1999. 13, 14, 15

[59] A. Rose, C. Wohlleber, S. Kassner, HF Schlaak, and R. Werthschutzky. **A novel piezoelectric driven laparoscopic instrument with multiple degree of freedom parallel kinematic structure**. In *Intelligent Robots and Systems, 2009. IROS 2009. IEEE/RSJ International Conference on*, pages 2162–2167. IEEE, 2009. 13, 14, 15

[60] K. Ikuta, S. Daifu, T. Hasegawa, and H. Higashikawa. **Hyper-finger for remote minimally invasive surgery in deep area**. *Medical Image Computing and Computer-Assisted Intervention–MICCAI 2002*, pages 173–181, 2002. 13, 14

[61] K. Harada, K. Tsubouchi, M.G. Fujie, and T. Chiba. **Micro manipulators for intrauterine fetal surgery in an open MRI**. In *Robotics and Automation, 2005. ICRA 2005. Proceedings of the 2005 IEEE International Conference on*, pages 502–507. IEEE, 2005. 13, 14, 15, 17

[62] H. Song, J. Chung, K. Kim, and J. Lee. **The Development of human-arm like manipulator for Laparoscopic Surgery with Force sensing**. In *Industrial Technology, 2006. ICIT 2006. IEEE International Conference on*, pages 1258–1262. IEEE, 2006. 13, 14

[63] H. Yamashita, N. Hata, M. Hashizume, and T. Dohi. **Handheld Laparoscopic Forceps Manipulator Using Multi-slider Linkage Mechanisms**. *Medical Image Computing and Computer-Assisted Intervention–MICCAI 2004*, pages 121–128, 2004. 13, 14, 15, 16

[64] P. Dario, M.C. Carrozza, M. Marcacci, S. D'Attanasio, B. Magnami, O. Tonet, and G. Megali. **A novel mechatronic tool for computer-assisted arthroscopy**. *Information Technology in Biomedicine, IEEE Transactions on*, **4**(1):15–29, 2000. 13, 14, 15

[65] J. Peirs, H. Van Brussel, D. Reynaerts, and G. De Gersem. **A flexible distal tip with two degrees of freedom for enhanced dexterity in endoscopic robot surgery**. In *Proceedings of the 13th Micromechanics Europe Workshop*, pages 271–274, 2002. 13, 14, 15, 17, 43, 48

[66] N. Simaan, R. Taylor, and P. Flint. **A dexterous system for laryngeal surgery**. In *Robotics and Automation, 2004. Proceedings. ICRA'04. 2004 IEEE International Conference on*, **1**, pages 351–357. IEEE, 2004. 13, 14, 15, 17, 22

[67] D. Asai, S. Katopo, J. Arata, S. Warisawa, M. Mitsuishi, A. Morita, S. Sora, T. Kirino, and R. Mochizuki. **Micro-neurosurgical system in the deep surgical field**. *Medical Image Computing and Computer-Assisted Intervention–MICCAI 2004*, pages 33–40, 2004. 13, 14, 15

[68] K. Xu, R.E. Goldman, J. Ding, P.K. Allen, D.L. Fowler, and N. Simaan. **System design of an insertable robotic effector platform for single port access (SPA) surgery**. In *Intelligent Robots and Systems, 2009. IROS 2009. IEEE/RSJ International Conference on*, pages 5546–5552. IEEE, 2009. 13, 14, 18, 22, 23, 47

[69] J. Peirs, D. Reynaerts, and H. Van Brussel. **Design of a shape memory actuated endoscopic tip**. *Sensors and Actuators A: physical*, **70**(1-2):135–140, 1998. 14, 15

[70] M. Minor and R. Mukherjee. **A dexterous manipulator for minimally invasive surgery**. In *Robotics and Automation, 1999. Proceedings. 1999 IEEE International Conference on*, **3**, pages 2057–2064. IEEE, 1999. 14, 15

[71] H. Fischer, B. Vogel, W. Pfleging, and H. Besser. **Flexible distal tip made of nitinol (NiTi) for a steerable endoscopic camera system**. *Materials Science and Engineering A*, **273**:780–783, 1999. 14, 15

[72] K. Ikuta, K. Sasaki, K. Yamamoto, and T. Shimada. **Remote Microsurgery System for Deep and Narrow Space-Development of New Surgical Procedure and Micro-robotic Tool**. *Medical Image Computing and Computer-Assisted Intervention–MICCAI 2002*, pages 163–172, 2002. 14, 15

[73] Y.J. Lee, J. Kim, S.Y. Ko, W.J. Lee, and D.S. Kwon. **Design of a compact laparoscopic assistant robot: KaLAR**. *ICCAS2003. Kroea*, 2003. 14, 15

[74] E. Dombre, M. Michelin, F. Pierrot, P. Poignet, P. Bidaud, G. Morel, T. Ortmaier, D. Sallé, N. Zemiti, P. Gravez, et al. **MARGE Project: Design, Modeling and Control of Assistive Devices for Minimally Invasive Surgery**. *Medical Image Computing and Computer-Assisted Intervention–MICCAI 2004*, pages 1–8, 2004. 14, 15

[75] P. Breedveld, JS Sheltes, EM Blom, and JEI Verheij. **A new, easily miniaturized steerable endoscope**. *Engineering in Medicine and Biology Magazine, IEEE*, **24**(6):40–47, 2005. 14, 15, 17, 43, 48

[76] U. Seibold, B. Kubler, and G. Hirzinger. **Prototype of instrument for minimally invasive surgery with 6-axis force sensing capability**. In *Robotics and Automation, 2005. ICRA 2005. Proceedings of the 2005 IEEE International Conference on*, pages 496–501. IEEE, 2005. 14, 15, 16

[77] N. Simaan et al. **Design and integration of a telerobotic system for minimally invasive surgery of the throat**. *The International journal of robotics research*, **28**(9):1134, 2009. 14, 15, 22

[78] GW Dachs and W.J. Peine. **A novel surgical robot design: Minimizing the operating envelope within the sterile field**. In *Engineering in Medicine and Biology Society, 2006. EMBS'06. 28th Annual International Conference of the IEEE*, pages 1505–1508. IEEE, 2006. 14, 15, 47

[79] A. Degani, H. Choset, A. Wolf, and M.A. Zenati. **Highly articulated robotic probe for minimally invasive surgery**. In *Robotics and Automation, 2006. ICRA 2006. Proceedings 2006 IEEE International Conference on*, pages 4167–4172. IEEE, 2006. 14, 15

[80] G. Chen, MT Pham, and T. Redarce. **Development and kinematic analysis of a silicone-rubber bending tip for colonoscopy**. In *Intelligent Robots and Systems, 2006 IEEE/RSJ International Conference on*, pages 168–173. IEEE, 2007. 14, 15

[81] M. Hashizume, T. Yasunaga, K. Tanoue, S. Ieiri, K. Konishi, K. Kishi, H. Nakamoto, D. Ikeda, I. Sakuma, M. Fujie, et al. **New real-time MR image-guided surgical robotic system for minimally invasive precision surgery**. *International Journal of Computer Assisted Radiology and Surgery*, **2**(6):317–325, 2008. 14, 15

[82] D.B. Camarillo, C.R. Carlson, and J.K. Salisbury. **Configuration tracking for continuum manipulators with coupled tendon drive**. *Robotics, IEEE Transactions on*, **25**(4):798–808, 2009. 14, 15

[83] H. Yamashita, S. Zuo, K. Masamune, H. Liao, and T. Dohi. **Nonmagnetic Rigid and Flexible Outer Sheath with Pneumatic Interlocking Mechanism for Minimally Invasive Surgical Approach**. *Medical Image Computing and Computer-Assisted Intervention–MICCAI 2009*, pages 418–425, 2009. 14, 15

[84] S. Thielmann, U. Seibold, R. Haslinger, G. Passig, T. Bahls, S. Joerg, M. Nickl, A. Nothhelfer, U. Hagn, and G. Hirzinger. **MICA - A new generation of versatile instruments in robotic surgery**. In *Intelligent Robots and Systems (IROS), 2010 IEEE/RSJ International Conference on*, pages 871–878. IEEE, 2010. 16

[85] A. Faraz and S. Payandeh. **Synthesis and workspace study of endoscopic extenders with flexible stem**. *Journal of Mechanical Design*, **119**:412, 1997. 18, 43

[86] J.R. Romanelli and D.B. Earle. **Single-port laparoscopic surgery: an overview**. *Surgical endoscopy*, **23**(7):1419–1427, 2009. 18

[87] J.D. Raman, K. Bensalah, A. Bagrodia, J.M. Stern, and J.A. Cadeddu. **Laboratory and clinical development of single keyhole umbilical nephrectomy**. *Urology*, **70**(6):1039–1042, 2007. 19, 52, 55

[88] A. Rane, P. Rao, and P. Rao. **Single-port-access nephrectomy and other laparoscopic urologic procedures using a novel laparoscopic port (R-port)**. *Urology*, **72**(2):260–263, 2008. 19

[89] J.R. Romanelli, L. Mark, and P.A. Omotosho. **Single port laparoscopic cholecystectomy with the TriPort system: a case report**. *Surgical Innovation*, **15**(3):223, 2008. 19

[90] F. Leblanc, BJ Champagne, KM Augestad, SL Stein, E. Marderstein, HL Reynolds Jr, and CP Delaney. **Single Incision Laparoscopic Colectomy: Technical Aspects, Feasibility, and Expected Benefits**. *Diagnostic and Therapeutic Endoscopy*, **2010**, 2010. 19

[91] P.F. Escobar, D. Starks, A.N. Fader, M. Catenacci, and T. Falcone. **Laparoendoscopic single-site and natural orifice surgery in gynecology**. *Fertility and Sterility*, 2010. 19

[92] R. Autorino, R.J. Stein, E. Lima, R. Damiano, R. Khanna, G.P. Haber, M.A. White, and J.H. Kaouk. **Current status and future perspectives in laparoendoscopic single-site and natural orifice transluminal endoscopic urological surgery**. *International Journal of Urology*, **17**(5):410–431, 2010. 20

[93] GV Rao, MJ Mansard, PK Ravula, P. Rebala, RR Dama, and DN Reddy. **Single-port surgery: Current applications and limitations**. *Asian Journal of Endoscopic Surgery*, **2**(3):56–64, 2009. 20

[94] A.D. Pryor, J.R. Tushar, and L.R. DiBernardo. **Single-port cholecystectomy with the TransEnterix SPIDER: simple and safe**. *Surgical endoscopy*, **24**(4):917–923, 2010. 20

[95] I.S. Gill, A.P. Advincula, M. Aron, J. Caddedu, D. Canes, P.G. Curcillo, M.M. Desai, J.C. Evanko, T. Falcone, V. Fazio, et al. **Consensus statement of the consortium for laparoendoscopic single-site surgery**. *Surgical endoscopy*, **24**(4):762–768, 2010. 21, 38, 55

[96] G.N. Box, H.J. Lee, R.J.S. Santos, J.B.A. Abraham, M.K. Louie, A.J.R. Gamboa, R. Alipanah, L.A. Deane, E.M. McDougall, and R.V. Clayman. **Rapid communication: robot-assisted NOTES nephrectomy: initial report**. *Journal of Endourology*, **22**(3):503–506, 2008. 21

[97] G.P. Haber, S. Crouzet, K. Kamoi, A. Berger, M. Aron, R. Goel, D. Canes, M. Desai, I.S. Gill, and J.H. Kaouk. **Robotic NOTES (Natural Orifice Translumenal Endoscopic Surgery) in reconstructive urology: initial laboratory experience**. *Urology*, **71**(6):996–1000, 2008. 21

[98] M.M. Desai, M. Aron, A. Berger, D. Canes, R. Stein, G.P. Haber, K. Kamoi, S. Crouzet, R. Sotelo, and I.S. Gill. **Transvesical robotic radical prostatectomy**. *BJU international*, **102**(11):1666–1669, 2008. 21

[99] J.H. Kaouk, R.K. Goel, G.P. Haber, S. Crouzet, and R.J. Stein. **Robotic single-port transumbilical surgery in humans: initial report**. *BJU international*, **103**(3):366–369, 2009. 21, 47

[100] J.H. Kaouk and R.K. Goel. **Single-port laparoscopic and robotic partial nephrectomy**. *European urology*, **55**(5):1163–1170, 2009. 22

[101] R.J. Stein, W.M. White, R.K. Goel, B.H. Irwin, G.P. Haber, and J.H. Kaouk. **Robotic laparoendoscopic single-site surgery using GelPort as the access platform**. *European urology*, **57**(1):132–137, 2010. 22

[102] A.A. Gumbs, L. Milone, P. Sinha, and M. Bessler. **Totally transumbilical laparoscopic cholecystectomy**. *Journal of Gastrointestinal Surgery*, **13**(3):533–534, 2009. 22

[103] S. Crouzet, G.P. Haber, W.M. White, K. Kamoi, R.K. Goel, and J.H. Kaouk. **Single-port, single-operator-light endoscopic robot-assisted laparoscopic urology: pilot study in a pig model**. *BJU international*, **105**(5):682–685, 2010. 22

[104] P. Allemann, J. Leroy, M. Asakuma, F. Al Abeidi, B. Dallemagne, and J. Marescaux. **Robotics May Overcome Technical Limitations of Single-Trocar Surgery: An Experimental Prospective Study of Nissen Fundoplication**. *Archives of Surgery*, **145**(3):267, 2010. 22, 33

[105] R.A. Joseph, A.C. Goh, S.P. Cuevas, M.A. Donovan, M.G. Kauffman, N.A. Salas, B. Miles, B.L. Bass, and B.J. Dunkin. **"Chopstick" surgery: a novel technique improves surgeon performance and eliminates arm collision in robotic single-incision laparoscopic surgery**. *Surgical endoscopy*, **24**(6):1331–1335, 2010. 22, 33, 34

[106] D.Q. Larkin, T.G. Cooper, C.J. Mohr, and D.J. Rosa. **Minimally invasive surgical system**, June 13 2007. US Patent App. 2008/0065102 A1. 22, 23, 47

[107] J. Ding, K. Xu, R. Goldman, P. Allen, D. Fowler, and N. Simaan. **Design, Simulation and Evaluation of Kinematic Alternatives for Insertable Robotic Effectors Platforms in Single Port Access Surgery**. In *Robotics and Automation (ICRA), 2010 IEEE International Conference on*, pages 1053–1058. IEEE. 23, 102

[108] M. Piccigallo, U. Scarfogliero, C. Quaglia, G. Petroni, P. Valdastri, A. Menciassi, and P. Dario. **Design of a Novel Bimanual Robotic System for Single-Port Laparoscopy**. *Mechatronics, IEEE/ASME Transactions on*, **15**(6):871–878, 2010. 23, 47

[109] D. Rattner and A. Kalloo. **ASGE/SAGES working group on natural orifice translumenal endoscopic surgery**. *Surgical Endoscopy*, **20**(2):329–333, 2006. 24, 38

[110] H. Feussner, D. Wilhelm, A. Meining, A. Schneider, A. Fiolka, S. Can, and H. Friess. **NOTES Technical Aspects-Hype or Hope?** *Surgical technology international*, **18**:26, 2009. 24

[111] D. Wilhelm, A. Meining, S. Von Delius, A. Fiolka, S. Can, C.H. von Weyhern, A. Schneider, and H. Feussner. **An innovative, safe and sterile sigmoid access (ISSA) for NOTES**. *Endoscopy*, **39**(5):401–406, 2007. 24, 104

[112] S. Can, A. Fiolka, D. Wilhelm, M. Burian, S. von Delius, A. Meining, A. Schneider, and H. Feussner. **Set of instruments for innovative, safe and sterile sigmoid access for natural-orifice transluminal endoscopic surgery**. *Biomedizinische Technik/Biomedical Engineering*, **53**(4):185–189, 2008. 24, 104

[113] S. Can, A. Fiolka, H. Mayer, A. Knoll, A. Schneider, D. Wilhelm, A. Meining, and H. Feussner. **The mechatronic support system "HVSPS" and the way to NOTES**. *Minimally Invasive Therapy & Allied Technologies*, **17**(6):341–345, 2008. 24, 103

[114] E. Della Flora, T.G. Wilson, I.J. Martin, N.A. O'Rourke, and G. Maddern. **Review of natural orifice translumenal endoscopic surgery (NOTES) for intra-abdominal surgery: experimental models, techniques and applicability to the clinical setting**. *Annals of surgery*, **247**(4):583–602, 2008. 24

[115] M.H. Sodergren, J. Clark, T. Athanasiou, J. Teare, G.Z. Yang, and A. Darzi. **Natural orifice translumenal endoscopic surgery: critical appraisal of applications in clinical practice**. *Surgical endoscopy*, **23**(4):680–687, 2009. 24

[116] M.F. McGee, M.J. Rosen, J. Marks, R.P. Onders, A. Chak, A. Faulx, V.K. Chen, and J. Ponsky. **A primer on natural orifice transluminal endoscopic surgery: building a new paradigm**. *Surgical innovation*, **13**(2):86, 2006. 24

[117] D.G. Fong, R.D. Pai, and C.C. Thompson. **Transcolonic endoscopic abdominal exploration: a NOTES survival study in a porcine model**. *Gastrointestinal endoscopy*, **65**(2):312–318, 2007. 24

[118] H. Feussner, S. Can, A. Fiolka, and A. Schneider. **Hybrid surgery-the way towards notes the challenge for computer science**. In *Biomedical Imaging: From Nano to Macro, 2008. ISBI 2008. 5th IEEE International Symposium on*, pages 1383–1386. IEEE, 2008. 24

[119] J. Marescaux, B. Dallemagne, S. Perretta, A. Wattiez, D. Mutter, and D. Coumaros. **Surgery without scars: report of transluminal cholecystectomy in a human being**. *Archives of Surgery*, **142**(9):823, 2007. 25

[120] C. Zornig, A. Emmermann, HA Von Waldenfels, H. Mofid, et al. **Laparoscopic cholecystectomy without visible scar: combined transvaginal and transumbilical approach**. *Endoscopy*, **39**(10):913–915, 2007. 25

[121] H. Feussner, S. Can, A. Fiolka, A. Schneider, and Wilhelm D. **Assistenzsysteme für die Single-Port-Chirurgie und die Chirurgie über natürliche Körperöffnungen (NOTES)**. In P.M Schlag, S. Eulenstein, and Lange T., editors, *Computerassistierte Chirurgie*, pages 545–551. Urban & Fischer in Elsevier, 2010. 25

[122] R. Autorino, J.A. Cadeddu, M.M. Desai, M. Gettman, I.S. Gill, L.R. Kavoussi, E. Lima, F. Montorsi, L. Richstone, J.U. Stolzenburg, et al. **Laparoendoscopic single-site and natural orifice transluminal endoscopic surgery in urology: a critical analysis of the literature**. *European urology*, 2010. 25

[123] S.N. Shaikh and C.C. Thompson. **Natural orifice translumenal surgery: Flexible platform review**. *World Journal of Gastrointestinal Surgery*, **2**(6):210, 2010. 25, 26, 27, 106

[124] L.L. Swanstrom, R. Kozarek, P.J. Pasricha, S. Gross, D. Birkett, P.O. Park, V. Saadat, R. Ewers, and P. Swain. **Development of a new access device for transgastric surgery**. *Journal of gastrointestinal surgery*, **9**(8):1129–1137, 2005. 25

[125] L.L. Swanstrom, M. Whiteford, and Y. Khajanchee. **Developing essential tools to enable transgastric surgery**. *Surgical endoscopy*, **22**(3):600–604, 2008. 26

[126] S. Horgan, G. Jacobsen, G.D. Weiss, J.S. Oldham Jr, P.M. Denk, F. Borao, S. Gorcey, B. Watkins, J. Mobley, K. Thompson, et al. **Incisionless revision of post-Roux-en-Y bypass stomal and pouch dilation: multicenter registry results**. *Surgery for Obesity and Related Diseases*, **6**(3):290–295, 2010. 26, 106

[127] G.O. Spaun, B. Zheng, and L.L. Swanstroem. **A multitasking platform for natural orifice translumenal endoscopic surgery (NOTES): a benchtop comparison of a new device for flexible endoscopic surgery and a standard dual-channel endoscope**. *Surgical endoscopy*, **23**(12):2720–2727, 2009. 26, 27, 106

[128] P.W. Dhumane, M. Diana, J. Leroy, and J. Marescaux. **Minimally invasive single-site surgery for the digestive system: A technological review**. *Journal of Minimal Access Surgery*, **7**(1):40, 2011. 26, 27, 35, 106

[129] S.J. Bardaro and L.L. Swanstrom. **Development of advanced endoscopes for natural orifice transluminal endoscopic surgery (NOTES)**. *Minimally Invasive Therapy & Allied Technologies*, **15**(6):378–383, 2006. 26

[130] A. Hattori, N. Suzuki, S. Suzuki, M. Hayashibe, Y. Otake, and S. Kobayashi. **General development plan of surgical robotic systems**. *Int J CARS*, **1**:201–203, 2006. 28

[131] SJ Phee, SC Low, ZL Sun, KY Ho, WM Huang, and ZM Thant. **Robotic system for no-scar gastrointestinal surgery**. *International Journal of Medical Robotics and Computer Assisted Surgery*, **4**(1):15, 2008. 28, 47

[132] D.J. Abbott, C. Becke, R.I. Rothstein, and W.J. Peine. **Design of an endoluminal NOTES robotic system**. In *Intelligent Robots and Systems, 2007. IROS 2007. IEEE/RSJ International Conference on*, pages 410–416. IEEE, 2007. 28, 47

[133] A.C. Lehman, N.A. Wood, J. Dumpert, D. Oleynikov, and S.M. Farritor. **Robotic natural orifice translumenal endoscopic surgery**. In *Robotics and Automation, 2008. ICRA 2008. IEEE International Conference on*, pages 2969–2974. IEEE, 2008. 28, 29

[134] K. Harada, E. Susilo, A. Menciassi, and P. Dario. **Wireless reconfigurable modules for robotic endoluminal surgery**. In *Robotics and Automation, 2009. ICRA'09. IEEE International Conference on*, pages 2699–2704. IEEE, 2009. 28, 29

[135] H. Feussner, D. Wilhelm, V. Dotzel, D. Papagoras, and E. Frimberger. **Combined endoluminal and endocavitary approaches to colonic lesions.** *Surgical technology international*, **11**:97, 2003. 32

[136] D. Wilhelm, S. von Delius, L. Weber, A. Meining, A. Schneider, H. Friess, R.M. Schmid, E. Frimberger, and H. Feussner. **Combined laparoscopic–endoscopic resections of colorectal polyps: 10-year experience and follow-up**. *Surgical endoscopy*, **23**(4):688–693, 2009. 32

[137] R.S. Chamberlain and S.V. Sakpal. **A comprehensive review of single-incision laparoscopic surgery (SILS) and natural orifice transluminal endoscopic surgery (NOTES) techniques for cholecystectomy**. *Journal of Gastrointestinal Surgery*, **13**(9):1733–1740, 2009. 35

[138] G.P. Haber, R. Autorino, H. Laydner, B. Yang, M.A. White, S. Hillyer, F. Altunrende, R. Khanna, G. Spana, I. Wahib, et al. **SPIDER Surgical System for Urologic Procedures With Laparoendoscopic Single-Site Surgery: From Initial Laboratory Experience to First Clinical Application**. *European Urology*, 2011. 36

[139] DM Herron and M. Marohn. **A consensus document on robotic surgery**. *Surgical Endoscopy*, **22**(2):313–325, 2008. 38, 40

[140] S. Can, H. Mayer, and A. Knoll. **NOTES: Neue Impulse aus Forschung und Entwicklung**. *Endoskopie heute*, **21**(04):226–230, 2008. 38

[141] J. Peirs, J. Clijnen, D. Reynaerts, H.V. Brussel, P. Herijgers, B. Corteville, and S. Boone. **A micro optical force sensor for force feedback during minimally invasive robotic surgery**. *Sensors and Actuators A: Physical*, **115**(2-3):447–455, 2004. 42

[142] B. Schuller, S. Can, and H. Feussner. **Robust Key-Word Spotting in Field Noise for Open-Microphone Surgeon-Robot Interaction**. *Proc. 5th Russian-Bavarian Conference on Bio-Medical Engineering, RBC-BME 2009, Munich, Germany*, 2009. 70

[143] A. Deguet, R. Kumar, R. Taylor, and P. Kazanzides. **The cisst libraries for computer assisted intervention systems**. In *MICCAI Workshop on Systems and Arch. for Computer Assisted Interventions, Midas Journal, September*, 2008. 71

[144] C. Staub, Y. Ning, S. Can, and A. Knoll. **A distributed software framework for robotic surgery**. In *MICCAI Workshop on Systems and Arch. for Computer Assisted Interventions, Midas Journal, August*, 2011. 71

[145] H. Lipkin, J. Munnae, G.M.M.D. Zhou, and W. Daley. **Endoscope Kinematics**. In *12th IFToMM World Congress, Besançon, June 18-21, 2007.*, 2007. 73

[146] P.I. Corke. **A robotics toolbox for MATLAB**. *Robotics & Automation Magazine, IEEE*, **3**(1):24–32, 1996. 75

[147] S. Can, H. Mayer, A. Knoll, A. Fiolka, A. Schneider, and H. Feussner. **A new, highly versatile mechatronic support system for single port minimally invasive surgery.** In *International Journal of Computer Assisted Radiology and Surgery (CARS)*, pages 280–281. Springer, 2008. 98

[148] S. Can, H. Mayer, A. Fiolka, A. Schneider, D. Wilhelm, H. Feussner, and A. Knoll. **The "Highly Versatile Single Port System" for laparoscopic surgery: Introduction and first clinical application**. In *4th European Conference of the International Federation for Medical and Biological Engineering*, pages 1650–1654. Springer, 2009. 98

[149] S. Can, A. Fiolka, A. Schneider, A. Knoll, and H. Feussner. **Single port manipulator for minimally invasive surgery**. In *Proceedings of the 3rd Hamlyn Symposium on Medical Robotics*, pages 23–24, 2010. 98

[150] S. Gillen, D. Wilhelm, A. Meining, A. Fiolka, E. Doundoulakis, A. Schneider, S. von Delius, H. Friess, and H. Feussner. **The ELITE model: construct validation of a new training system for natural orifice transluminal endoscopic surgery (NOTES)**. *Endoscopy*, **41**(5):395–399, 2009. 99, 104

[151] H. Mayer, I. Nagy, and A. Knoll. **Kinematics and modeling of a system for robotic surgery**. *On Advances in Robot Kinematics*, pages 181–190, 2004. 117